Recycling Sediments Between Source and Sink During a Eustatic Cycle: Systems of Late Quaternary Northwestern Gulf of Mexico Basin

John B. Anderson [a], Davin J. Wallace [b*], Alexander R. Simms [c], Antonio B. Rodriguez [d], Robert W. R. Weight [e], and Z. Patrick Taha [f]

[a] *Department of Earth Science, Rice University, Houston, TX, 77005, USA, email: johna@rice.edu*

[b] *Department of Marine Science, University of Southern Mississippi, Stennis Space Center, MS, 39529, USA, email: davin.wallace@usm.edu*

[c] *Department of Earth Science, University of California, Santa Barbara, CA, 93106, USA, email: asimms@geol.ucsb.edu*

[d] *Institute of Marine Sciences, University of North Carolina at Chapel Hill, Morehead City, NC, 28557, USA, email: abrodrig@email.unc.edu*

[e] *BHP Billiton, Unconventional Exploration, 1360 Post Oak Blvd., Houston, TX, 77056, USA, email: robertweight@gmail.com*

[f] *Chevron U.S.A. Inc., 1400 Smith St, Houston, TX, 77002, USA, email: zapataha@yahoo.com*

* Corresponding author

Phone: 281-352-3073

Fax: 228-688-1121

Email: davin.wallace@usm.edu

ABSTRACT

The Northwestern Gulf of Mexico Basin is an ideal natural laboratory to study and understand source-to-sink systems. An extensive grid of high-resolution seismic data, hundreds of sediment cores and borings and a robust chronostratigraphic framework were used to examine the evolution of late Quaternary depositional systems of the northwestern Gulf of Mexico throughout the last eustatic cycle (~125 ka to Present). The study area includes fluvial systems with a wide range of drainage basin sizes, climate settings and water and sediment discharges. Detailed paleogeographic reconstructions are used to derive volumetric estimates of sediment fluxes (Volume Accumulation Rates). The results show that the response of rivers to sea-level rise and fall varied across the region. Larger rivers, including the former Mississippi, Western Louisiana (presumably the ancestral Red River), Brazos, Colorado and Rio Grande rivers, constructed deltas that advanced across the shelf in step-wise fashion during Marine Isotope Stages (MIS) 5-2. Sediment delivery to these deltas increased during the overall sea-level fall due to increases in drainage basin area and erosion of sediment on the inner shelf, where subsidence is minimal, and transport of that sediment to the more rapidly subsiding outer shelf. The sediment supply from the Brazos River to its delta increased at least 3-fold and the supply of the Colorado River increased at least 6-fold by the late stages of sea-level fall through the lowstand. Repeated filling and purging of fluvial valleys from ~119-22 ka contributed to the episodic growth of falling-stage deltas.

During the MIS 2 lowstand (~22-17 ka), the Mississippi River abandoned its falling-stage fluvial-deltaic complex on the western Louisiana shelf and drained to the Mississippi Canyon. Likewise, the Western Louisiana delta was abandoned, presumably due to merger

of the Red River with the Mississippi River, terminating growth of the Western Louisiana delta. The Brazos River abandoned its MIS 3 shelf margin delta to merge with the Trinity, Sabine and Calcasieu rivers and together these rivers nourished a lowstand delta and slope fan complex. The Colorado and Rio Grande rivers behaved more as point sources of sediment to thick lowstand delta-fan complexes.

Lowstand incised valleys exhibited variable morphologies that mainly reflect differences in onshore and offshore relief and the time intervals these valleys were occupied. They are deeper and wider than falling stage channel belts and are associated with a shelf-wide surface of erosion (sequence boundary).

During the early MIS 1 (~17 ka to ~ 10 ka) sea-level rise, the offshore incised valleys of the Calcasieu, Sabine, Trinity, Brazos, Colorado, and Rio Grande rivers were filled with sediment. The offshore valleys of smaller rivers of central Texas would not be filled until the late Holocene, mainly by highstand mud. The lower, onshore portions of east Texas incised valleys were filled with sediment mainly during the Holocene, with rates of aggradation in the larger Brazos and Colorado valleys being in step with sea-level rise. Smaller rivers filled their valleys with back-stepping fluvial, estuarine and tidal delta deposits that were offset by flooding surfaces. In general, the sediment trapping capacity of bays increased as evolving barrier islands and peninsulas slowly restricted tidal exchange with the Gulf and valley filling led to more shallow, wider bays. A widespread period of increased riverine sediment flux and delta growth is attributed to climate change during MIS 1, between ~ 11.5-8.0 ka, and occurred mainly under cool-wet climate conditions.

Relatively small sea-level oscillations during the MIS 1 transgression (~17 ka to ~ 4.0 ka) profoundly influenced coastal evolution, as manifested by landward stepping shorelines, on the order of tens of kilometers within a few thousand years. The current barriers, strand plains and chenier plains of the study area formed at different times over the past ~8 ka, due mainly to differences in sand supply and the highly variable relief on the MIS 2 surface on which these systems formed.

Modern highstand deposition on the continental shelf formed the Texas Mud Blanket, which occurs on the central Texas shelf and records a remarkable increase in fine-grained sediment supply. This increase is attributed to greater delivery of sediments from the Colorado and Brazos rivers, which had filled their lower valleys and abandoned their transgressive deltas by late Holocene time, and to an increase in westward directed winds and surface currents that delivered suspended sediments from the Mississippi River to the Texas shelf.

Collectively, our results demonstrate that source-to-sink analyses in low gradient basin settings requires a long-term perspective, ideally a complete eustatic cycle, because most of the sediment that was delivered to the basin by rivers underwent more than one cycle of erosion, transport and sedimentation that was regulated by sea-level rise and fall. Climate was a secondary control. The export of sediments from the hinterland to the continental shelf was not directly in step with temperature change, but rather varied between different fluvial-deltaic systems.

1. Introduction

Many laboratory flume experiments and numerical modeling studies, as well as conceptual models, have attempted to bridge the gap between sedimentary processes and strata formation. Advancing and testing the validity of those types of models can be done using regional geological data across a margin influenced by multiple distinct fluvial systems and spanning enough time to record autocyclic and allocyclic influences. We contend that the late Quaternary provides the best time interval for this research because sea-level history is well constrained relative to the rest of geological time, centennial to millennial-scale chronostratigraphic resolution is achievable and, depending on location, subsidence and paleoclimate histories are best constrained. The late Quaternary is also the only time when high-resolution seismic data provides vertical and horizontal resolution at both outcrop and stratigraphic-bedding scales.

The northwestern Gulf of Mexico provides an excellent field area for this type of research because the continental shelf experiences relatively high subsidence, the sediment discharge of rivers varies widely, and knowledge of paleoclimate change is steadily improving. In addition, the continental shelf physiography and oceanography varies significantly across the study area, which has resulted in different sediment accumulation and dispersal patterns. Finally, the northwestern Gulf of Mexico has a long tradition of sedimentological and stratigraphic research that provides an important framework for source-to-sink research.

We describe sediment delivery, transport and deposition within and between fluvial, deltaic, coastal, shelf and upper slope depocenters of the northwestern Gulf of Mexico in the late Quaternary. Note, Bhattacharya et al. (this volume) and Bentley et al. (this volume) discuss development of source-to-sink systems in the northern Gulf in the Cretaceous and Cenozoic, respectively. In addition, Blum et al. (2013) provide a recent and thorough review of the literature on the response of Quaternary fluvial systems to allogenic and autogenic forcings, including examples from the northwestern Gulf of Mexico.

Our study area includes several rivers that have a wide range of drainage-basin size, relief, and geology (Fig. 1). These rivers have highly variable discharge and sediment yields that reflect the strong climate gradient of the region, mainly precipitation, and anthropogenic influences (Table 1). Currently, drainage-basin area correlates poorly with sediment discharge, which is partly due to differences in precipitation, land-use practices, and water management across the study area. In the past, rivers like the Colorado and Rio Grande had larger sediment discharges that were more consistent with their drainage-basin areas.

Our research focused on the last glacial eustatic cycle (~125 ka to Present) for which sea-level history is well known (Fig. 2). We greatly benefited from results of prior studies, in particular the extraordinary detailed work of Berryhill and colleagues (Berryhill, 1987), which was based on dense grids of high-resolution seismic data from the western Louisiana and south Texas continental shelves.

Our early research focused on stratigraphic variability of the continental shelf and upper slope across the northern Gulf (Anderson et al., 2004). Since then, we have completed detailed studies of the onshore Calcasieu (Milliken et al., 2008a), Sabine (Milliken et al., 2008b), Trinity (Anderson et al., 2008), Brazos (Taha and Anderson, 2008), Colorado (previously unpublished), Lavaca (Maddox et al., 2008), Copano (Troiani et al., 2011), Nueces (Simms et al., 2008) and Baffin Bay (Simms et al., 2010) fluvial valleys. We have also conducted extensive research on barrier islands and peninsulas, shelf banks, tidal deltas and the Brazos wave-dominated delta (e.g., Siringan and Anderson, 1993; Rodriguez et al., 2000a,b, 2004; Simms et al., 2006a; Wallace et al., 2009, 2010; Wallace and Anderson, 2010, 2013; summarized in Anderson et al., 2014). Finally, we recently completed a study of the Texas Mud Blanket (Weight et al., 2011), which dominates highstand sedimentation on the continental shelf. These studies included detailed lithofacies analysis, based largely on sediment core analyses, coupled with high-resolution seismic data to integrate lithofacies and stratigraphy. A robust chronostratigraphic framework allows us to assemble results from these previous studies into a basin-scale analysis of how lithofacies and stratigraphy have varied in response to allogenic and autogenic forcings.

2. Methods

This review is based on over two decades of research that was heavily focused on data acquisition and analysis of hundreds of sediment cores (vibracores, pneumatic hammer cores and drill cores), hundreds of water-well and oil industry platform-boring descriptions and thousands of kilometers of high-resolution seismic data (Fig. 3).

A range of seismic sources, including a 50 inch^3 Generator-Injector (GI) air gun, 15 inch^3 water gun, multi-element sparker, boomer and chirp, were used for seismic-data acquisition in order to obtain maximum stratigraphic resolution at different water depths and stratigraphic thicknesses. All are single-channel data and most of these data were digitally acquired and processed using band-pass filters and gain adjustment.

Sedimentological work included detailed lithological descriptions, identification of sedimentary structures, grain size, macro- and micro-faunal analyses, magnetic susceptibility and clay mineralogy. Hundreds of radiocarbon dates, oxygen isotope profiles and micropaleontological data provide chronostratigraphic constraints on relative age assignments derived from seismic stratigraphic analysis (see Anderson et al., 2004 for details). Using these combined data, we apply basic sequence stratigraphic techniques and terminology to subdivide the stratigraphic section into systems tracts (Fig. 4) that are constrained using the sea-level curve and associated Marine Oxygen Isotope (MIS) stages shown in Figure 2.

These are as follows:

Highstand Systems Tract (MIS 5e), 124-119 ka

Falling-Stage Systems Tract (MIS 5-3), ~119-22 ka

Lowstand Systems Tract (MIS 2), ~22-17 ka

Transgressive Systems Tract (MIS 1), ~17-4.0 ka

Current Highstand (MIS 1), ~4.0 ka-Present.

We use our seismic grids and chronostratigraphic results (Anderson et al., 2004; Weight et al., 2011) to derive sediment Volume Accumulation Rates (VAR; in km^3/kyr) over millennial time scales. These values are converted to Mass Accumulation Rates (MAR; 10^6 t/yr) in order to compare these long-term rates to sediment discharge rates derived using the QBART method (Syvitski and Milliman, 2007). It is noteworthy that, while both values are expressed in 10^6 t/yr, the two methods are quite different, in particular the time intervals considered, as our MAR approach averages over millennial time scales while the QBART method utilizes modern conditions (Table 1). The MAR calculations assume that the sediment volume is entirely quartz (density of 2.65 g/cm^3) with a porosity value of 40%, which is similar to previous studies in the region (Pirmez et al., 2012; Weight et al., 2011). This calculation is done using the relationship between mass (m_{sp}), volume (V_{sp}) and density (ρ_{sp}) of the solid phase (sp) of sediments:

$$M_{sp} = V_{sp}\ \rho_{sp} \qquad (1)$$

See Weight et al. (2011) for further details.

3. Study area

3.1. Subsidence and Basin Physiography

Regional basin subsidence is highly variable, ranging from 0.03 mm/yr along inland portions of the coast to >1.0 mm/yr at the shelf margin (Paine, 1993; Anderson et al., 2004; Simms et al., 2013). Thus, during the last eustatic cycle (~125 ka to Present), less than one meter of subsidence occurred along the current coastline while the shelf margin experienced more than 100 meters of subsidence. This seaward increase in subsidence and sediment accommodation is manifest as a wedge of strata deposited during the last eustatic cycle (Fig. 4). Subsidence rates also increased near large depocenters on the shelf, a response to sediment loading and compaction (Simms et al., 2013).

It is well established that shelf physiography is regulated by fluvial sediment flux (Olariu and Steele, 2009). Variations in continental shelf physiography across the study area are the result of differences in sediment input and the degree to which accommodation was filled by sedimentation over multiple eustatic cycles (Anderson et al., 2004), both of which are largely governed by underlying large structures (e.g., San Marcos and Sabine Arches-Fig. 3). In particular, relatively low sediment input, due to the diversion of rivers by a structural high across the San Marcos Arch, has resulted in a prominent embayment on the central Texas shelf (Fig. 5).

3.2. Climate and Paleoclimate

Currently, four major climate regimes are found across the region (Thornthwaite, 1948): humid (western Louisiana and far east Texas), wet subhumid (east central Texas), dry subhumid (central Texas), and semiarid (south Texas). Most notably, mean annual precipitation ranges widely (50 to 150 cm per year; Fig. 1), but temperature differences from east to west across the study area are minimal. In addition, onshore relief and geology are significantly different across the region. Larger rivers (Brazos, Colorado and Rio Grande, Fig. 1) have drainage basins that span variable relief, climate, vegetation type and cover, and geology. These rivers are characterized by flashy flow, with greater discharge and sediment supply to the coast during floods that occur at decadal time scales (Rodriguez et al., 2000a; Fraticelli, 2006; Carlin and Dellapenna, 2014). Smaller rivers (e.g., Calcasieu, Sabine, Trinity, Lavaca, Nueces rivers; Fig. 1) drain mostly coastal-plain areas, and as a result, watersheds are characterized by similar low relief but different vegetation cover and geology. These smaller rivers exhibit considerable variability in sediment discharge that reflects the strong precipitation gradient across the region (Fig. 1).

Several studies have focused on the post-glacial climatic history (~18 ka to Present) of Texas based on multiple proxies, such as ^{13}C variations in organics and carbonates (Humphrey and Ferring, 1994; Wilkins and Currey, 1999; Nordt et al., 2002), faunal shifts (Toomey et al., 1993; Buzas-Stephens et al., 2014), presence of C4 grasses (Nordt et al., 1994), and calcium oxalate (Russ et al., 2000). These studies have shown that numerous shifts between cold-wet and warm-dry conditions occurred over millennial time scales (Fig.

6) driven both by atmospheric and oceanographic changes (North American Monsoon, PDO, ENSO; e.g., Toomey et al., 1993; Buzas-Stephens et al., 2014). Independent studies have shown that sediment supply to the basin varied through time and at different temporal scales due to changes in vegetation cover and river discharge, which are largely driven by climate (Fraticelli, 2006; Hidy et al., 2014). In general, climate variability increases toward the west and south. Central Texas was predominately cool-wet from ~18 ka to 7.5 ka, and warm-dry from ~7.5 ka to 3.5 ka (Humphrey and Ferring, 1994; Nordt et al., 1994, 2002; Toomey et al., 1993). Since 3.5 ka, the paleoclimate in central Texas was characterized by fluctuations between millennial scale periods of cool-wet and warm-dry conditions (Buzas-Stephens et al., 2014). While the climate records in west Texas are considerably shorter, they also suggest that the past ~6 ka has been characterized by centennial to millennial periods of cool-wet and warm-dry conditions (Wilkins and Currey, 1999; Russ et al., 2000).

3.3. Oceanographic Setting

The Texas coast has a diurnal, microtidal range (<1 m) (Morton, 1994). Along the northwestern Gulf of Mexico, the shoreline is typically influenced by fair-weather near-shore waves that range between 30 and 60 cm in height with 2 to 6 second periods. Due to the coastline shape, the prevailing southeasterly winds and waves drive longshore currents that flow from east to west in east Texas and from south to north in south Texas. These currents therefore converge offshore central Texas (Lohse, 1955; Curray, 1960; Morton, 1979; Oey, 1995). The Gulf of Mexico is frequently impacted by severe storms and hurricanes and during these times, wave heights and periods can be enhanced. Intense hurricanes (likely category 3 and higher) have impacted the Texas coast over the late Holocene at a time-averaged rate of 0.46% (annual landfall probability) (Wallace and Anderson, 2010), meaning they strike at any single location about once every 200 years.

Wind-driven currents dominate oceanographic circulation on the continental shelf. A counterclockwise gyre is a dominant feature on the central Texas shelf. It is driven by strong westward coastal currents and by an eastward current that flows along the shelf margin (Fig. 7). West of the Mississippi River, the Louisiana-Texas Coastal Current dominates shelf circulation (Cochrane and Kelly, 1986; Oey, 1995; Jarosz and Murray, 2005). During fall, winter, and spring, flow is to the west on the Louisiana shelf and toward the southwest on the Texas shelf; during the summer the flow periodically reverses. Circulation on the continental slope is strongly influenced by eddies spinning off from the loop current that migrate from east to west and onto the central Texas continental shelf (Shideler, 1981; Rudnick et al., 2015; Fig. 7). Currents in water depths of 2000 meters can exceed 85 cm/s above the bottom (Hamilton and Lugo-Fernandez, 2001).

4. Systems Tract Evolution

4.1. Previous Highstand and Falling Stage (MIS 5-3)

During MIS 5e, ice-equivalent sea levels were 6-9 m higher than present (Kopp et al., 2009, 2013; Dutton and Lambeck, 2012). In the northern Gulf of Mexico region, glacio-isostatic effects resulted in local relative sea levels of ~8-10 m above present (Muhs et al., 2011; Simms et al., 2013). This resulted in the formation of a prominent shoreline during this period of relatively stable sea level, locally known as the Ingleside Shoreline (Price, 1933; Shepard and Moore, 1955; Paine, 1993; Otvos and Howat, 1996; Simms et al., 2013) (Fig. 3). The shoreline was dated near Galveston Bay and Matagorda Bay using optically stimulated luminescence, with ages ranging between 119-128 ka (Simms et al., 2013). Original beach ridges are locally preserved. The shoreline is absent locally where removed by fluvial erosion or buried by eolian deposits. Its similarity to the modern shoreline suggests that coastal-sediment delivery and dynamics were similar during MIS 5e as today.

4.1.1. Falling-Stage Channel Belts

The first and most detailed studies of falling-stage deposits on the continental shelf were conducted by Berryhill and colleagues (Berryhill, 1987). Suter (1987) mapped fluvial channels on the western Louisiana continental shelf, which were interpreted to have formed during "Early Wisconsin" time (Fig. 8). Suter and Berryhill (1985) mapped and described shelf-margin deltas on the western Louisiana and east Texas continental shelves. Studies by Coleman and Roberts (1988a, b) and Wellner et al. (2004) provided chronostratigraphic documentation that the older ("Early Wisconsin") channels mapped by Suter (1987) and their associated shelf-margin deltas are MIS 5-3 falling-stage deposits. Relatively high subsidence and sediment accumulation in this area facilitated preservation of these deposits.

The channels mapped by Suter (1987) can be subdivided into two separate drainage systems. The eastern drainage complex (paleo-Mississippi River channel complex) is characterized by somewhat wider, more closely spaced channels that occupied an area at least 150-km wide (Fig. 8). The eastern set of channels display lateral accretion, generally less than a kilometer, indicating modest channel sinuosity. The age of the eastern shelf margin delta, which Suter and Berryhill (1985) called the "Mississippi Delta", is not directly constrained but is assumed to be a MIS 3 feature since the Mississippi River is known to have avulsed to a new location at the Mississippi Canyon by MIS 2 time. The western channel complex is on the order of 80 kilometers in width, although the western boundary is poorly defined by our data. It is characterized by channels that converge seaward (Fig. 8). The western channel complex exhibits a general northeast to southwest orientation, perhaps indicating a westward-dip to the shelf during this time interval (Suter and Berryhill, 1985). Individual channels are in excess of 35-meters deep, with width-to-depth ratios generally greater than 30:1 (Suter, 1987). The western channel complex nourished a large shelf margin delta, the Western Louisiana delta (Fig. 8), during MIS 3 until ~33,000 radiocarbon years ago (Wellner et al., 2004).

The Texas shelf differs from the western Louisiana shelf in that it has fewer and more widely spaced falling-stage channels. This may be partly due to lower subsidence on the Texas shelf, which resulted in erosion of shallow channels, especially on the inner shelf. But it was also likely that the fluvial geomorphology of the two areas was different.

4.1.2. Falling-Stage Deltas

We distinguish fluvial-dominated deltas as having clinoform heights greater than the depth of wave erosion, which in the western Gulf is in the range of -8 to -10 meters (Rodriguez et al., 2001; Wallace et al., 2010). We can further characterize the shapes of these deltas (e.g., highly lobate versus elongate) based on variations in clinoform dips as revealed in seismic records. Highly lobate deltas display greater variability in clinoform angles, reflecting variations in the directions of progradation of individual lobes. To a first order, delta shape is controlled by the rate of sediment delivery versus rates of sea-level rise and fall (i.e., changes in accommodation) (Driscoll and Karner, 1999). As we will demonstrate, falling-stage deltas tend to be elongate in a dip direction, a product of rapid basinward growth forced by sea-level fall. In contrast, transgressive fluvial-dominated deltas display highly lobate shapes and lowstand deltas display slope-parallel elongation.

During the overall fall in sea level, the ancestral Mississippi, Western Louisiana, Brazos, Colorado and Rio Grande rivers constructed large deltas on the shelf (Fig. 9). Detailed sequence stratigraphic analysis revealed that the growth of these deltas was strongly regulated by the episodic nature of the overall sea-level fall (Morton and Suter, 1996; Wellner et al., 2004; Abdulah et al., 2004; Banfield and Anderson, 2004) (Fig. 2). They experienced phases of seaward progradation across the inner shelf during MIS 5e-d, 5c-b and 5a-4 (Figs. 2 and 9). Episodes of delta growth were interrupted by landward shifts (back-stepping) during periods of sea-level rise (MIS 5d-c and 5b-a; Fig. 2). Slow subsidence and low accommodation on the inner shelf resulted in the upper portions of these falling-stage deltas being eroded. In particular, their sandy mouth-bar deposits, which occur in the upper part of the delta succession, were eroded.

During MIS 4, sea level fell to ~-80 meters and then during MIS 3 rose to between ~-60 and ~-30 meters, followed by a gradual fall to ~-80 to ~-90 meters at the end of MIS 3 (Fig. 2). The MIS 3 rise is discernible as a prominent flooding surface that separates MIS 3 delta clinoforms from MIS 5 deposits (Fig. 4). All four deltas experienced rapid and continuous growth to the shelf margin and into water depths of up to ~80 meters during MIS

3 (Anderson et al., 2003; Anderson, 2005). This phase of seaward growth resulted in a downward shift in clinoforms and mouth-bar sands that down-cut into prodelta muds (Fig. 10).

The observed response of falling-stage deltas to high-frequency sea-level oscillations has been recognized in other areas, including the Gulf of Cadiz (Hernández-Molina et al., 2000) and Gulf of Lions (Lobo et al., 2004; Labaune et al., 2005).

4.1.2.1. Sediment Supply Through Time

We use the VAR values for falling-stage deltas to estimate the long-term (millennial-scale) sediment delivery to individual fluvial/deltaic systems (Table 1). These are minimum estimates because it is not possible to account for the volume of fine-grained sediments that bypassed the shelf. Furthermore, we do not account for onshore deposits of MIS 5e.

Our estimates for the Brazos system are as follows:

- Stage 5e-5b: ~1.10 km^3/kyr
- Stage 5a-4: ~1.35 km^3/kyr
- Stage 3: ~3.5 km^3/kyr.

The observed ~3-fold increase in VAR during the overall falling stage is attributed, in part, to recycling of sediments from the inner shelf to the outer shelf. This recycling occurred during repeated episodes of transgression and regression during MIS 5 through MIS 3 time

(Fig. 2). Evidence for recycling exists in our seismic data and cores as prominent transgressive and regressive surfaces (Fig. 4), which are erosional unconformities. This recycling also resulted in an overall increase in the sand-to- mud ratio of the falling-stage deltas, due to progressive removal of silts and clays, to produce extensive sandy mouth bars (Fig. 10).

During the same time interval that large deltas prograded across the western Louisiana and east and south Texas shelves, the central Texas shelf, where no large rivers exist, experienced seaward progradation of coastal deposits that filled only about 20% of the total accommodation formed by subsidence on the outer shelf (Eckles et al., 2004) (Fig. 9). This contributed to the bathymetric embayment (Central Texas Embayment) on the central Texas shelf (Fig. 5), which is situated between the ancestral Colorado and Rio Grande deltas. This shelf embayment later became the location of highstand mud accumulation.

4.2. Lowstand

The major lowstand depositional systems of the study area include incised valleys on the continental shelf and delta-fan complexes, hemiplegic drapes and contourites on the continental slope (Fraticelli and Anderson, 2003) (Fig. 11).

4.2.1. Incised Valleys

Between ~ 28 ka and 18 ka, sea level fell continuously from ~-80 to ~-120 meters, exposing the entire continental shelf (Fig. 2). During this time interval, rivers continued to erode and extend their valleys seaward, marking the final phase of fluvial incision and creation of the MIS 2 sequence boundary. Using dense grids of seismic profiles acquired in the 1970's by the USGS and by Texaco Oil Company and augmented by our own data (Fig. 3), Simms et al. (2007) constructed a digital elevation map of the MIS 2 surface that shows the incised valleys on the continental shelf (Fig. 11). The onshore valleys that are now bays were mapped in considerable detail using tighter grids of seismic data, sediment cores and platform borings (Anderson and Rodriguez, 2008) (Fig. 12). A map of the Brazos incised valley was constructed using aerial photographs supplemented by hundreds of water-well descriptions (Taha and Anderson, 2008). The onshore Colorado and Rio Grande incised valleys have not been mapped in detail.

Relative to falling-stage channels, incised valleys are significantly wider (from a few kilometers to tens of kilometers wide at the current shoreline) and deeper. The incised valleys average 40-m deep near the present shoreline, whereas falling-stage channels, with the exception of those of the western Louisiana continental shelf, are generally less than 20-m deep and less than a kilometer wide (including lateral accretion). With the exception of the more ramp-like central Texas shelf, incised valleys are discernable to the shelf edge.

The cross-sectional profiles of individual valleys vary widely, ranging from relatively narrow (e.g., Baffin Bay and Sabine valleys) to broad and terraced (e.g., Trinity and Lavaca valleys, which are now occupied by Galveston and Matagorda bays, respectively) (Fig. 12). Terraced morphology was a product of stepped down-cutting due to the episodic nature of sea-level fall (Fisk, 1944; Thomas and Anderson, 1994; Blum et al., 1995; Rodriguez et al., 2005). Both the Colorado and Brazos valleys bifurcated in an offshore direction while the Calcasieu, Sabine and Trinity valleys converged (Fig. 11). The offshore Brazos, Sabine and

Trinity valleys were similar in width and depth, despite differences in their drainage-basin areas and discharge (Table 1). In part, these similarities were likely due to variations in the depth of transgressive ravinement along the shelf, which removed the upper, wider and more morphologically variable portions of these valleys. The different valley morphologies and drainage patterns have been attributed mainly to differences in the river profiles relative to continental-shelf gradients (Greene et al., 2007; Simms et al., 2007). But, there were also probably differences in the response of these rivers to sea-level fall. Some valleys experienced multiple episodes of erosion and fill during the last eustatic cycle, while others were occupied only during a portion of the cycle (e.g., stages 3-1). This is particularly true in the lower-valley reaches where avulsions must have occurred. In general, smaller rivers such as the Trinity River occupied the same valley throughout MIS 5-2 (Fig. 11). The Brazos valley, on the other hand, avulsed during the late (MIS 3) falling stage. Fluvial valleys of the central Texas shelf can be traced only a few tens of kilometers across the shelf. These valleys were formed by rivers that flowed across a prograded shoreline that terminated on the mid-shelf, resulting in a significant gradient change with time (Eckles et al., 2004). In contrast, the Rio Grande valley provides another unique fluvial geomorphology, one where a single, relatively narrow valley on the inner shelf widens and deepens seaward, reaching a depth of ~100 meters at the shelf margin (Suter and Berryhill, 1985; Banfield and Anderson, 2004) (Fig. 13).

This complex sea-level and physiographic control on valley morphology has been observed in other locations, for example the Manfredonia Incised Valley of the south Adriatic continental shelf. There, Maselli et al. (2014) demonstrated significant upstream deepening of the valley, which they connected with fluvial incision of the MIS 5e highstand coastal prism and associated subaqueous clinoform under the influence of MIS 5-4 sea-level changes. Shallowing downstream and narrowing of valleys primarily was related to increased sea-level fall rates at the MIS 3-2 transition on a flatter mid-outer shelf. Ultimately, the interplay between sea-level change, stream power and load, and the physiography of the shelf controlled the duration of incision, valley morphology and drainage pattern.

4.2.2. Lowstand Deltas and Fans

Even before sea level fell to its lowest point (MIS 2; Fig. 2), the Mississippi, Western Louisiana, Brazos, Colorado and Rio Grande rivers had constructed deltas situated at the shelf margin (Suter and Berryhill, 1985; Abdulah et al., 2004; Wellner et al., 2004; Banfield and Anderson, 2004; Figs. 8 and 9). But, the point at which these deltas reached the shelf margin and delivered sediments to the continental slope varied. The Mississippi, Western Louisiana, Brazos, and Colorado deltas occupied the shelf margin and upper slope by MIS 3 time (Fig. 9) while the Rio Grande delta lagged behind, being mostly an MIS 2 feature (Anderson, et al., 1996; Abdulah et al., 2004; Banfield and Anderson, 2004; Anderson, 2005).

Prior to the MIS 2 lowstand, the Mississippi, Western Louisiana, and Brazos deltas were abandoned by their fluvial sources. Bentley et al. (this volume) review late Quaternary sedimentation on the Mississippi fan. The Brazos River avulsed to a new location along the eastern margin of its MIS 3 delta and merged with the ancestral Trinity River. Radiocarbon ages indicate that the Brazos River avulsion occurred between ~36 ka and 20 ka (Fraticelli and Anderson, 2003) and that the Western Louisiana MIS 3 delta was abandoned by ~ 36 ka (Wellner et al., 2004). Upstream of where the Brazos and Trinity valleys merged on the outer shelf, the Sabine and Calcasieu valleys converged with the Trinity Valley (Fig. 11). Sediment from these combined drainage basins nourished a prominent lowstand delta and slope fan complex that occupied four salt-withdrawal minibasins on the upper slope (Satterfield and Behrens, 1990; Anderson et al., 1996, 2004; Morton and Suter, 1996; Winker, 1996; Beaubouef and Friedmann, 2000; Badalini et al., 2000; Pirmez et al., 2012) (Fig. 14).

Because the Brazos River abandoned its MIS 3 delta, the delta was not incised by a lowstand valley and thus was not a significant source of sediment to the lowstand delta-fan system. The MIS 3 Western Louisiana delta may, however, have been a source of sediment to the newly established Brazos-Trinity (B-T) lowstand delta (Wellner et al., 2004). Platform borings from the seaward terminus (shelf edge) of the B-T valley sampled up to 30 m of sand (Anderson et al., 1996), which is consistent with thickness estimates from seismic facies analyses (Morton and Sutter, 1996).

Pirmez et al. (2012) conducted a detailed study of the B-T depositional system, including 2D and 3D seismic data analysis and sedimentological and chronostratigraphic analyses of sediment cores, including drill cores, from the four upper slope minibasins located down dip of the B-T lowstand delta (Fig. 14). They used seismic and chronostratigraphic data to derive a total volume of 62.2 km^3 for sediment accumulation in the minibasins during the most recent glacial-eustatic cycle. They then combined their chronostratigraphic results with maps from Prather (2012) to estimate sediment flux to the basin during this time interval. Their results showed that deposition in the upper minibasin began by 24.3 ka, which was approximately coeval with the formation of the B-T MIS 2 delta, and that sediment delivery to the basin had largely ended by ~15 ka (Pirmez et al., 2012).

Unlike the B-T system, the Colorado River remained fixed at its outer shelf location and nourished its shelf-margin delta throughout MIS 3-2, with an approximately six-fold increase in VAR over that time interval (Table 1). The Colorado shelf margin delta was deeply incised during the lowstand, and contributed to the supply of sediment to two canyons that connect with two slope fans (Lehner, 1969; Tatum, 1977; Woodbury et al., 1978; Rothwell et al., 1991; Abdulah et al., 2004) (Fig. 11).

The ancestral Rio Grande River incised valley widened and deepened seaward into a prominent canyon head (Fig. 13). The lowstand delta was mapped by Berryhill (1987) and Banfield and Anderson (2004), and the slope fan was mapped by Sidner et al. (1978) and Rothwell et al. (1991) (Fig. 11). By the end of the lowstand, the river had constructed a thick, wedge-shaped delta/fan complex that filled this valley and canyon head with up to 100 meters of sediment (Fig. 13), and tectonics considerably influenced the thickness of the delta (Berryhill, 1987). A single core from the lowstand delta sampled a 30-m thick package of silty sand, sandy silt and sand (Banfield and Anderson, 2004).

Chronostratigraphic data for the Rio Grande falling stage delta are not sufficient to derive reliable VAR estimates. Banfield and Anderson (2004) noted seaward expansion of the delta and argued that the sediment discharge during the falling stage and lowstand was significantly greater than at present. They attributed this increase in sediment supply to the delta to recycling of sediment from the inner shelf and wetter climate conditions within the drainage basin at that time, resulting in greater erosion within the drainage basin and increased river discharge.

4.3. Transgression

The post-LGM (Last Glacial Maximum) sea-level history for the northern Gulf of Mexico is well constrained, especially for the past 10 ka (Fig. 15).

Figure 16 shows the major transgressive depositional systems of the study area, including incised-valley fills, deltas and coastal deposits. Between ~17 ka and ~10 ka the rate of rise was so rapid that only a thin veneer of early transgressive strata was deposited on the outer shelf, except on the western Louisiana shelf where MIS 1 estuarine, fluvial and marine deposits blanketed the shelf (Suter, 1987). The other exception was the Trinity-Sabine-Brazos delta, which continued to grow during the early part of the transgression, as indicated by a shift from progradational to aggradational clinoforms (Fig. 17) and by a radiocarbon age of ~14 ka from near the top of the delta (Wellner et al., 2004).

After ~10 ka, the rate of sea-level rise slowed progressively from an average rate of 4.2 mm/yr to 1.4 mm/yr (Fig. 15). This slower rise resulted in a decrease in the rate of transgression and thicker transgressive deposits on the inner shelf. As a result, the record of sedimentation since ~ 10 ka is more complete than earlier periods (Anderson et al., 2014). This includes sand banks, which are coastal barriers that were overstepped during transgression to form sand banks (Rodriguez et al., 1999), incised-valley fill deposits and isolated fluvial-dominated deltas.

Sediment supply to the continental shelf apparently increased between ~ 11.5 ka and 5.0 ka as indicated by the formation of lobate deltas of the Brazos (Abdulah et al., 2004), Colorado (Van Heijst et al., 2001) and Rio Grande (Banfield and Anderson, 2004) rivers. These deltas sit on top of the MIS 2 sequence boundary and display highly variable clinoform angles, reflecting lobate shapes (Fig. 18). Radiocarbon ages from the Brazos (Abdulah et al., 2004) and Colorado (Van Heijst et al., 2001) deltas confirm their MIS 1 ages.

4.3.1. Incised-Valley Infilling

Simms et al. (2006b) characterized overfilled valleys, those that are filled entirely with fluvial sediments, and under-filled valleys, those that contain estuarine and marine sediments. Overfilled valleys include the Brazos and Colorado valleys and most likely the Rio Grande valley. Figure 19 is a highly exaggerated (vertical scale 300x) digital elevation map that contrasts the under-filled Trinity valley and the overfilled Brazos valley. Note that the under-filled Trinity valley is well defined north of the coastal plain, whereas the Brazos valley has less topographic expression. All under-filled valleys have been flooded to create bays (i.e., Calcasieu, Sabine, Trinity/San Jacinto, Matagorda, Copano, San Antonio, Corpus Christi and Baffin bays). The overall stratigraphic architecture of these valleys have been studied in detail (Milliken et al., 2008a,b; Anderson et al., 2008; Maddox et al., 2008; Simms et al., 2008, 2010; Troiani et al., 2011) and are characterized by deepening-upward successions of fluvial, bayhead delta, bay and tidal deposits that back-step landward (Fig. 20). Thomas and Anderson (1994) argued that this back-stepping stratigraphic architecture resulted from the episodic nature of sea-level rise, with flooding surfaces separating supposedly contemporaneous bayhead delta, open bay, and tidally influenced lower bay deposits. This concept was later tested using detailed seismic and drill core analyses of modern bays (Anderson and Rodriguez, 2008) (Fig. 21). Results showed that some of the flooding surfaces in separate bays appear to be contemporaneous, and are thus interpreted as having been caused by rapid rates of sea-level rise (Anderson et al., 2010). However, other flooding surfaces formed at different times in different bays, which indicates that they resulted from periods of decreased sediment supply or from variations in the rate of bay flooding regulated by the antecedent topography of the valleys (Rodriguez et al., 2005; Simms and Rodriguez, 2014).

The offshore bayhead deltas mapped by Thomas (1990) and Thomas and Anderson (1994) are significantly larger than the modern Trinity delta, yet they formed over similar time intervals. Direct age control of the offshore deltas is lacking, but the age of the youngest delta (Delta 3, Fig. 20) is well constrained (Fig. 21). This delta experienced its most rapid phase of growth between ~9.6 and 7.7 ka. This phase of growth occurred at the same time the Brazos and Colorado rivers constructed their most recent fluvial-dominated deltas on the inner shelf (Van Heijst et al., 2001; Abdulah et al., 2004). The much smaller modern Trinity delta formed over the past ~2,600 years (Fig. 21). The different growth rates imply either variations in the sediment supplied by the Trinity River or inherent changes in accommodation due to predictable morphological changes at flooded tributary junctions (e.g., Simms and Rodriguez, 2014).

Taha and Anderson (2008) examined the Brazos River incised valley in detail using over 400 water-well descriptions to map the valley and characterize its fill (Fig. 22). Radiocarbon ages from sediment cores were used to constrain rates of aggradation within the valley (Abbott, 2001; Taha and Anderson, 2008) (Figs. 23 and 24). The lower 60 km of the Brazos valley contains 28.6 km^3 of sediment, mostly fine-grained Holocene floodplain deposits with isolated channels (Fig. 22). The majority of the valley fill is younger than ~20 ka, and rates of aggradation 40-km inland increased after 12 ka and decreased after 6 ka as aggradation gradually shifted up valley (Figs. 23 and 24). Aggradation in the lower 40-km length of the onshore valley tracked sea-level rise closely (Taha and Anderson, 2008), but there were no times when the rate of rise exceeded sediment supply as indicated by the absence of marine flooding surfaces and estuarine sediments within the valley fill. Lowstand deposits occur only in the base of the valley (Fig. 24). The proportion of sandy channels relative to fine-grained floodplain silts and clays decreased through time in the upper part of the valley, a result of valley widening outpacing channel stacking even after aggradation rates decreased (Fig. 25).

We recently conducted a similar study to the Brazos investigation in the lower Colorado River incised valley using over 600 water-well descriptions. To date, only a single drill core has been used to measure the rate of aggradation within the valley, but it revealed a rate of valley aggradation nearly identical to the Brazos valley at approximately the same distance of 40 km from the coast (Fig. 24).

4.3.2. Transgressive Ravinement

Seismic profiles from the continental shelf show many examples of fluvial channels and deltas decapitated by the transgressive ravinement surface (e.g., Abdulah et al., 2004; Wellner et al., 2004) (Figs. 10 and 26). Sediment core transects that cross the modern shoreface and inner shelf revealed that preservation of barrier and shoreface deposits is minimal and that marine muds onlapped the decapitated shoreface at a depth of between -8 and -10 m, indicating that this is the depth of transgressive ravinement along the Texas coast (Siringan and Anderson, 1994; Rodriguez et al., 2004; Wallace et al., 2010). The depth of transgressive ravinement was generally below the depth of late Holocene river channels, so these channels were, for the most part, eroded.

4.4. Current Highstand

4.4.1. Coastal Evolution

The current highstand began ~4.0 ka, when the rate of sea-level rise slowed to ~0.4 to 0.6 mm/yr (Fig. 15-see references therein). It was around this time that most of the current strandplains, barrier islands, peninsulas and chenier plains began to form, although the actual timing of their formation varied by a few thousand years (Anderson et al., 2014) (Fig. 27). In fact, throughout the modern highstand these coastal features have had a highly variable response to sea-level rise, which reflected differences in rates of sediment supply and underlying relief of the Pleistocene surface on which coastal features were formed. Sand delivery from smaller rivers was shut off several thousand years earlier when their valleys were flooded to create bays. Only the Brazos, Colorado and Rio Grande rivers contributed sediment directly to the basin. In addition to these fluvial sources, considerable volumes of sand came from offshore (Anderson et al., 2014).

Using the -8 to -10 m depth for the transgressive ravinement surface, Weight et al. (2011) calculated sediment production rates for the area that includes the ancestral Brazos and Colorado deltas in 1000-year time slices. Total sediment production from ravinement of these sources was ~61.0 km^3 (Weight et al., 2011). Based on seismic facies, platform borings and sediment cores, a conservative sand estimate of the eroded material is 60%, yielding a total volume of ~36.6 km^3 of sand that was made available to the coastal system. We estimate a total sand volume of 13 ± 3 km^3 within the modern barrier island systems of the Texas coast, based on data from Bolivar Peninsula (Rodriguez et al., 2004), Galveston Island (Bernard et al., 1959; Rodriguez et al., 2004), Follets Island (Bernard et al., 1970; Morton, 1994; Wallace et al., 2010), Matagorda Peninsula (Wilkinson and McGowen, 1977), Matagorda Island (Wilkinson, 1975), San José Island (Anderson et al., 2014), Mustang Island (Simms et al., 2006a), North Padre Island (Fisk, 1959), and South Padre Island (Wallace and Anderson, 2010). More than 75% of this total volume exists within the Central Texas barrier islands (Matagorda Peninsula, Matagorda Island, San José Island, Mustang Island, and North Padre Island), primarily due to their older ages and converging longshore currents and associated deposition. Over time, longshore currents are removing sediment from east and south Texas barriers and depositing it along the central Texas coast. We estimate a total sand volume of ~22.5 ± 2.5 km^3 on the inner shelf based on the area of the northwestern Gulf of Mexico (50,000 km^2) shelf and total sand thicknesses, mostly storm beds, within late Holocene sediments (Hayes, 1967; Snedden et al., 1988; Wallace and Anderson, 2013). Thus, the sand budget of the Texas coast is balanced using offshore sources.

A detailed sediment budget analysis by Wallace et al. (2010) examined sand sources and sinks along the upper Texas coast. This study included washover, shoreface, and tidal delta fluxes, and determined an annual volumetric sand flux of 84,000 m^3/yr is being transported towards central Texas. The offshore sand flux due to hurricanes was estimated to be <5,000 m^3/yr (Wallace and Anderson, 2013), and therefore, this less likely influenced Holocene coastal evolution (Siringan and Anderson, 1994; Wallace et al., 2009). Detailed sand fluxes are not currently known for south and central Texas barrier systems. However, given the order of magnitude differences between thicknesses of east and south Texas barriers relative to central Texas barriers (Anderson et al., 2014) it is clear that longshore currents have exerted the first-order control on sand erosion and deposition over millennial timescales.

4.4.2. Estuarine Sinks

Thomas and Anderson (1994) demonstrated that bay evolution within the Trinity River incised valley (ancestral Galveston Bay) was characterized by episodes of tidal-inlet and tidal delta development within the offshore valley and argued that these tidal deposits recorded times when barrier islands and peninsulas existed, even though these barriers were not always preserved on the adjacent continental shelf due to transgressive ravinement. Periods of shoreline stability were interrupted by landward shifts in bayhead delta, bay and tidal deltas that were tens of kilometers in distance (Figs. 20 and 21). With each landward step, a new phase of bay and barrier evolution began. As the bay was filled with sediment it evolved from a deep, narrow bay to a broad, shallow bay (Fig. 28), which implies significant changes in bay circulation through time. The long, narrow, open-mouthed bay may have experienced stronger, resonating tidal circulation, similar to modern Chesapeake Bay (Zhong et al., 2008). This period of greater tidal influence was recorded by a large amount of tidal inlet/delta strata that occurred in the lower portion of the bay (Fig. 21). Modern Galveston Bay is a broad and shallow bay with a narrow tidal inlet and tidal delta that is significantly smaller than its predecessors (Figs. 20, 21 and 28). It is characterized by complex tidal circulation with wind-generated currents and waves playing a strong role in sediment re-suspension and dispersal. With barrier island and chenier development during the late Holocene, the sediment-trapping capacity of the bay has increased through time, resulting in increased accumulation of bay mud and a new phase of bayhead delta progradation during the last several millennia (Fig. 21). Detailed studies of Calcasieu Lake (Milliken et al., 2008a), Sabine Lake (Milliken et al., 2008b), Matagorda Bay (Maddox et al., 2008), Corpus Christi Bay (Simms et al., 2008), Copano Bay (Troiani et al., 2011), and Baffin Bay (Simms et al., 2010) revealed similar styles of bay evolution.

4.4.3. Texas Mud Blanket

The dominant highstand feature on the continental shelf is the Texas Mud Blanket (TMB), which is up to 50-m thick and covers the entire central Texas shelf (Fig. 29). Weight et al. (2011) conducted a detailed study of the mud blanket using a relatively dense grid (~3000 km) of high-resolution seismic data and several long cores that penetrated the deposit. They acquired a robust radiocarbon stratigraphy to examine the evolution of the mud blanket, including volume and flux calculations and XRD analyses aimed at identifying the source of the deposit. The results showed that the TMB accumulated mainly during the late Holocene and that rates of accumulation were inversely correlated with rates of sea-level rise (Fig. 30). One exception, an early episode of growth, began ~ 9 ka, with the accumulation of 41 km^3 of sediment between ~9.0 ka and ~8 ka. This sediment was derived mainly through transgressive ravinement of shelf strata and coincided with a period of growth of the Brazos, Colorado and Rio Grande deltas. However, it was not until ~3.5 ka that the most rapid phase of TMB deposition occurred, with a total of 172 km^3 of accumulation during this period (Fig. 30). Mineralogical results indicated that the sediment came mainly from the Colorado, Brazos and Mississippi rivers. This was a marked increase in sediment delivery from these rivers.

By the late Holocene, the Brazos and Colorado rivers had filled their lower valleys with sediment, thus eliminating onshore accommodation and increasing sediment delivery to the Gulf. Weight et al. (2011) argued that the dramatic increase in sediment delivery from the Mississippi River to the TMB at this time was best explained by an increase in southeasterly winds, which drove westward-flowing marine currents in the northwestern Gulf.

5. Discussion

5.1. Subsidence and Accommodation

The creation of accommodation by subsidence is essential for preservation of sedimentary deposits, especially during the late Quaternary when the frequency of sea-level rise and fall was rapid. Subsidence rates on the Louisiana coastal plain and inner shelf are relatively high (mm's/yr), which has allowed preservation of relatively thick falling-stage (MIS 5) fluvial and deltaic deposits (Berryhill, 1987; Coleman and Roberts, 1988 a,b; Wellner et al., 2004) (Fig. 8). In Texas, subsidence rates on the coastal plain and inner shelf are a fraction of a mm/yr (Paine, 1993; Simms et al., 2013) and relief on the lowstand surface of erosion (MIS 2 sequence boundary, Fig. 11) indicates significant fluvial erosion of falling-stage deposits. In addition, transgressive ravinement occurs to depths of -8 to -10 meters

(Siringan and Anderson, 1994; Rodriguez et al., 2001; Wallace et al., 2010) and has further eroded late Quaternary strata on the continental shelf.

During MIS 5 through MIS 2, sea level fell and rose repeatedly, with magnitudes of fall that were in the range of 30 to 50 m and rises of a few tens of meters (Fig. 2). Thus, portions of the continental shelf experienced multiple episodes of subaerial fluvial erosion and transgressive ravinement. The result was minimal preservation of late Quaternary sediments on the inner shelf and recycling of eroded sediments to the outer shelf where subsidence was as much as two orders of magnitude higher than on the inner shelf (Anderson et al., 2004). Through time, this resulted in removal of highstand and early falling-stage deposits on the inner shelf and higher sediment-flux rates to the outer shelf. Repeated recycling of sediments on the inner shelf resulted in enrichment of sand on the outer shelf.

The importance of subsidence and accommodation on erosion and recycling of sediments from a slowly-subsiding inner continental shelf to a faster-subsiding outer shelf is also illustrated using the west Florida continental shelf, where subsidence is minimal. There, late Quaternary deposits are quite thin on the inner shelf. Falling-stage and lowstand deposits exist only on the outer continental shelf and upper slope in the form of sand-dominated shelf-margin deltas. The feeder channels of these deltas have been completely eroded (Bart and Anderson, 2004; McKeown et al., 2004). Reworking of these deltas during transgression has resulted in a transgressive sheet sand that extends from west Florida to Mississippi, the MAFLA Sheet Sand (McBride et al., 2004).

5.2. Fluvial Incision and Valley Shape

Using flume experiments, Strong and Paola (2008) examined valley shape as a function of rate of base-level change and other factors. They describe continuous down-cutting during base-level fall and valley widening that ultimately results in a diachronous erosion surface.

We observe different valley morphologies for different rivers that formed during the same relative fall in sea level (Figs 11, 12). This is attributed to variable relief and the fact that different valleys were occupied at different times during the overall fall. The Mississippi, western Louisiana, and Brazos rivers abandoned their falling stage channel belts and deltas and cut lowstand valleys during MIS 2. Other rivers, such as the Trinity River, occupied the same valley throughout the falling stage and lowstand and are, therefore, true cross-shelf paleovalleys (Blum et al., 2013). Thus, different valley morphologies result from processes acting over different time scales, but each of the rivers we have studied has a lowstand valley that is part of a discernable, both in seismic data and cores, shelf-wide surface of erosion (Simms et al., 2007, Fig. 11).

5.3. Valley Aggradation and Purging

Blum and Törnqvist (2000) proposed two end-member source-to-sink models. Their “vacuum cleaner model” called for cannibalization and evacuation of sediment from the alluvial valley during sea-level fall. However, they questioned the concept of incision and complete bypass of sediments from alluvial valleys for larger fluvial systems. Their “conveyor belt model” called for more continuous sediment supply from the drainage basin. Blum and Womack (2009) argued that the Brazos and Colorado mixed bedrock-alluvial paleo-valleys behaved as conveyor belt systems with sediment storage and release governed mainly by climate oscillations. Blum et al. (2013) hypothesized that periods of incision are associated with sediment export minima, whereas periods of lateral migration and channel-belt construction result in increased sediment flux from rivers to basins. Blum and Womack (2009) further suggested that, although sediment flux is moderated by coastal-plain storage, sediment discharge to the ocean is less during glacial periods compared to interglacial periods, resulting in a net increase in sediment flux during warm intervals.

Our results demonstrate that the greatest sediment storage capacity for incised valleys occurs in the lower 50 to 100 kilometers of these valleys where they are wider, deeper and more susceptible to changes in sea level. Our data also demonstrate that the lower Brazos and Colorado valleys are filled mainly with Holocene fluvial sediments; lowstand deposits are confined to the deepest portions of these valleys (Figs. 23 and 24). We did not observe marine flooding surfaces in either valley, hence, aggradation within these valleys kept pace with, and was largely in sync with, sea-level rise (Taha and Anderson, 2008, Fig. 24). We also observe that aggradation rates decrease through time and up valley, despite the decreasing accommodation as deposition shifted up valley. This decrease in aggradation was associated with nearly an order-of-magnitude decrease in the rate of sea-level rise (from 5.0 mm/yr to 0.6 mm/yr, Fig. 24), which suggests that sediment bypass increased in the late Holocene. This is consistent with the observation that both the Brazos and Colorado rivers became important sources for the TMB during the late Holocene (Weight et al., 2011).

It is widely argued that a time lag exists between the onset of sea-level fall and upstream adjustment to that fall, resulting in out of phase erosional and depositional cycles at the coast (e.g., Van Heijst and Postma, 2001). Hence, aggradation can occur in the upper reaches of a river valley during sea-level fall and incision can occur during sea-level rise. Such was the case in the upper Colorado valley, where Blum and Valastro (1994) demonstrated a phase of floodplain aggradation ~20-14 ka, followed by incision after that time. The most rapid aggradation of the lower onshore Brazos and Colorado valleys occurred ~12-6 ka and was in step with a sea-level rise (Taha and Anderson, 2008; Fig. 24). Hence, erosion and aggradation in the upper and lower valleys of these rivers were out of phase.

We calculate ~28.6 km^3 of lowstand and transgressive sediments occupy the Brazos valley and estimate a similar volume for the Colorado valley, based on its similar size and stratigraphy. Thus, considerable erosion and creation of accommodation within the lower valley occurred during the falling stage and lowstand. Approximately 24.0 km^3 of the Brazos valley fill was deposited since ~8 ka, yielding a VAR of ~3.0 km^3/kyr for this time interval. The similar size and aggradation rates for the Colorado valley suggests a similar VAR.

Blum et al.'s (2013) argument that the long-term sediment yields of rivers are not significantly influenced by valley purging during sea-level fall is based on the assumption that periods of net export from the incised valley occurred only a few times over an ~60 ka period. However, given the rapid aggradation rates within the lower Brazos and Colorado valleys, we might assume that similar cycles of valley aggradation and purging occurred several times during the MIS 5 through 2 sea-level oscillations, assuming similar sediment yields of the rivers over this period. Episodes of sea-level rise (MIS 5d-c, MIS 5b-a, MIS 4-3) occurred over time intervals of 10 to 20 ka and the magnitudes of rise were 20 to 30 m (Fig. 2), or about the same as the sea-level rise associated with aggradation of the lower Brazos and Colorado valleys after ~ 12 ka. Based on our VAR estimates for the Brazos valley (~3.0

km^3/kyr) for this time interval, this was sufficient to have contributed significantly to the falling-stage MIS 5e-5b delta (VAR$\sim$1.10 km^3/kyr), the MIS 5a-4 delta (VAR$\sim$1.35 km^3/kyr), and the MIS 3 delta (VAR$\sim$3.5 km^3/kyr). In addition to valley storage and purging, there were also significant expansions of the Brazos and Colorado drainage areas due to merging of coastal plain streams and rivers into these rivers (Anderson et al., 2004; Blum and Womack, 2009; Blum et al., 2013) and recycling of sediments from the inner to the outer shelf. This scenario of increased sediment delivery to the basin during the falling stage explains the observed episodes of progradation that are interrupted by flooding and associated delta back-stepping that occurred during relatively brief periods of sea-level rise. It does not account for the volume of sediment that would have been eroded from the delta and lost from the system, and the relatively high sand content of the late falling-stage (MIS 3) deltas implies significant loss of fines.

The Brazos is currently a suspended-load-dominated river with an average 11:1 ratio of suspended load to bed load sediment (Paine and Morton, 1989). A total of 5 transgressive channels occupy the Brazos incised valley between the coast and 65-km inland (Fig. 22). Their ages are reasonably well constrained using the radiocarbon-based stratigraphy for the valley-fill succession. On average, the river avulsed about every 2,400 years and the suspended load to bed load ratio did not change significantly during the past $\sim$12 ka.

The style of aggradation for under-filled valleys (Calcasieu, Sabine, Trinity, Lavaca, Copano, Nueces and Baffin Bay valleys) was different from that of overfilled valleys. Only the deepest part of under-filled valleys contain lowstand and early transgressive fluvial sediments; the majority of their valley fill consists of bayhead delta, bay and tidal delta deposits that are younger than $\sim$ 10 ka (Simms et al., 2006b; Milliken et al., 2008a, b, Anderson et al., 2008; Maddox et al., 2008; Simms et al., 2008, 2010; Troiani et al., 2011) (Fig. 21), indicating that they too were purged of older sediments during the falling stage and lowstand. The lower 50 km of the onshore Trinity incised valley contains ~12.0 km^3 of sediment. Of this, ~3.0 km^3 is fluvial sediment and the remaining ~9.0 km^3 is mostly fine-grained bayhead delta and bay deposits that are younger than ~10 ka, yielding a Holocene VAR of about 0.9 km^3/kyr, or about one third the VAR for the Brazos River. Today the Brazos River sediment discharge is approximately twice that of the combined Trinity and San Jacinto Rivers (Table 1).

5.4. Climate-Induced Changes in the Sediment Discharge of Rivers

Results from numerical modeling studies by Perlmutter et al. (1998) suggest that changes in the delivery of sediment from the hinterland are most pronounced during transitions between wet and dry climatic conditions. Hidy et al. (2014) used cosmogenic ^{10}Be to determine Texas river catchment denudation rates, largely from glacial or interglacial interval terrace deposits over the past half million years. Their results indicate that these rates are 30–35% higher during interglacial periods relative to glacial periods, and are connected broadly with temperature. Given these findings, what can be deduced from the sedimentary record?

Paleoclimate records for Texas (Toomey et al., 1993; Humphrey and Ferring, 1994; Nordt et al., 1994, 2002; Wilkins and Currey, 1999; Russ et al., 2000; Buzas-Stephens et al., 2014) indicated millennial-scale oscillations in temperature and precipitation (Fig. 6). So, climate-controlled variations in sediment supply likely occurred at a faster pace than the 120 ka glacial/interglacial cycles. Indeed, along the northwestern Gulf Coast climatic changes, especially precipitation, were not always in sync with global climate change and, as is the case today, indicate variable patterns across Texas. Further complicating the relationship between climate and sediment yields of rivers is the fact that the larger rivers, including the Brazos, Colorado and Rio Grande rivers, span more than one climate zone.

Our study has revealed Brazos, Colorado and Rio Grande deltas resting above the MIS 2 sequence boundary, indicating that these deltas formed during the MIS 1 sea-level rise. Limited radiocarbon age control and the locations and water depths of these deltas indicate formation between ~11.5 and ~8.0 ka. Of these three, the Colorado delta was mapped in the greatest detail (Snow, 1998) and yielded a total volume of 10.8 km^3 (Van Heijst et al., 2001). During this time interval, the VAR = 3.09 km^3/kyr (MAR of 4.91 10^6 t/yr), which is almost twice the estimated current flux of 2.8 10^6 t/yr (Table 1). This does not account for loss of fine-grained sediments, transgressive ravinement of the delta or for the sediments that were accumulating in the lower portion of the onshore valley during this time interval. This episode of high sediment discharge and delta growth occurred when the average rate of sea-level rise was 4.2 mm/yr (Fig. 15) and culminated when the climate in Texas was in transition from a prolonged cool-wet interval to warm-dry conditions associated with the Climatic Optimum (Fig. 6). Following this time, aggradation shifted onshore to the Brazos and Colorado valleys, and presumably the Rio Grande valley, and offshore delta growth has been restricted to wave-dominated deltas that have been mostly eroded by transgressive ravinement (Abdulah et al., 2004; Banfield and Anderson, 2004).

Evidence for climate-induced changes in the sediment supply during the Holocene comes also from the Calcasieu, Sabine-Neches, Trinity, Lavaca, and Nueces incised-valley fill successions. Extensive and thick bayhead delta deposits within these valleys record episodes of significant growth during the early Holocene (Anderson et al., 2008; Milliken et al., 2008a,b; Maddox et al., 2008; Simms et al., 2008), as illustrated using the Trinity incised valley (Fig. 21). After ~7.5 ka, bayhead deltas decreased in size and sedimentation within the bays and became dominated by estuarine processes. By the late Holocene, sedimentation within Baffin Bay shifted from that of dominant fluvial influence to the current unique suite of more arid depositional environments (Simms et al., 2010), striking evidence for the shift from cool-wet conditions of the early Holocene to warm-dry conditions of the mid-late Holocene in south Texas (Fig. 6).

In summary, our results indicate that the export of sediments from the hinterland to the continental shelf (e.g., Romans et al., This Volume) was not directly in step with global temperature change, but rather varied in response to higher frequency climate oscillations between warm-dry and cool-wet conditions.

5.5. Lowstand Fan Deposition

During the MIS 2 lowstand, the B-T, Colorado and Rio Grande Rivers all supplied slope fans with sediment. What these slope fans hold in common is that they all exist down slope of shelf-margin deltas that remained relatively fixed in their locations during the culminating MIS 2 drop in sea level. The exception to this was the Western Louisiana delta, which was abandoned by its fluvial feeders prior to the MIS 2 fall, although this shelf-margin delta may have been a source of sediment for the B-T fan. Of these three slope fan systems, only the B-T system has been studied in detail and it is the only system in which the timing of fan evolution is constrained (Prather, 2012; Pirmez et al., 2012).

Satterfield and Behrens (1990) and Winker (1996) proposed a "fill and spill" model whereby four minibasins on the upper slope and down-dip of the B-T valley were filled in successive fashion. Pirmez et al. (2012) concluded that, of the ~62 km^3 of sediment that accumulated in all four minibasin since ~115 ka, ~49 km^3 accumulated since ~24.3 ka and that 83% of that sediment accumulated in Basin I, the upper-most basin. Their results showed a dramatic (40-fold) increase in flux after ~24 ka.

Pirmez et al. (2012) recognized four components of the sediment budget in their source-to-sink analysis of the B-T system: (1) sediment delivered directly from the river drainage basins; (2) sediments generated locally by erosion in various parts of the system; (3) sediment accumulated on the shelf and in outer-shelf deltas; and (4) deep water contributed material. Using a simple triangle wedge of uniform (120 m) thickness spread along the entire extent of the lowstand delta and an average sediment porosity of 40%, they estimated a volume of 45 km^3. They further estimated that 20-25 km^3 of sediment was delivered to the fan complex between 24.3 and 15.3 ka, which is about a quarter of the total sediment discharge (based on modern sediment discharge rates) for the combined Trinity, Sabine and Brazos rivers (~11 km^3/ka), during this time interval. Thus, of the four perceived sources of sediment to the B-T lowstand delta and slope fan complex, a large portion was accounted for by direct sediment supply from rivers.

Pirmez et al. (2012) concluded that sediment flux to the B-T fan did not vary in response to higher frequency oscillations of sea level during MIS 4 or at the end of MIS 3 and that sediment supply continued even after sea-level rise began at the end of MIS 2. This was consistent with continued growth of the B-T delta at this time (Wellner et al., 2004).

5.6. Transgressive and Highstand Processes

At the end of MIS 2, sea level rose rapidly, forcing the shoreline to migrate landward at rates of a few tens of meters per year. During this time, falling-stage deltas were decapitated by transgressive ravinement, providing the main source of sand for the evolving coastal system (Anderson et al., 2014) and a source of silt and clay in the initial growth of the Texas Mud Blanket (Weight et al., 2011). On the inner shelf and inland, incised valleys were filled with sediment. Aggradation within these valleys was dominated by sea-level rise and, for the most part, was complete by the late Holocene.

The overall stratigraphic signature of the transgression was one of landward stepping coastal deposits and incised-valley fill deposits. This back-stepping stratigraphic character resulted, in part, from the episodic nature of sea-level rise, which was punctuated by episodes of rapid rise that varied by many meters in a century, in the case of Meltwater Pulse 1A (Fairbanks, 1989), to small amplitude (sub-meter) events, such as the well documented 8.2 ka sea-level event (Törnqvist et al., 2004a; Rodriguez et al., 2010). This episodic nature of sea-level rise is considered to be characteristic of glacial eustasy because of the multiple variables that control ice-sheet retreat (Anderson et al., 2013). Hence, this punctuated style of coastal evolution on low gradient continental shelves should be typical of "ice house" conditions.

Approximately 4,000 years ago, the rate of sea-level rise in the northern Gulf of Mexico decreased from an average rate of 1.4 mm/yr to an average rate between 0.4 mm/yr to 0.6 mm/yr (Fig. 15). This was when most of the coastal barriers of Texas began to form, although the timing of their formation varied along the coast (Fig. 27). Formation of barriers resulted in greater trapping capacity of bays, so the delivery of sediment from smaller rivers to the Gulf of Mexico was minimal during the current highstand.

The TMB was the dominant depositional feature of the western Gulf during the late Holocene (Fig. 29). It filled a large embayment in the central Texas shelf between the falling-stage Colorado and Rio Grande deltas, had a total volume of 172 km^3, and formed mainly after 3.5 ka, indicating an average VAR of ~49 km^3/kyr (81 x 10^6 t/yr) (Fig. 30). This was, by far, the highest VAR at any time during the last glacial-eustatic cycle for any depositional system in the study area. Clay mineralogical analyses of the TMB showed that most of this sediment came from the Mississippi River and the remaining portion came from the combined Brazos and Colorado rivers (Weight et al., 2011).

Weight et al. (2011) argued that by ~ 4 ka, accommodation within the lower Brazos and Colorado incised valleys had been filled, resulting in greater sediment throughput and delivery to the TMB. Our VAR estimate derived from aggradation rates for the lower Brazos valley for the period between 8 ka to Present is 3.0 km^3/kyr. Given the similar aggradation histories for the lower Brazos and Colorado valleys, we assume a similar VAR for the Colorado River during this time interval. Thus, the combined Brazos and Colorado rivers likely contributed less than 10% of the total volume of sediment composing the TMB.

Weight et al. (2011) point out that the flux to the TMB is only about 20% of the current Mississippi River sediment discharge. Thus, it is believed that the Mississippi River, which is approximately 1,000 kilometers to the east, was the main contributor of sediment to the TMB. There are other places across the planet where sediment is transported great distances from its source (e.g., Wright and Nittrouer, 1995; Allison et al., 2000; Liu et al., 2009; Ridente et al., 2009; Walsh and Nittrouer, 2009), but the TMB is one of the best documented in terms of its distribution, thickness and chronostratigraphic constraints on deposition.

5.7. The Anthropocene and Future Directions

It is beyond the scope of this paper to describe and discuss the human impact on the natural source-to-sink system. However, there is little question that humans have assumed a major role in sediment delivery, distribution and deposition in modern time. This is manifest as modern sediment yields of some rivers that are disproportionate with drainage-basin size and precipitation, undernourished deltas and coasts and, in the case of the modern Brazos delta, complete alteration of the delta location (see Anderson et al., 2014 for recent review). This paper provides a framework (Fig. 31) for future work aimed at quantifying natural and anthropogenic influences on sedimentation and will hopefully provide a natural laboratory for refining quantitative source-to-sink models aimed at linking sedimentary processes to the stratigraphic record.

6. Conclusions

1. This study demonstrates that source-to-sink analysis in low gradient basin settings requires a long-term perspective because most of the sediment delivered to the basin by rivers undergoes more than one cycle of sedimentation (Fig. 31). Sediment supply to depocenters was dominated by episodic sea-level change during the falling stage

(MIS 5-3), and during the transgression (MIS 1) by episodic sea-level rise and climate-controlled variations in sediment supply.

2. During the falling stage, high-frequency oscillations in sea level (tens of meters over millennial time scales), coupled with low rates of subsidence on the inner shelf, resulted in erosion and recycling of sediments from the inner shelf and an overall increase in sediment delivery to the outer shelf where subsidence is much faster (Fig. 31).
3. Filling and purging of incised valleys and expansion of source areas via merging of coastal plain rivers and streams contributed to the increased sediment delivery to deltas during the overall sea-level fall. Recycling led to winnowing of fines and enrichment of sand that accumulated in delta mouth bars, lowstand deltas, and slope fans.
4. Climate influence on sediment supply to individual depocenters was spatially and temporally variable. As a result, we observe no simple relationship between temperature and the delivery of sediment to the basin. However, changes in precipitation likely contributed to observed changes in sediment supply at millennial time scales and contributed to this variability.
5. Slope fans of the northwestern Gulf basin experienced unique evolution due to different influences and connectivity to falling-stage and lowstand deltas that were important sources of sediment to these fans.
6. The lower reaches of the incised valleys of the study area, regardless of discharge and size, were deeply eroded during the MIS 2 lowstand and aggradation of these valleys occurred mainly during the MIS 1 transgression. The Brazos, Colorado and Rio

Grande rivers filled their valleys with fluvial sediments while smaller rivers filled their valleys with fluvial, bayhead delta, bay, and tidal-delta deposits.

7. During the MIS 1 transgression, falling-stage deltas were reworked by transgressive ravinement, providing the principle sand source for modern coastal environments.
8. Episodic sea-level rise during the MIS 1 transgression (~17 ka to ~4.0 ka) profoundly influenced coastal evolution, as manifested by landward stepping shorelines and bay environments on the order of tens of kilometers within a few thousand years.
9. During the current Holocene highstand (~4.0 ka-Present), silts and clays delivered to the northwestern Gulf by the Mississippi, Brazos and Colorado rivers accumulated in a thick and extensive mud blanket on the central Texas shelf, the Texas Mud Blanket. This remarkable increase in the delivery of fine-grained sediments to the shelf is attributed mainly to an increase in westward-directed winds and surface currents that delivered suspended sediments from the Mississippi River to the Texas shelf.

Acknowledgements

The authors wish to thank the National Science Foundation, the Gulf of Mexico Quaternary Seismic Stratigraphy Consortium, and the David Worthington Fund for financial support. We also wish to thank the many graduate students who contributed to this research (Ken Abdulah, Niranjan Aryal, Laura Banfield, Louis Bartek, Philip Bart, Brenda Eckles, Michelle Fassell, Rodrigo Fernández, Carmen Fraticelli, Mike Hamilton, Heather McKeown, Kristy Milliken, Jessica Maddox, Sabrina Sarzalejo, Lauren Simkins, Fernando Siringan, Jennifer Snow, Mark Thomas, Taylor Troiani, Max Van Heijst, and Julia Wellner) and numerous colleagues, too many to name, who provided valuable feedback and discussion over the past three decades. We would also like to thank the editor J.P. Walsh, and two anonymous reviewers whose insightful comments significantly improved this paper.

References

Abbott, J.T., 2001. Houston Area Geoarcheology: A framework for archeological investigation, interpretation, and cultural resource management in the Houston highway district. Archeological Studies Program Report 27, Texas Department of Transportation, Environmental Affairs Division, Austin, 235 p.

Abdulah, K.C, Anderson, J.B., Snow, J.N., Holdford-Jack, L., 2004. The late Quaternary Brazos and Colorado Deltas, Offshore Texas, U.S.A. – Their evolution and the factors that controlled their deposition, in: Anderson, J.B., Fillon, R. H. (Eds.), Late Quaternary stratigraphic evolution of the northern Gulf of Mexico margin. Society for Sedimentary Geology, Special Publication 79, 237-270.

Allison, M.A., Kineke, G.C., Gordon, E.S., and Goñi, M.A., 2000. Development and reworking of a seasonal flood deposit on the inner continental shelf off the Atchafalaya River. Continental Shelf Research 20, 2267–2294.

Anderson, J.B., 2005. Diachronous development of Late Quaternary shelf-margin deltas in the northwestern Gulf of Mexico: implications for sequence stratigraphy and deep-water reservoir occurrence, in: Giosan, L., Bhattacharya, J.P. (Eds.), River Deltas- Concepts, models, and examples. Society for Sedimentary Geology, Special Publication 83, 257–276.

Anderson, J.B., and Rodriguez, A.B. (Eds.), 2008. Response of upper gulf coast estuaries to Holocene climate change and sea-level rise. Geological Society of America, Special Paper 443, 146 p.

Anderson, J.B., Abdulah, K., Sarzalejo, S., Siringan, F., Thomas, M.A., 1996. Late Quaternary sedimentation and high-resolution sequence stratigraphy of the east Texas shelf. Geological Society, Special Publication 117, 95-124.

Anderson, J.B., Kirshner, A.E., Simms, A.R., 2013. Constraints on Antarctic Ice Sheet configuration during and following the last glacial maximum and its episodic contribution to sea-level rise. Geological Society of London, Special Publication 381, 215-232. http://dx.doi.org/10.1144/SP381.13.

Anderson, J., Milliken, K., Wallace, D., Rodriguez, A., Simms, A., 2010. Coastal impact underestimated from rapid sea level rise. EOS Transactions of the American Geophysical Union, 91, 205–206.

Anderson, J.B., Rodriguez, A., Abdulah, K.C., Fillon, R.H., Banfield, L.A., McKeown, H.A., Wellner, J.S., 2004. Late Quaternary stratigraphic evolution of the northern Gulf of Mexico: A synthesis, in: Anderson, J.B., Fillon, R. H. (Eds.), Late Quaternary stratigraphic evolution of the northern Gulf of Mexico margin. Society for Sedimentary Geology, Special Publication 79, 1-23.

Anderson, J.B., Rodriguez, A.B., Milliken, K.T., Taviani, M., 2008. The Holocene evolution of the Galveston Bay complex, Texas: Evidence for rapid change in estuarine environments, in: Anderson, J.B. Rodriguez, A.B. (Eds.), Response of upper Gulf Coast estuaries to Holocene Climate Change and Sea-Level Rise. Geological Society of America, Special Paper 443, 89-104.

Anderson, J.B., Wallace, D.J., Simms, A.R., Rodriguez, A.B., Milliken, K.T., 2014. Variable response of coastal environments of the northwestern Gulf of Mexico to sea-level rise and climate change: Implications for future change. Marine Geology 352, 348-366.

Anderson, J., Wellner, J., Abdulah, K., Sarzalejo, S., 2003. Late Quaternary shelf-margin delta and slope-fan complexes of the east Texas-western Louisiana margin: Variable response to eustasy and sediment supply, in: Shelf margin deltas and linked down slope petroleum systems. Global significance and future exploration potential, 23rd Annual GCSSEPM Foundation Bob F. Perkins Research Conference, 1-12.

Aslan, A., Blum, M.D., 1999. Contrasting styles of Holocene avulsion, Texas Gulf Coastal Plain, USA, in: Smith, N.D., Rogers, J. (Eds.), Fluvial Sedimentology VI. Blackwell Publishing Ltd., Oxford, UK, doi: 10.1002/9781444304213.ch15.

Badalini, G., Kneller, B., Winker, C.D., 2000. Architecture and processes in the late Pleistocene Brazos–Trinity turbidite system, Gulf of Mexico continental slope. Deep-Water Reservoirs of the World. Proc. GCSSEPM 20th Annu. Res. Conf., 16–34.

Banfield, L.A., Anderson, J.B., 2004. The Late Quaternary evolution of the Rio Grande Delta: Complex response to eustasy and climate change, in: Anderson, J.B., Fillon, R. H. (Eds.), Late Quaternary stratigraphic evolution of the northern Gulf of Mexico margin. Society for Sedimentary Geology, Special Publication 79, 289-306.

Bard, E., Hamelin, B., Fairbanks, R.G., 1990. U-Th ages obtained by mass spectrometry in corals from Barbados: sea level during the past 130, 000 years. Nature 346, 456-458.

Bart, P.J., Anderson, J.B., 2004. Late Quaternary stratigraphic evolution of the Alabama and west Florida outer continental shelf, in: Anderson, J.B., Fillon, R. H. (Eds.), Late

Quaternary stratigraphic evolution of the northern Gulf of Mexico margin. Society for Sedimentary Geology, Special Publication 79, 43-53.

Beaubouef, R.T., Friedmann, S.J., 2000. High resolution seismic/sequence stratigraphic framework for the evolution of Pleistocene intra slope basins, Western Gulf of Mexico: Depositional models and reservoir analogs, in: Weimer, P., Slatt, R.M., Bouma, A.H., Lawrence, D.T. (Eds.), Gulf Coast Section, SEPM, 20th Annual Research Conference, Deep-Water Reservoirs of the World, Houston, TX, 40 - 60.

Bentley et al., This Volume

Bernard, H.A., Major, C.F., Jr., Parrott, B.S., 1959. The Galveston barrier island and environments: A model for predicting reservoir occurrence and trend. Transactions-Gulf Coast Association of Geological Societies 9, 221-224.

Bernard, H.A., Major, C.F., Jr., Parrott, B.S., LeBlanc, R.J., 1970. Recent sediments of southeast Texas: A field guide to the Brazos alluvial and deltaic plains and the Galveston barrier island complex. University of Texas, Bureau of Economic Geology Guidebook 11, Austin, TX, 132 p.

Berryhill, H.L., 1987. The continental shelf off south Texas, in: Berryhill, H.L. (Ed.), Late Quaternary facies and structure, northern Gulf of Mexico: Interpretations from seismic data. American Association of Petroleum Geologists, Studies in Geology 23, 11-79.

Bhattacharya et al., This Volume

Blum, M.D., Valastro, S. Jr., 1994. Late Quaternary sedimentation, lower Colorado River, Gulf coastal plain of Texas. Geological Society of America Bulletin 106, 1002–1016.

Blum, M.D., Hattier-Womack, J., 2009. Climate change, sea-level change, and fluvial sediment supply to deepwater depositional systems, in: Kneller, B., Martinsen, O.J., and McCaffrey,

B. (Eds.), External controls on deep-water depositional systems. Society for Sedimentary Geology, Special Publication 92, 15-39.

Blum, M., Martin, J., Milliken, K., Garvin, M., 2013. Paleovalley systems: Insights from Quaternary analogs and experiments. Earth Science Reviews 116, 128-169.

Blum, M.D., Morton, R.A., Durbin, J.M., 1995. "Deweyville" terraces and deposits of the Texas Gulf coastal plain. Transactions- Gulf Coast Association of Geological Societies 45, 53-60.

Blum, M.D., and Törnqvist T.E., 2000. Fluvial responses to climate and sea-level change: A review and look forward. Sedimentology 47, 2-48.

Buzas-Stephens, P., Livsey, D.N., Simms, A.R., Buzas, M.A., 2014. Estuarine foraminifera record Holocene stratigraphic changes and Holocene climate changes in ENSO and the North American monsoon: Baffin Bay, Texas. Palaeogeography, Palaeoclimatology, Palaeoecology 404, 44-56.

Carlin, J.A., Dellapenna, T.M., 2014. Event-driven sedimentation on a low-gradient, low-energy shelf: The Brazos River subaqueous delta, northwestern Gulf of Mexico. Marine Geology 353, 21-30.

Chappell, J., Omura, A., Esat, T, McCulloch, M., Pandilfi, J., Ota, Y., Pillans, B., 1996. Reconciliation of late Quaternary sea levels derived from coral terraces at Huon Peninsula with deep sea oxygen isotope records. Earth and Planetary Science Letters 141, 227–236.

Cochrane, J.D., Kelly, F.J., 1986. Low-frequency circulation on the Texas-Louisiana continental shelf. Journal of Geophysical Research 91, 10645–10659. doi:10.1029/JC091iC09p10645.

Coleman, J.M., Roberts, H.H, 1988a. Sedimentary development of the Louisiana continental shelf related to sea level cycles: Part I- sedimentary sequences. Geo-Marine Letters 8, 63–108.

Coleman, J.M., Roberts, H.H, 1988b. Sedimentary development of the Louisiana continental shelf related to sea level cycles: Part II- seismic response. Geo-Marine letters 8, 109–119.

Curray, J.R., 1960. Sediments and history of Holocene transgression, continental shelf, northwestern Gulf of Mexico, in: Shepard, F.P., Phleger, F.B., van Andel, T.H. (Eds.), Recent Sediments, Northwestern Gulf of Mexico. American Association of Petroleum Geologists, 221–266.

Driscoll, N.W., Karner, G.D., 1999. Three-dimensional quantitative modeling of clinoform development. Marine Geology 154, 383–398.

Dutton, A., Lambeck, K., 2012. Ice volume and sea level during the last interglacial. Science 337, 216-219.

Eckles, B.J., Fassell M.L., Anderson, J.B., 2004. Late Quaternary evolution of the wave-storm-dominated Central Texas Shelf, in: Anderson, J.B., Fillon, R. H. (Eds.), Late Quaternary stratigraphic evolution of the northern Gulf of Mexico margin. Society for Sedimentary Geology, Special Publication 79, 271-288.

Fairbanks, R.G., 1989. A 17,000-year glacio-eustatic sea level record: influence of glacial melting rates on the Younger Dryas event and deep-ocean circulation. Nature 342, 637-642.

Fisk, H.N., 1944. Geological investigation of the alluvial valley of the lower Mississippi River. Vicksburg, Mississippi, U.S. Army Corps of Engineers, Mississippi River Commission, 78 p.

Fisk, H.N., 1959. Padre Island and the Laguna Madre flats, coastal south Texas. Proceedings of the 2nd Coastal Geography Conference, Louisiana State University, Baton Rouge, 103-151.

Fraticelli, C.M., 2006. Climate forcing in a wave-dominated delta: The effects of drought-flood cycles on delta progradation. Journal of Sedimentary Research 76, 1067–1076.

Fraticelli, C., Anderson, J., 2003. The impact of the Brazos deltaic system on upper slope stratigraphic sequence evolution, in: Shelf margin deltas and linked down slope petroleum systems. Global significance and future exploration potential, 23rd Annual GCSSEPM Foundation Bob F. Perkins Research Conference, 281-313.

Greene, D.L., Jr. Rodriguez, A.B., Anderson, J.B., 2007. Seaward-branching coastal-plain and piedmont incised-valley systems through multiple sea-level cycles: Late Quaternary examples from Mobile Bay and Mississippi Sound, U.S.A. Journal of Sedimentary Research 77, 139-158.

Hamilton, P. and Lugo-Fernandez, A., 2001. Observations of high speed deep currents in the northern Gulf of Mexico. Geophysical Research Letters 28. doi: 10.1029/2001GL013039.

Hayes, M.O., 1967. Hurricanes as geological agents, south Texas coast. American Association of Petroleum Geologists Bulletin 51, 937–942.

Hernández-Molina, F.J., Somoza, L., Lobo, F., 2000. Seismic stratigraphy of the Gulf of Cádiz continental shelf: A model for Late Quaternary very high-resolution sequence stratigraphy and response to sea-level fall. Geological Society of London, Special Publication 172, 329-362.

Hidy, A.J., Gosse, J.C., Blum, B.D., Gibling, M.R., 2014. Glacial-interglacial variation in denudation rates from interior Texas, USA, established with cosmogenic nuclides. Earth and Planetary Science Letters 390, 209-221.

Humphrey, J.D., Ferring, C.R., 1994. Stable isotopic evidence for latest Pleistocene and Holocene climatic change in north-central Texas. Quaternary Research 41, 200-213.

Jarosz, E., Murray, S. P., 2005. Velocity and transport characteristics of the Louisiana-Texas Coastal Current, in: Sturges, W., Lugo-Fernandez, A. (Eds.), Circulation in the Gulf of Mexico: Observations and Models. American Geophysical Union, Washington, D. C. doi: 10.1029/161GM11.

Kopp, R.E., Simons, F.J., Mitrovica, J.X., Maloof, A.C., Oppenheimer, M., 2009. Probabilistic assessment of sea level during the last interglacial stage. Nature 462, 863-867.

Kopp, R.E., Simons, F.J., Mitrovica, J.X., Maloof, A.C., Oppenheimer, M., 2013. A Probabilistic assessment of sea level variations within the last interglacial stage. Geophysical Journal International, 193, 711-716.

Labaune, C., Tesson, M., Gensous, B., 2005. Integration of high and very high-resolution seismic reflection profiles to study Upper Quaternary deposits of a coastal area in the western Gulf of Lions, SW France. Marine Geophysical Researches 26, 109-122.

Labeyrie, L.D., Duplessy, J.C., Blanc, P.L., 1987. Variations in mode of formation and temperature of oceanic deep waters over the past 125,000 years. Nature 327, 477–482.

Lehner, P., 1969. Salt tectonics and Pleistocene stratigraphy on continental slope of northern Gulf of Mexico. AAPG Bulletin 53, 2431-2479.

Liu, J.P., Xue, Z., Ross, K., Wang, H.J., Yang, Z.S., Li, A.C., Gao, S., 2009. Fate of sediments delivered to the sea by Asian large rivers: Long-distance transport and formation of remote alongshore clinothems. The Sedimentary Record 7, 4–9.

Livsey, D., Simms, A.R., 2013. Holocene sea-level change derived from microbial mats. Geology 41, 971-974.

Lobo, F.J., Tesson, M., Gensous, B., 2004. Stratal architectures of late Quaternary regressive-transgressive cycles in the Roussillon Shelf (SW Gulf of Lions, France). Marine and Petroleum Geology 21, 1181-1203.

Lohse, E.A., 1955. Dynamic geology of the modern coastal region, northwest Gulf of Mexico, in: Hough, J.L., Menard, H.W. (Eds.), Finding Ancient Shorelines. Society of Economic Paleontologists and Mineralogists Special Publication 3, 99–105.

Maddox, J., Anderson, J.B., Milliken, K.T., Rodriguez, A.B., Dellapenna, T.M., Giosan, L., 2008. The Holocene Evolution of the Matagorda and Lavaca estuary complex, Texas, USA, in: Anderson, J.B. Rodriguez, A.B. (Eds.), Response of upper Gulf Coast estuaries to Holocene Climate Change and Sea-Level Rise. Geological Society of America, Special Paper 443, 105-119.

Maselli, V., Trincardi, F., Asioli, A., Ceregato, A., Rizzetto, F., and Taviani, M., 2014. Delta growth and river valleys: The influence of climate and sea level changes on the South Adriatic shelf (Mediterranean Sea). Quaternary Science Reviews 99, 146-163.

McBride, R.A., Moslow, T.F, Roberts, H.H., Diecchio, R., 2004. Late Quaternary geology of the northeastern Gulf of Mexico shelf: Sedimentology, depositional history, and ancient analogs of a major shelf sand sheet of the modern transgressive systems tract, in: Anderson, J.B., Fillon, R. H. (Eds.), Late Quaternary stratigraphic evolution of the northern Gulf of Mexico margin. Society for Sedimentary Geology, Special Publication 79, 55-83.

McGowen, J.H., Garner, L.E., Wilkinson, B.H., 1977. The Gulf shorelines of Texas: Processes, characteristics, and factors in use. The University of Texas at Austin, Bureau of Economic Geology Geological Circular 77-3, 27 p.

McKeown, H.A., Bart, P.J., Anderson, J.B., 2004. High-Resolution stratigraphy of a sandy, ramp-type margin- Apalachicola, Florida, U.S.A., in: Anderson, J.B., Fillon, R. H. (Eds.), Late Quaternary stratigraphic evolution of the northern Gulf of Mexico margin. Society for Sedimentary Geology, Special Publication 79, 25-41.

Milliken, K.T., Anderson, J.B., Rodriguez, A.B., 2008a. Record of dramatic Holocene environmental changes linked to eustasy and climate change in Calcasieu Lake, Louisiana, USA, in: Anderson, J.B. Rodriguez, A.B. (Eds.), Response of upper Gulf Coast estuaries to Holocene Climate Change and Sea-Level Rise. Geological Society of America, Special Paper 443, 43-63.

Milliken, K.T., Anderson, J.B., Rodriguez, A.B., 2008b. Tracking the Holocene evolution of Sabine Lake through the interplay of eustasy, antecedent topography, and sediment supply variations, Texas and Louisiana, USA, in: Anderson, J.B. Rodriguez, A.B. (Eds.), Response of upper Gulf Coast estuaries to Holocene Climate Change and Sea-Level Rise. Geological Society of America, Special Paper 443, 65-88.

Milliken, K.T., Anderson, J.B., Rodriguez, A.B., 2008c. A new composite Holocene sea-level curve for the northern Gulf of Mexico, in: Anderson, J.B. Rodriguez, A.B. (Eds.), Response of upper Gulf Coast estuaries to Holocene Climate Change and Sea-Level Rise. Geological Society of America, Special Paper 443, 1-11.

Milliman, J.D., and Syvitski, J.P.M., 1992. Geomorphic/tectonic control of sediment discharge to the ocean: The importance of small mountainous rivers. The Journal of Geology 100, 525–544.

Morton, R.A., 1979. Temporal and spatial variations in shoreline changes and their implications, examples from the Texas Gulf Coast. Journal of Sedimentary Research 49, 1101–1111.

Morton, R.A., 1994. Texas barriers, in: Davis, R.A. (Ed.), Geology of Holocene Barrier Island Systems. Springer-Verlag, Berlin, 75–114.

Morton, R.A., Suter, J.R., 1996. Sequence stratigraphy and composition of Late Quaternary shelf margin deltas, northern Gulf of Mexico. AAPG Bulletin 80, 505-530.

Muhs, D. R., Simmons, K. R., Schumann, R. R., Halley, R. B., 2011. Sea-level history of the past two interglacial periods: New evidence from U-series dating of reef corals from south Florida. Quaternary Science Reviews 30, 570-590.

Nordt, L.C., Boutton, T.W., Hallmark, C.T., Waters, M.R., 1994. Late Quaternary vegetation and climate changes in central Texas based on the isotope composition of organic carbon. Quaternary Research 41, 109-120.

Nordt, L.C., Boutton, T.W., Jacob, J.S., Mandel, R.D., 2002. C_4 plant productivity and climate-CO_2 variations in south-central Texas during the Late Quaternary. Quaternary Research 58, 182-188.

Oey, L.-Y., 1995. Eddy-and wind-forced shelf circulation. Journal of Geophysical Research: Oceans 100, 8621-8637.

Olariu, C., Steel, R.J., 2009. Influence of point-source sediment-supply on modern shelf-slope morphology: implications for interpretation of ancient shelf margins. Basin Research 21, 484-501.

Otvos, E.G., Howat, W.E., 1996. South Texas Ingleside Barrier; Coastal sediment cycles and vertebrate fauna. Late Pleistocene stratigraphy revised. Transactions of the Gulf Coast Association of Geological Societies 46, 333-344.

Paine, J. G., 1993. Subsidence of the Texas coast: Inferences from historical and late Pleistocene sea levels. Tectonophysics 222, 445-458.

Paine, J.G., Morton, R.A., 1989. Shoreline and vegetation-line movement, Texas Gulf Coast, 1974 to 1982. The University of Texas at Austin, Bureau of Economic Geology, Geological Circular 89-1, 50 p.

Perlmutter, M.A., Radovich, B.J., Mattheus, M.D., Kendall, C.G., 1998. The impact of high-frequency sedimentation cycles on stratigraphic interpretation, in: Gradstein, F.M., Sandvik, K.O., and Milton, N.J. (Eds.), Sequence Stratigraphy—Concepts and Applications. Norwegian Petroleum Society, Special Publication 8, 141–170.

Pirmez, C., Prather, B.E., Mallarino, G., O'Hayer, W.W., Droxler, A.W. and Winker, C.D., 2012. Chronostratigraphy of the Brazos-Trinity depositional system, western Gulf of Mexico: Implications for deepwater models, in: Prather, B.E., Deptuck, M.E., Mohrig, D., Van Hoorn, B., Wynn, R.B. (Eds.), Application of the principles of seismic geomorphology to continental slope and base-of-slope systems: Case studies from seafloor and near-seafloor analogues. SEPM Special Publication 99, 111-143.

Prather, B.E., 2012. Controls on reservoir distribution, architecture, and stratigraphic trapping in slope settings. Principles of Geologic Analysis, 553-579. doi: 10.1016/B978-0-444-53042-4.00020-0

Price, W.A., 1933. Role of diastrophism in topography of Corpus Christi area, south Texas. AAPG Bulletin 17, 907-962.

Ridente, D., Trincardi, F., Piva, A., Asioli, A., 2009. The combined effect of sea level and supply during Milankovitch cyclicity: Evidence from shallow-marine $\delta^{18}O$ records and sequence architecture (Adriatic margin). Geology 37, 1003-1006.

Rodriguez, A.B., Anderson, J.B., Siringan, F.P., Taviani, M., 1999. Sedimentary Facies and genesis of Holocene sand banks on the east Texas inner continental shelf, in: Sneddin, J., Bergman, K. (Eds.), Isolated shallow marine sand bodies. SEPM Special Publication 64, 165-178.

Rodriguez, A.B., Hamilton, M.D., Anderson, J.B., 2000a. Facies and evolution of the modern Brazos Delta, Texas: Wave versus flood influence. Journal Sedimentary Research 70, 283-295.

Rodriguez, A. B., Anderson, J. B., Banfield, L. A., Taviani, M., Abdulah, K., Snow, J. N. 2000b. Identification of a −15 m Wisconsin shoreline on the Texas inner continental shelf. Palaeogeography, Palaeoclimatology, Palaeoecology 158, 25-43.

Rodriguez, A.B., Fassell, M.L., Anderson, J.B., 2001. Variations in shoreface progradation and ravinement along the Texas coast, Gulf of Mexico. Sedimentology 48, 837-853.

Rodriguez, A.B., Anderson, J.B., Siringan, F.P., Taviani, M., 2004. Holocene evolution of the east Texas coast and inner continental shelf: Along-strike variability in coastal retreat rates. Journal of Sedimentary Research 74, 405-421.

Rodriguez, A.B., Anderson, J.B., Simms, A.R., 2005. Terrace inundation as an autocyclic mechanism for parasequence formation: Galveston Estuary, Texas, U.S.A. Journal of Sedimentary Research 75, 608-620.

Rodriguez, A.B., Simms, A.R., Anderson, J.B., 2010. Bay-head deltas across the northern Gulf of Mexico back step in response to the 8.2 ka cooling event. Quaternary Science Reviews 29, 3983-3993.

Romans et al., This Volume

Rothwell, R.G., Kenyon, N.H., McGregor, B.A., 1991. Sedimentary features of the south Texas continental slope as revealed by side-scan sonar and high-resolution seismic data. AAPG Bulletin 75, 298-312.

Rudnick, D.L., Gopalakrishnan, G., Cornuelle, B.D., 2015. Cyclonic Eddies in the Gulf of Mexico: Observations by underwater gliders and simulations by numerical model. Journal of Physical Oceanography 45, 313–326.

Russ, J., Loyd, D.H., Boutton, T.W., 2000. A paleoclimate reconstruction for southwestern Texas using oxalate residue from lichen as a paleoclimate proxy. Quaternary International 67, 29-36.

Satterfield, W.M., Behrens, E.W., 1990. A late Quaternary canyon/channel system, northwest Gulf of Mexico continental slope. Marine Geology 92, 51-67.

Seaber, P.R., Kapinos, F.P., Knapp, G.L., 1987. Hydrologic Unit Maps. US Geological Survey Water-Supply Paper 2294, 1–63.

Shackleton, N. J., 1987. Oxygen isotopes, ice volume and sea level. Quaternary Science Reviews 6, 183-190.

Shepard, F.P., 1953. Sedimentation rates in Texas estuaries and lagoons. AAPG Bulletin 37, 1919–1934.

Shepard, F.P., Moore, D.G., 1955. Central Texas coast sedimentation: Characteristics of sedimentary environment, recent history, and diagenesis: Part 2. AAPG Bulletin 39, 1463-1593.

Shideler, 1981. Development of the benthic nephloid layer on the south Texas continental shelf, western Gulf of Mexico. Marine Geology 41, 37-61.

Sidner, B. R., Gartner, S., Bryant, W. R., 1978. Late Pleistocene geologic history of Texas outer continental shelf and upper continental slope, in: Bouma, A. H., Moore, G. T., Coleman, J. M. (Eds.), Framework, facies, and oil-trapping characteristics of the upper continental margin. AAPG Studies in Geology 7, 243-266.

Simms, A.R., Anderson, J.B., Blum, M., 2006a. Barrier-island aggradation via inlet migration: Mustang Island, Texas. Sedimentary Geology 187, 105–125.

Simms, A. R., Anderson, J. B., Taha, Z.P., Rodriguez, A.B., 2006b. Overfilled versus underfilled incised valleys: Lessons from the Quaternary Gulf of Mexico, in: Dalrymple, R., Leckie, D., Tillman, R. (Eds.), Incised valleys in time and space. SEPM Special Publication 85, 117-139.

Simms, A.R., Anderson, J.B., Milliken, K.T., Taha, Z.P., Wellner, J.S., 2007. Geomorphology and age of the oxygen isotope stage 2 (last lowstand) sequence boundary on the northwestern Gulf of Mexico continental shelf, in: Davies, R.J., Posamentier, H.W., Wood, L.J., and Cartwright, J.A. (Eds.), Seismic geomorphology: Applications to hydrocarbon exploration and production. Geological Society, London, Special Publication 277, 29–46.

Simms, A.R., Anderson, J.B., Rodriguez, A.B., Taviani, M., 2008. Mechanisms controlling environmental change within an estuary: Corpus Christi Bay, Texas, USA, in: Anderson, J.B., Rodriguez, A.B. (Eds.), Response of upper Gulf Coast estuaries to Holocene Climate Change and Sea-Level Rise. Geological Society of America, Special Paper 443, 121-146.

Simms, A. R., Aryal, N., Miller, L., Yokoyama, Y., 2010. The incised valley of Baffin Bay, Texas: A tale of two climates. Sedimentology 57, 642-669.

Simms, A.R., Rodriguez, A.B., 2014. Where do coastlines stabilize following rapid retreat? Geophysical Research Letters 41, 1698-1703. doi:10.1002/2013GL058984.

Simms, A. R., Anderson, J. B., DeWitt, R., Lambeck, K., Purcell, A., 2013. Quantifying rates of coastal subsidence since the last interglacial and the role of sediment loading. Global and Planetary Change 111, 296-308.

Sionneau, T., Bout-Roumazeilles, V., Biscaye, P. E., Van Vliet-Lanoe, B., Bory, A., 2008. Clay mineral distributions in and around the Mississippi River watershed and Northern Gulf of Mexico: Sources and transport patterns. Quaternary Science Reviews 27, 1740-1751.

Siringan, F.P., Anderson, J.B., 1993. Seismic facies, architecture, and evolution of the Bolivar Roads tidal inlet/delta complex, East Texas Gulf Coast. Journal of Sedimentary Petrology 63, 794-808.

Siringan, F.P., Anderson, J.B., 1994. Modern shoreface and inner-shelf storm deposits off the east Texas coast, Gulf of Mexico. Journal of Sedimentary Research 64, 99–110.

Smyth, W.C., 1991. Seismic facies analysis and depositional history of an incised valley system, Galveston Bay area, Texas. Unpublished M.S. thesis, Rice University, Houston, TX, 170 p.

Snedden, J.W., Nummedal, D., Amos, A.F., 1988. Storm and fair-weather combined-flow on the central Texas continental shelf. Journal of Sedimentary Petrology 58, p. 580–595.

Snow, J.N., 1998. Late Quaternary highstand and transgressive deltas of the ancestral Colorado River: Eustatic and climate controls on deposition. Unpublished M.A. thesis, Rice University, Houston, TX, 138 p.

Strong, N., Paola, C., 2008. Valleys that never were: Time surfaces versus stratigraphic surfaces. Journal of Sedimentary Research 78, 579-593.

Suter, J.R. Berryhill, H.L., 1985. Late Quaternary shelf-margin deltas, Northwest Gulf of Mexico. AAPG Bulletin, 69 77-91.

Suter, J.R., 1987. Ancient fluvial systems and Holocene deposits, southwestern Louisiana continental shelf, in Berryhill, H.L. (Ed.), Late Quaternary facies and structure, northern Gulf of Mexico: Interpretations from seismic data. American Association of Petroleum Geologists, Studies in Geology 23, 81-129.

Sylvia, D.A., Galloway, W.E., 2006. Morphology and stratigraphy of the late Quaternary lower Brazos valley: Implications for paleo-climate, discharge and sediment delivery. Sedimentary Geology 190, 159-175.

Syvitski, J.P., Milliman, J.D., 2007. Geology, geography, and humans battle for dominance over the delivery of fluvial sediment to the coastal ocean. The Journal of Geology 115, 1–19.

Taha, Z.P., Anderson, J.B., 2008. The influence of valley aggradation and listric normal faulting on styles of river avulsion: A case study of the Brazos River, Texas, USA. Geomorphology 95, 429-448.

Tatum, T. E., 1977. Shallow geologic features of the upper continental slope, northwestern Gulf of Mexico. Unpublished Master's thesis, Texas A&M University, College Station, TX, 122 p.

Thomas, M.A., 1990. The impact of long-term and short-term sea level changes on the evolution of the Wisconsinan-Holocene Trinity/Sabine incised valley system, Texas Continental Shelf. Unpublished Ph.D. Dissertation, Rice University, Houston, TX, 247 p.

Thomas, M.A., Anderson, J.B., 1994. Sea-Level controls on the facies architecture of the Trinity/Sabine incised-valley system, Texas continental shelf, in: Dalrymple, R., Boyd, R., Zaitlin, B.A. (Eds.), Incised-Valley systems. SEPM Special Publication 51, Tulsa, Oklahoma, 63-82.

Thornthwaite, C.W., 1948. An approach toward a rational classification of climate. Geographical Review 38, 55–94.

Toomey, R.S., III, Blum, M.D., Valastro, S., Jr., 1993. Late Quaternary climates and environments of the Edwards Plateau, Texas. Global and Planetary Change 7, 299-320.

Törnqvist, T.E., Bick, S.J., González, J.L., Van der Borg, K., De Jong, A.F.M., 2004a. Tracking the sea-level signature of the 8.2 ka cooling event: new constraints from the Mississippi Delta. Geophysical Research Letters 31, L23309.

Törnqvist, T.E., González, J.L., Newsom, L.A., Van der Borg, K., De Jong, A.F.M., Kurnik, C.W., 2004b. Deciphering Holocene sea-level history on the U.S. Gulf Coast: a high-resolution record from the Mississippi Delta. Geological Society of America Bulletin 116, 1026–1039.

Törnqvist, T.E., Bick, S.J., Van der Borg, K., De Jong, A.F.M., 2006. How stable is the Mississippi Delta? Geology 34, 697-700.

Toscano, M.A., Macintyre, I.G., 2003. Corrected western Atlantic sea-level curve for the last 11,000 years based on calibrated 14C dates from Acropora palmata framework and intertidal mangrove peat. Coral Reefs 22, 257–270. doi: 10.1007/s00338-003-0315-4.

Troiani, B. T., Simms, A. R., Dellapenna, T., Piper, E., Yokoyama, Y., 2011. The importance of sea-level and climate change, including changing wind energy, on the evolution of a coastal estuary: Copano Bay, Texas. Marine Geology 280, 1-12, 12a, 17-19.

Van Heijst, M.W.I.M., Postma, G., 2001. Fluvial response to sea-level changes: A quantitative analogue, experimental approach. Basin Research 13, 269–292.

Van Heijst, M.W.I.M., Postma, G., Meijer, X.D., Snow, J.N., Anderson, J.B., 2001. Quantitative analogue flume-model study of river-shelf systems: Principles and verification exemplified by the Late Quaternary Colorado river-delta evolution. Basin Research 13, 243-268.

Wallace, D.J., Anderson, J.B., Fernández, R., 2010. Transgressive ravinement versus depth of closure: A geological perspective from the upper Texas Coast. Journal of Coastal Research 26, 1057-1067.

Wallace, D.J., Anderson, J.B., 2013. Unprecedented erosion of the upper Texas Coast: Response to accelerated sea-level rise and hurricane impacts. Geological Society of America Bulletin 125, 728-740.

Wallace, D.J. Anderson, J.B., 2010. Evidence of similar probablility of intense hurricane strikes for the Gulf of Mexico over the late Holocene. Geology 38, 511–514.

Wallace, D.J., Anderson, J.B., Rodriguez, A.B., 2009. Natural versus anthropogenic mechanisms of erosion along the upper Texas coast, in: Kelley, J.T., Pilkey, O.H., Cooper, J.A.G. (Eds.), America's Most Vulnerable Coastal Communities. Geological Society of America Special Paper 460, 137–147.

Walsh, J.P., Nittrouer, C.S., 2009. Understanding fine-grained river-sediment dispersal on continental margins. Marine Geology 263, 34-45.

Weight, R.W.R., Anderson, J.B., Fernández, R., 2011. Rapid mud accumulation on the central Texas shelf linked to climate change and sea-level rise. Journal of Sedimentary Research 81, 743-764.

Wellner, J.S. Sarzalejo, S., Logoe, M., Anderson, J.B., 2004. The Late Quaternary stratigraphic evolution of the west Louisiana-East Texas continental shelf, in: Anderson, J.B., Fillon, R. H. (Eds.), Late Quaternary stratigraphic evolution of the northern Gulf of Mexico margin. Society for Sedimentary Geology, Special Publication 79, 217-236.

Wilkins, D.E., Currey, D.R., 1999. Radiocarbon chronology and δ13C analysis of mid- to late-Holocene aeolian environments, Guadalupe Mountains National Park, Texas, USA. The Holocene 9, 363-371.

Wilkinson, B.H., McGowen, J.H., 1977. Geologic approaches to the determination of long-term recession rates, Matagorda Peninsula, Texas. Environmental Geology 1, 359-365.

Wilkinson, B.H., 1975. Matagorda Island, Texas: The evolution of a Gulf coast barrier complex. Geological Society of America Bulletin 86, 959-967.

Williams, S.J., Prins, D.A., Meisburger, E.P., 1979. Sediment distribution, sand resources and geologic character of the inner continental shelf off Galveston County, Texas. United States Army Corps of Engineers, Miscellaneous Report 79-4, 159 p.

Winker, C.D., 1996. High-resolution seismic stratigraphy of a late Pleistocene submarine fan ponded by salt-withdrawal mini-basins on the Gulf of Mexico continental slope.

Offshore Technology Conference Proceedings, OTC 8024, 619-628.

Woodbury, H. O., Spotts, J. H., Akers, W. H., 1978. Gulf of Mexico continental-slope sediments and sedimentation, in: Bouma, A.H., Moore, G.T., Coleman, J.M. (Eds.), Framework, facies, and oil-trapping characteristics of the upper continental margin. AAPG Studies in Geology, 7, 117-137.

Wright, L.D., Nittrouer, C.A., 1995. Dispersal of river sediments in coastal seas: six contrasting cases. Estuaries 18, 494-508.

Zhong, L., Li, M., Foreman, M.G.G., 2008. Resonance and sea level variability in Chesapeake Bay. Continental Shelf Research 28, 2565-2573.

Figure Captions

1. Map showing drainage basins of rivers that drain into the northern Gulf of Mexico. The area is characterized by a significant difference in precipitation from east to west across the area as shown by average precipitation gradients (modified from Anderson et al., 2004).
2. Composite oxygen isotope records (modified from Labeyrie et al., 1987; Shackleton, 1987; open circles = Bard et al., 1990; closed circles and triangles = Chappell et al., 1996; Anderson et al., 2004) calibrated with U-Th dates on corals used as a proxy sea-level curve for this paper. Also shown are the marine oxygen isotope stages (MIS). The most poorly constrained portion of the curve is the initial MIS 3 lowstand and highstand (designated with arrows), which have uncertainties of up to 30 meters. Modified from Anderson et al., 2004.

3. Rice University high-resolution seismic data used for this study. The box designates the area on the western Louisiana continental shelf where dense (average one mile spacing) grids of high-resolution seismic data acquired by the USGS (see Berryhill, 1987) and Texaco Oil Company (see Wellner et al., 2004) were available for this investigation. Also shown are the locations of bays where detailed studies have been conducted. LC=Lake Calcasieu, SL=Sabine Lake, GB=Galveston Bay, MG=Matagorda Bay, CB=Copano Bay, CCB=Corpus Christi Bay and BB=Baffin Bay. The approximate location of the Ingleside Paleoshoreline is shown (from Simms et al., 2013). Also shown are the trends of the San Marcos and Sabine Arches.
4. Interpreted seismic lines G-300x and Line G-90Y, two connecting dip-oriented profiles collected along the depositional axis of the falling-stage Brazos delta (modified from Rodriguez et al., 2000b; Anderson et al., 2004). Major seismic surfaces are also shown.
5. Bathymetric map and profiles illustrating variation in Texas continental shelf physiography. Also shown is the trend of the San Marcos Arch.
6. Summary of late Pleistocene - Holocene paleoclimate investigations from Texas (modified from Weight et al., 2011).
7. Major surface currents of the northern Gulf of Mexico. Also shown is the coastal convergence zone (from McGowen et al., 1977). Solid arrows represent mean current directions and dashed arrows show migratory loop currents. LCR=loop current ring and CR=cyclonic rings (modified from Sionneau et al., 2008).
8. Falling-stage (MIS 5-3) channels of the western Louisiana continental shelf (modified from Suter and Berryhill, 1985). The dashed lines subdivide three distinct channel belts. The eastern channel belt merges seaward with the Mississippi shelf margin delta. A

second, narrower western channel belt merges with MIS 3 Western Louisiana delta (WDL). The western most channel belt includes the Calcasieu and Sabine channels. See Suter (1987) and Suter and Berryhill (1985) for more detailed map and discussion. MRCC=Mississippi River channel complex; WCC= Western channel complex.

9. Paleogeographic map showing major falling-stage depositional systems of the study area (modified from Suter and Berryhill, 1985; Anderson et al., 2004). Note the repeated cycles of progradation and backstepping exhibited by the Brazos delta.

10. Paleogeographic map of MIS 3 falling-stage deltas on the western Louisiana and east Texas continental shelves (modified from Anderson et al., 2004). Sandy mouth bars highlighted in yellow. Also shown are seismic lines 34 and 12 that illustrate seismic facies used to map these deltas. Note cut-and-fill, chaotic seismic faces characteristic of sandy mouth bar facies. Two oil company platform borings near line 34 provide lithological ground truth for seismic facies interpretations, with yellow indicating sand and gray representing mud. Note also that mouth bars are incised into prodelta muds, a result of falling sea level (forced regression). See Abdulah et al. (2004) and Wellner et al. (2004) for details. Two-Way Travel Time in seconds.

11. Paleogeographic map showing major lowstand depositional systems (modified from Anderson et al., 2004; Simms et al., 2007; Anderson and Rodriguez, 2008; Pirmez et al., 2012) plotted on a digital elevation map of the MIS 2 exposure surface (sequence boundary).

12. Detailed maps of incised valleys beneath Sabine (Sabine valley), Galveston (Trinity valley), Matagorda (Lavaca valley) and Baffin (Baffin valley) bays illustrating differences in valley geomorphology (modified from Williams et al., 1979; Smyth, 1991; Maddox et

al., 2008; Rodriguez et al., 2005). Also shown are valley cross sections to illustrate similarities in valley fills.

13. Structure contour map of Rio Grande incised valley and associated lowstand delta-fan complex (modified from Banfield and Anderson, 2004).
14. Bathymetric map (modified from GeoMapApp) of east Texas continental slope showing salt-withdrawal minibasins where small fans associated with the Brazos-Trinity (B-T) lowstand valley accumulated (within orange box). Also shown is the approximate location of the MIS 2 lowstand valley and delta and seismic section G-410 (modified from Anderson et al., 2004) illustrating the lowstand delta and fan deposits within one of these minibasins and the location of Seismic profile H-29 (Fig. 17). MIS 2-1 RS = MIS 2-1 ravinement surface, SB2 = MIS 2 sequence boundary, 5e MFS = MIS 5e maximum flooding surface. Small lowercase letters designate stratigraphic units as shown in figure 17.
15. Composite linear regression Gulf of Mexico sea-level index-point curve for the past 10,000 years (modified from Milliken et al., 2008c; Anderson et al., 2014). See these references for full methodologies, error bars for points, and nonlinear regression.
16. Paleogeographic map showing major depositional systems of the MIS 1 transgression (compiled from Snow, 1998; Van Heijst et al., 2001; Anderson et al., 2004; Banfield and Anderson, 2004; Simms et al., 2007; Anderson and Rodriguez, 2008; Weight et al., 2011). Arrows show direction of back-stepping valley fill facies.
17. Seismic profile (HI-) 29 showing lowstand Trinity-Sabine-Brazos delta (modified from Wellner et al., 2004). Letters designate individual clinoform units based on the seismic stratigraphic analysis of Wellner et al. (2004). Note the downward shift in offlap break for clinoform sets c-g followed by an upward shift for clinoforms h-j. The slope-parallel

shape of the delta indicates that these shifts record changes in sea level and not lobe shifting events. This indicates that growth of the delta continued after sea level began to rise, which is supported by radiocarbon ages (modified from Wellner et al., 2004).

18. Seismic line 36b across transgressive Rio Grande delta showing varying clinoform dips indicative of lobe shifting. Also shown is the sequence boundary as defined by Banfield and Anderson (2004). The map shows the reconstruction of the delta based on seismic lines shown with gray lines (modified from Banfield and Anderson, 2004).
19. Highly exaggerated (300X) digital elevation map showing the sediment underfilled Trinity incised valley, now occupied by Galveston Bay, and the sediment overfilled Brazos incised valley. Dashed white lines denote valleys. Compiled from Aslan and Blum, 1999; Anderson et al., 2004; Taha and Anderson, 2008. The ~ 50 km wide coastalplain, which is characterized by relatively flat relief, is also designated.
20. Map showing contemporaneous back-stepping bayhead deltas (1-4) and tidal inlet (1-V) pairs within the offshore Trinity valley (modified from Thomas and Anderson, 1994).
21. Stratigraphic section along the axis of the Trinity incised valley (modified from Anderson et al., 2008), now occupied by Galveston Bay, constructed from seismic lines and drill cores collected along the valley axis (vertical lines with core numbers). Also shown are radiocarbon ages obtained from cores and approximate depths and ages of flooding surfaces that correspond to back-stepping bay facies.
22. Oblique 3-D perspective of the Brazos incised valley showing channels that merge upstream into an avulsion node. Map is based on more than 400 water well descriptions (Taha and Anderson, 2008). Channel sands were not mapped for either Jones Creek or the modern Brazos River.

23. Axial (A-A’) profile for the Brazos valley illustrating aggradation history based on radiocarbon ages (from Bernard et al., 1970; Abbott et al., 2001; Sylvia and Galloway, 2006; Taha and Anderson, 2008) for the Brazos incised valley (modified from Taha and Anderson, 2008). Map shows locations of profiles.
24. Cross-valley profile (B-B’) for the Brazos valley (see Fig. 23 and caption for transect location and references). Also shown is a comparison of aggradation rates between the Colorado and Brazos incised valleys, along-strike and 40 km from the modern coastline (modified from Taha and Anderson, 2008). Note the similarity between aggradation rates from 12 to 6 ka, based on calibrated radiocarbon ages from 6 cores (5 cores in the Brazos and 1 core in the Colorado). The composite Holocene sea-level curve for the northern Gulf of Mexico (see figure 15) is shown with blue lines denoting 6 ka and older. Note that aggradation tracks sea-level rise.
25. Vertical distribution of 8,800 m of Clay and Sand descriptions from water wells logged in the lower 60 km of the Brazos Valley. All chosen cutting descriptions are positioned above the inferred Stage 2 sequence boundary, with surface elevations between 0 and 16 m above sea level, depending on distance from coast.
26. Seismic profile across offshore falling-stage channel, which is characterized by chaotic-complex seismic facies, and transgressive ravinement surface capped by acoustically laminated seismic facies of Holocene marine mud (modified from Wellner et al., 2004). An oil company platform boring that sampled the channel is also shown. Sa=sand, Si=interbedded sand and mud, and M=marine mud.
27. Summary of Texas barrier island evolution showing variable timing of formation of different barriers (modified from Anderson et al., 2014). Also shown is the composite

Holocene sea-level curve (see figure 15) for the northern Gulf of Mexico and historical shoreline migration rates. Orange arrows designate ages of major contemporaneous flooding surfaces in area bays.

28. Paleogeographic reconstructions illustrating the Holocene evolution of Galveston Bay (modified from Anderson et al., 2008). Note that the bay evolves from deep and narrow to broad and shallow as the valley is flooded and filled with sediment. Also shown is a cross section of the valley illustrating changes in bay area and shape through time (see figure 12).
29. Interpreted and uninterpreted seismic Line 1 illustrating acoustically laminated character of the Texas Mud Blanket and map showing distribution of the mud blanket (modified from Weight et al., 2011). Also shown is the location of Line 1. Conversion of two-way travel time to meters was done using 1807m/s and is only valid above sequence boundary.
30. Sediment flux history for the Texas Mud Blanket related to the sea-level record (modified from Weight et al., 2011- see for full descriptions of references for this figure).
31. Summary figure illustrating sedimentary events and associated stratigraphic architecture for Falling Stage, Lowstand, Transgressive and Highstand Systems Tracts. Also shown is the relevant section of the sea-level curve for each systems tract.

Table Caption

1. Table describing depocenter location, MIS Stage, the relevant time interval, and calculated volumes/sediment fluxes. Also shown are the modern rivers and their associated sediment discharge values.

Figure 1

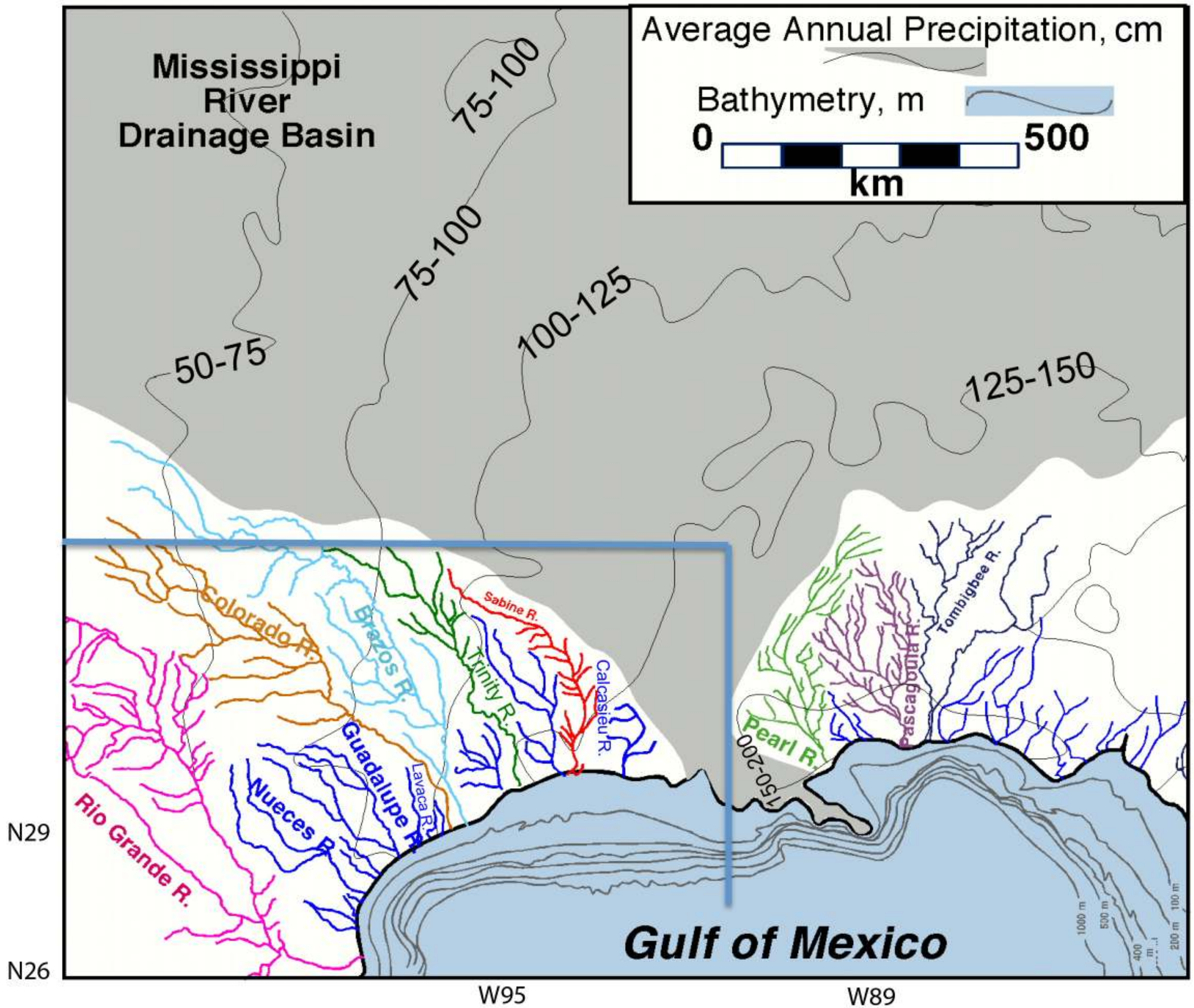

Average Annual Precipitation, cm
Bathymetry, m
0
500
km
Mississippi
River
Drainage Basin
75-100
75-100
100-125
50-75
125-150
Colorado R.
Brazos R.
Trinity R.
Sabine R.
Calcasieu R.
Guadalupe R.
Lavaca R.
Nueces R.
Rio Grande R.
Pearl R.
Pascagoula R.
Tombigbee R.
150-200
Gulf of Mexico
N29
N26
W95
W89

Figure 2

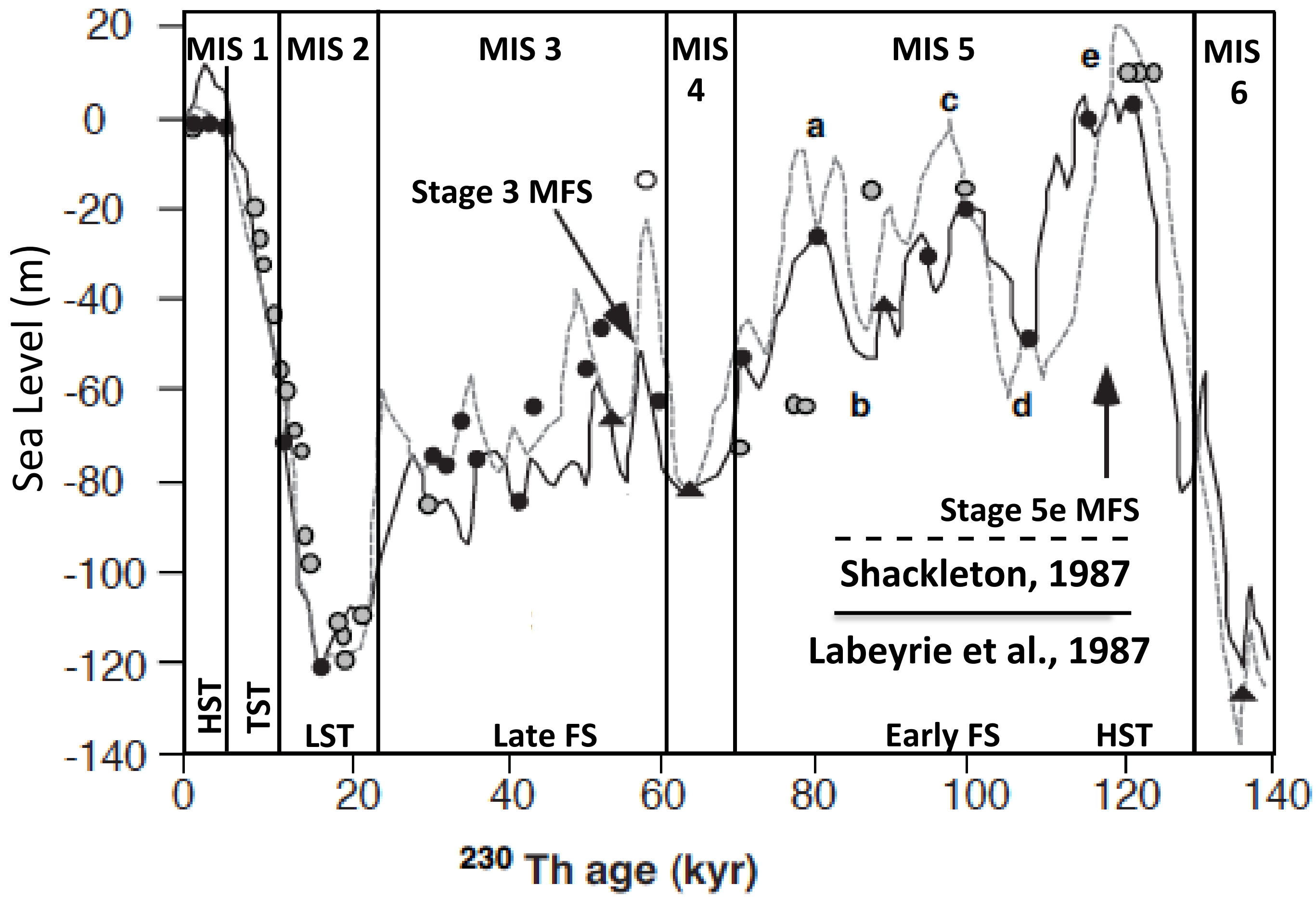

MIS 1
MIS 2
MIS 3
MIS 4
MIS 5
MIS 6
a
b
c
d
e
Stage 3 MFS
Stage 5e MFS
Shackleton, 1987
Labeyrie et al., 1987
HST
TST
LST
Late FS
Early FS
HST
Sea Level (m)
20
0
-20
-40
-60
-80
-100
-120
-140
0
20
40
60
80
100
120
140
230 Th age (kyr)

Figure 3

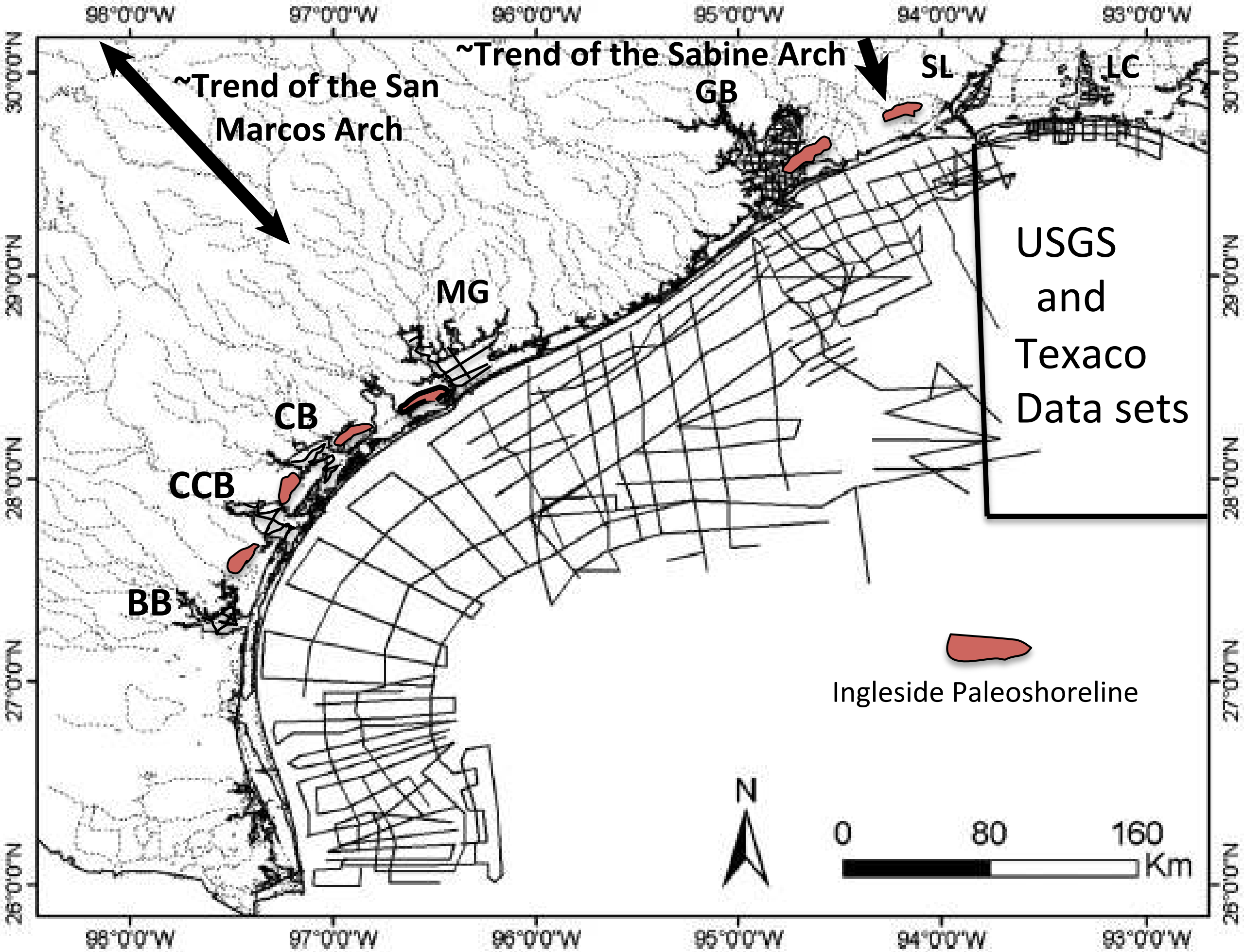
98°0'0"W
97°0'0"W
96°0'0"W
95°0'0"W
94°0'0"W
93°0'0"W
30°0'0"N
29°0'0"N
28°0'0"N
27°0'0"N
26°0'0"N
~Trend of the San Marcos Arch
~Trend of the Sabine Arch
GB
SL
LC
MG
CB
CCB
BB
USGS and Texaco Data sets
Ingleside Paleoshoreline
N
0
80
160
Km

Figure 4

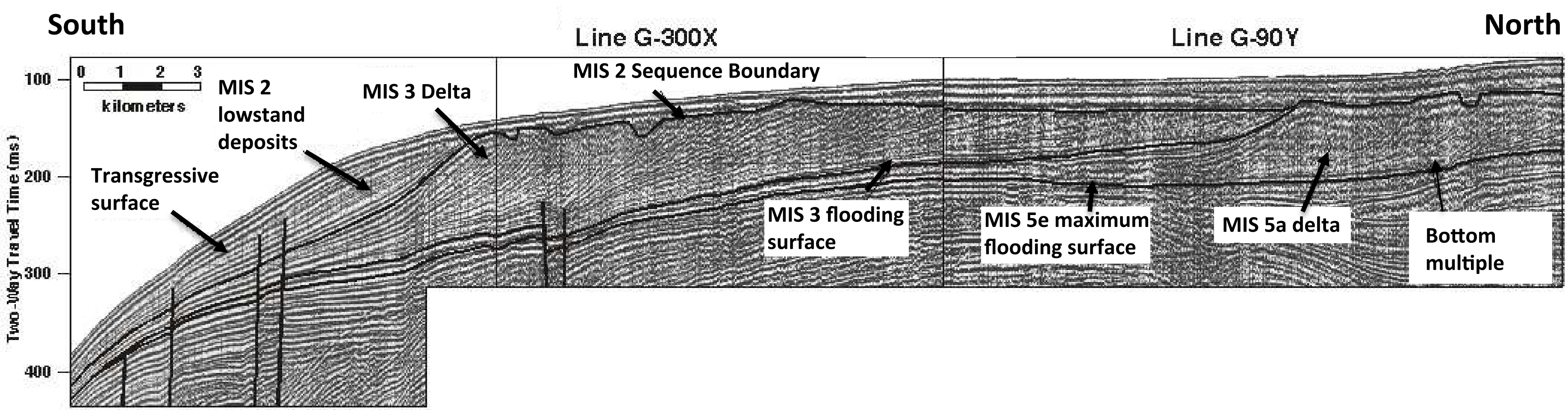
South
Line G-300X
Line G-90Y
North
0 1 2 3
kilometers
MIS 2 lowstand deposits
MIS 3 Delta
MIS 2 Sequence Boundary
Transgressive surface
MIS 3 flooding surface
MIS 5e maximum flooding surface
MIS 5a delta
Bottom multiple
Two-Way Travel Time (ms)
100
200
300
400

Figure 5

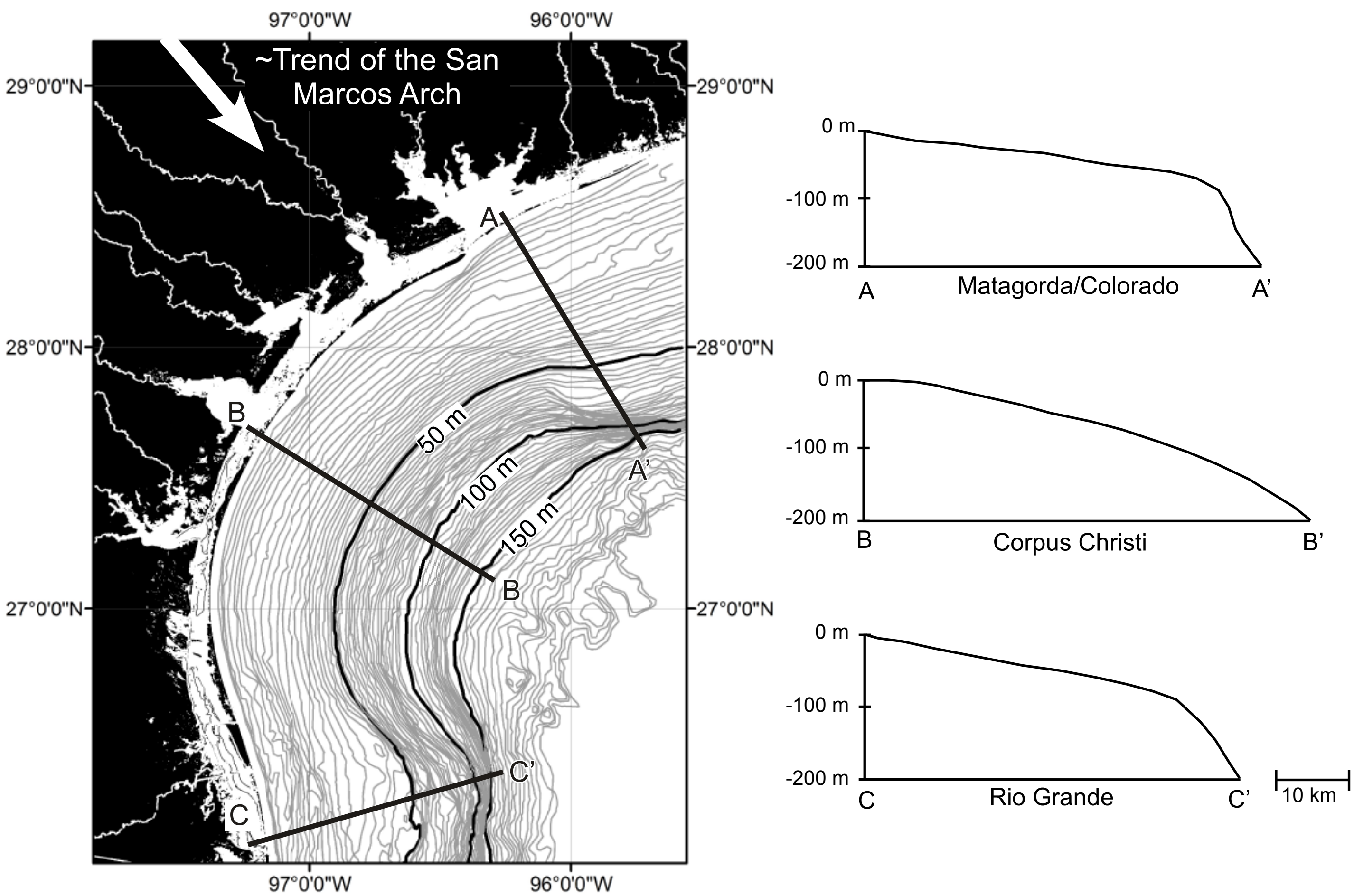

~Trend of the San Marcos Arch
97°0'0"W
96°0'0"W
29°0'0"N
28°0'0"N
27°0'0"N
A
A'
B
B
C
C'
50 m
100 m
150 m
0 m
-100 m
-200 m
Matagorda/Colorado
Corpus Christi
B'
Rio Grande
10 km

Figure 6

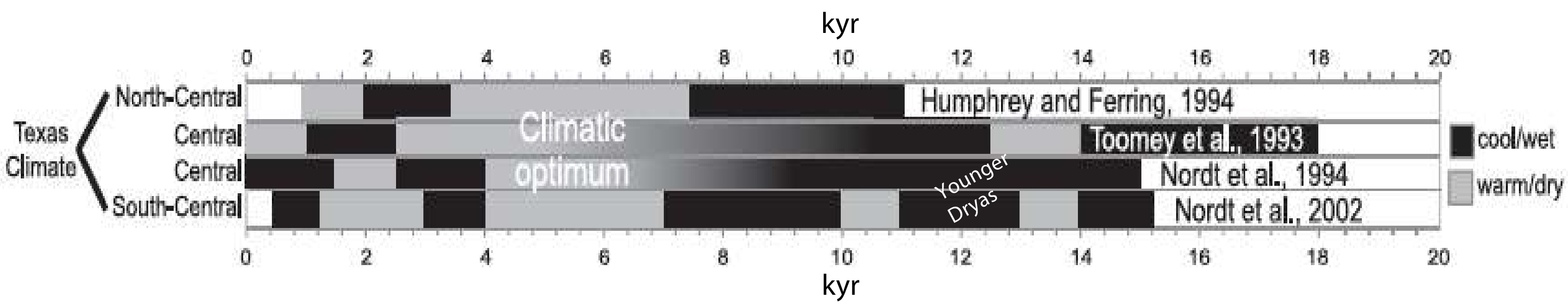

kyr
0
2
4
6
8
10
12
14
16
18
20
Texas
Climate
North-Central
Central
Central
South-Central
Humphrey and Ferring, 1994
Toomey et al., 1993
Nordt et al., 1994
Nordt et al., 2002
Climatic
optimum
Younger
Dryas
cool/wet
warm/dry

Figure 7

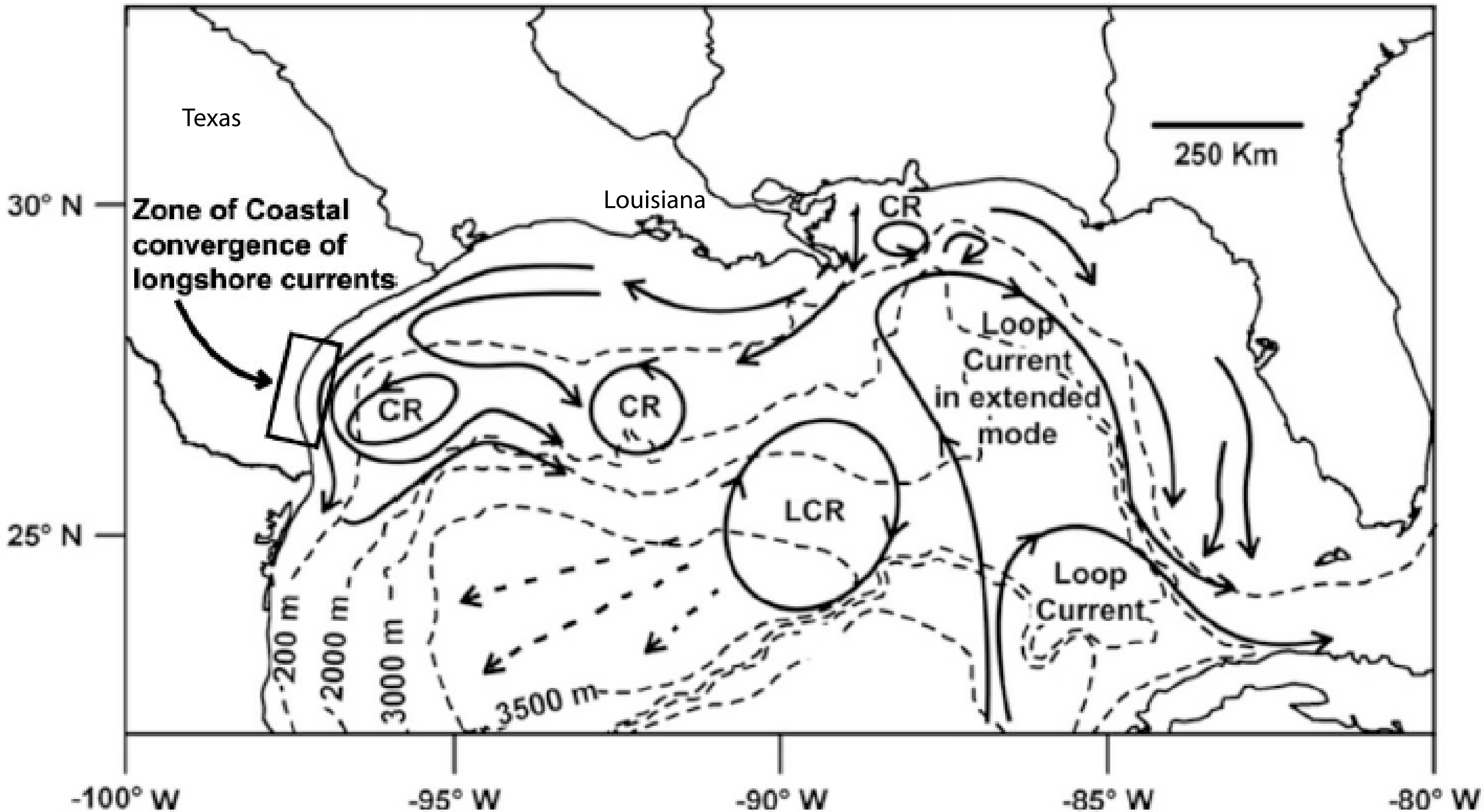

Texas
Louisiana
250 Km
30° N
25° N
Zone of Coastal convergence of longshore currents
CR
CR
CR
LCR
Loop Current in extended mode
Loop Current
200 m
2000 m
3000 m
3500 m
-100° W
-95° W
-90° W
-85° W
-80° W

Figure 8

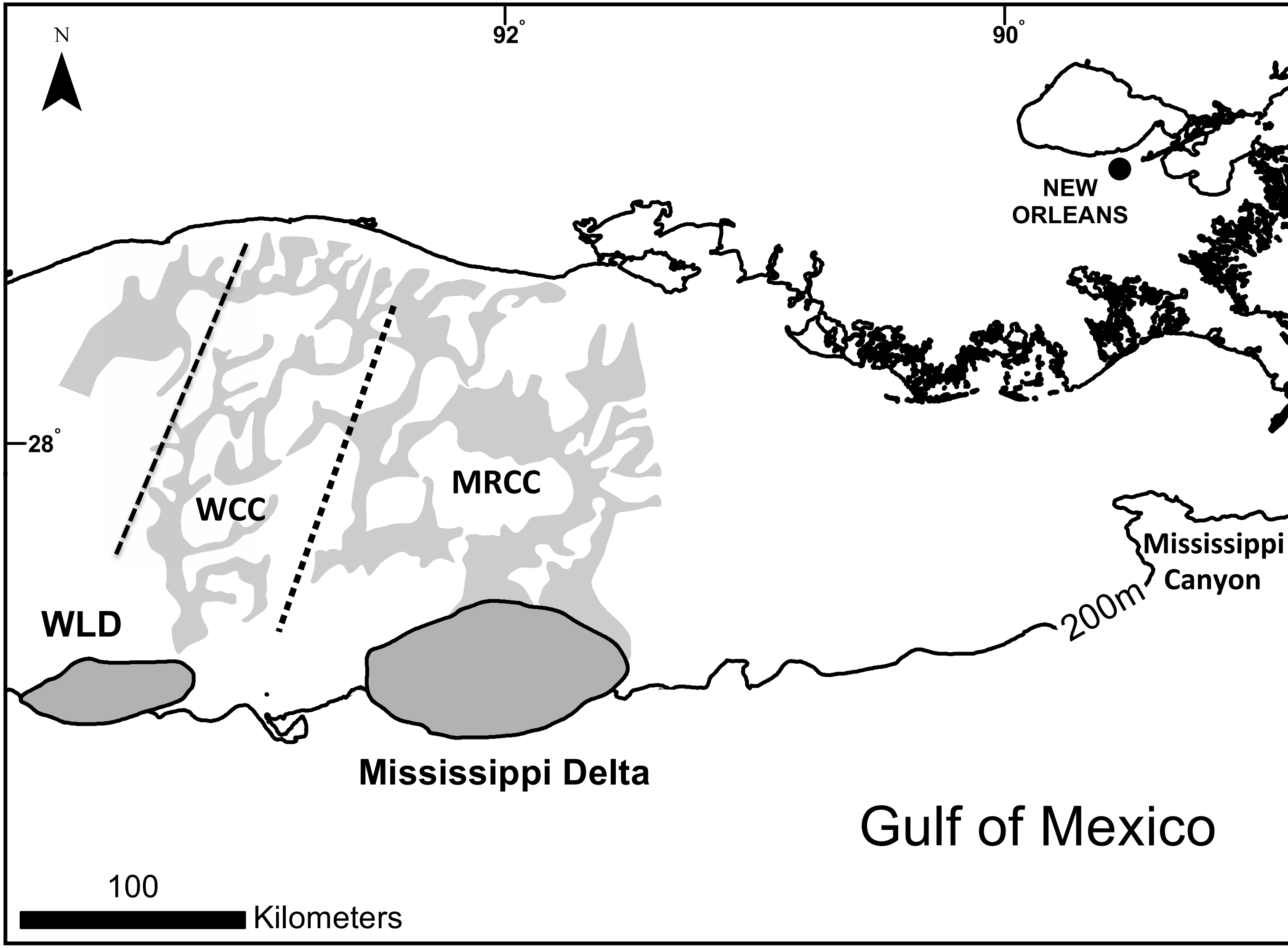
N
92°
90°
28°
NEW
ORLEANS
WCC
MRCC
WLD
Mississippi
Canyon
200m
Mississippi Delta
Gulf of Mexico
100
Kilometers

Figure 9

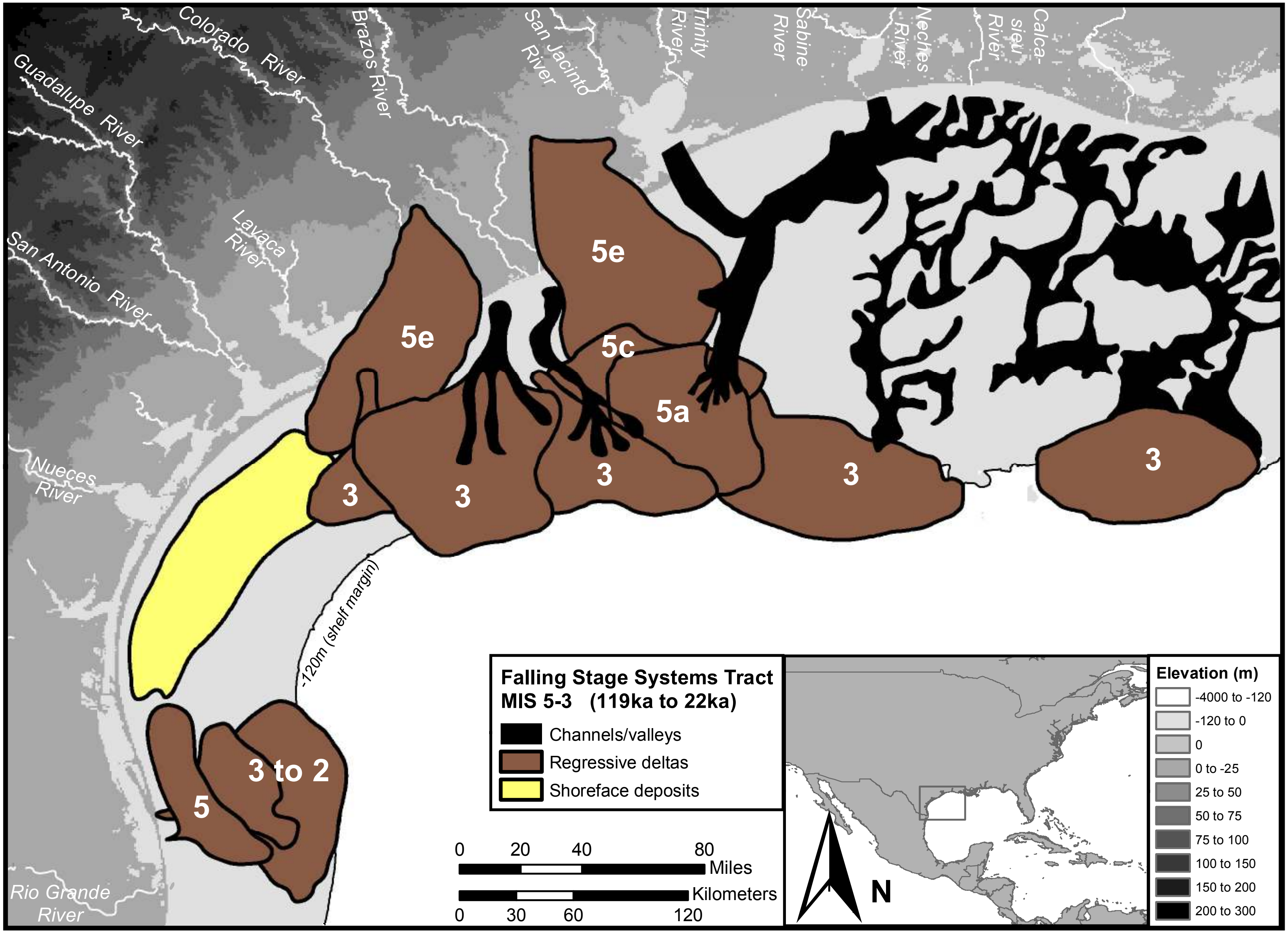
Colorado River
Brazos River
San Jacinto River
Trinity River
Sabine River
Neches River
Calcasieu River
Guadalupe River
Lavaca River
San Antonio River
Nueces River
Rio Grande River
-120m (shelf margin)
5e
5e
5c
5a
3
3
3
3
3
3
5
3 to 2
Falling Stage Systems Tract
MIS 5-3 (119ka to 22ka)
Channels/valleys
Regressive deltas
Shoreface deposits
0 20 40 80 Miles
0 30 60 120 Kilometers
N
Elevation (m)
-4000 to -120
-120 to 0
0
0 to -25
25 to 50
50 to 75
75 to 100
100 to 150
150 to 200
200 to 300

Figure 10

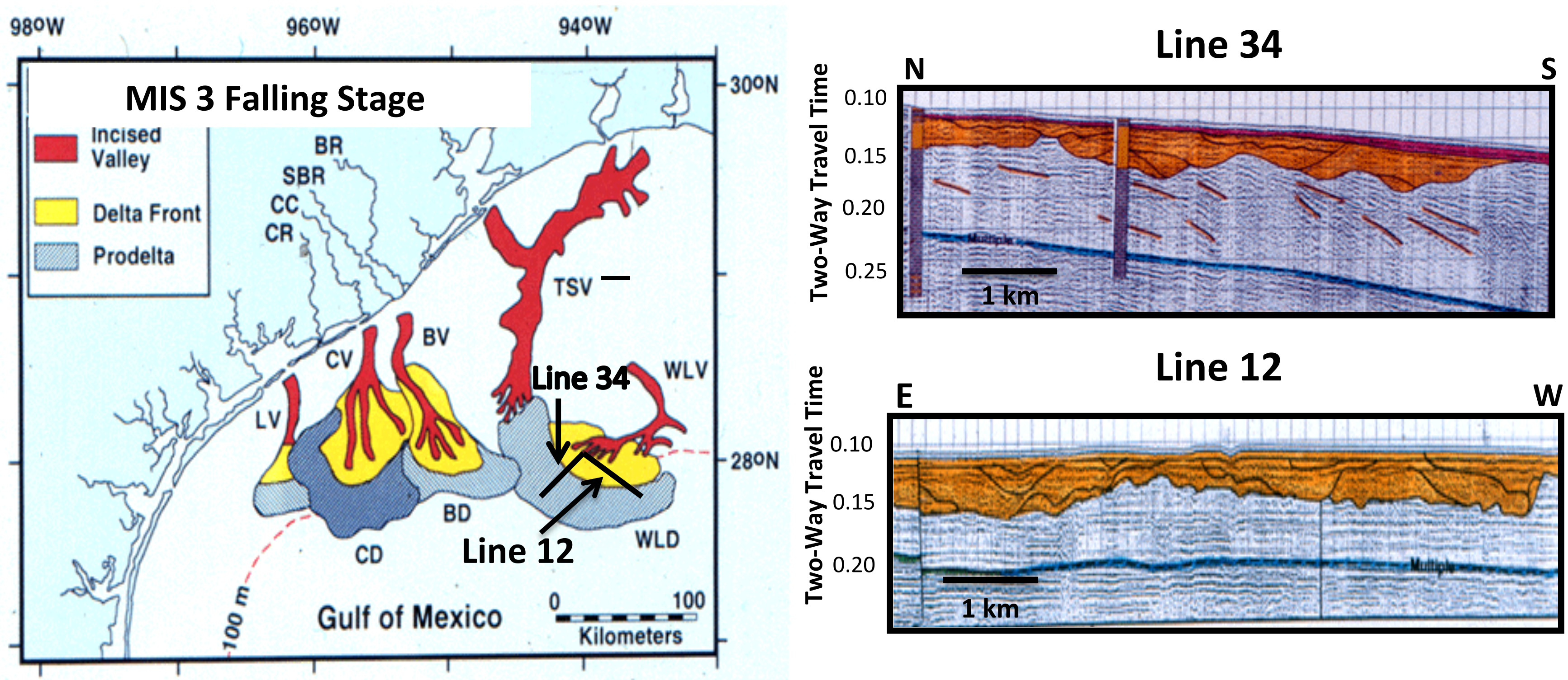
MIS 3 Falling Stage
Incised Valley
Delta Front
Prodelta
98°W
96°W
94°W
30°N
28°N
BR
SBR
CC
CR
TSV
BV
CV
LV
WLV
Line 34
Line 12
BD
CD
WLD
100 m
Gulf of Mexico
0
100
Kilometers
Line 34
N
S
Two-Way Travel Time
0.10
0.15
0.20
0.25
1 km
Line 12
E
W
Two-Way Travel Time
0.10
0.15
0.20
1 km

Figure 11

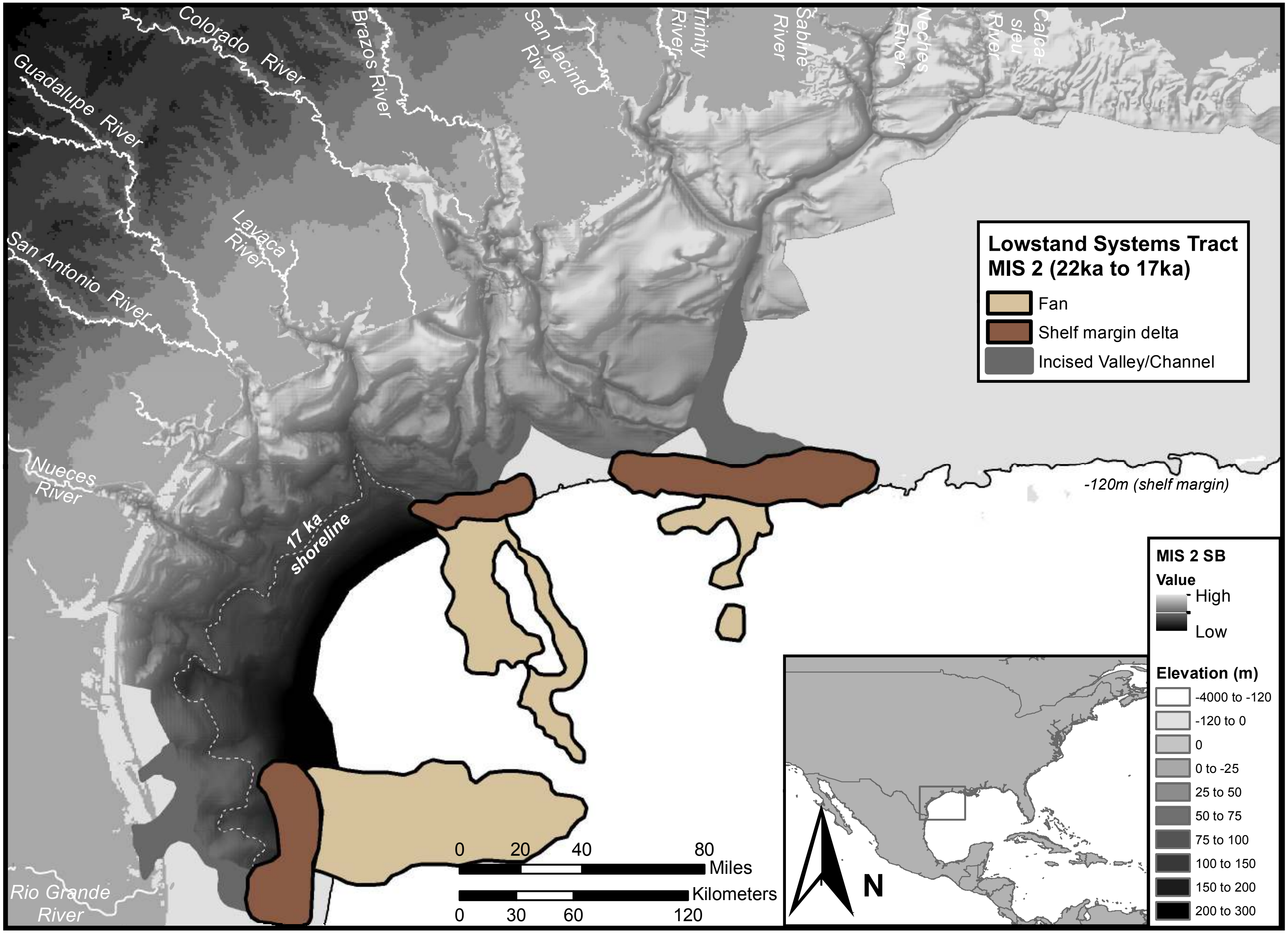
Colorado River
Brazos River
San Jacinto River
Trinity River
Sabine River
Neches River
Calcasieu River
Guadalupe River
Lavaca River
San Antonio River
Nueces River
Rio Grande River
17 ka shoreline
-120m (shelf margin)
Lowstand Systems Tract
MIS 2 (22ka to 17ka)
Fan
Shelf margin delta
Incised Valley/Channel
MIS 2 SB
Value
High
Low
Elevation (m)
-4000 to -120
-120 to 0
0
0 to -25
25 to 50
50 to 75
75 to 100
100 to 150
150 to 200
200 to 300
0 20 40 80
Miles
Kilometers
0 30 60 120
N

Figure 12

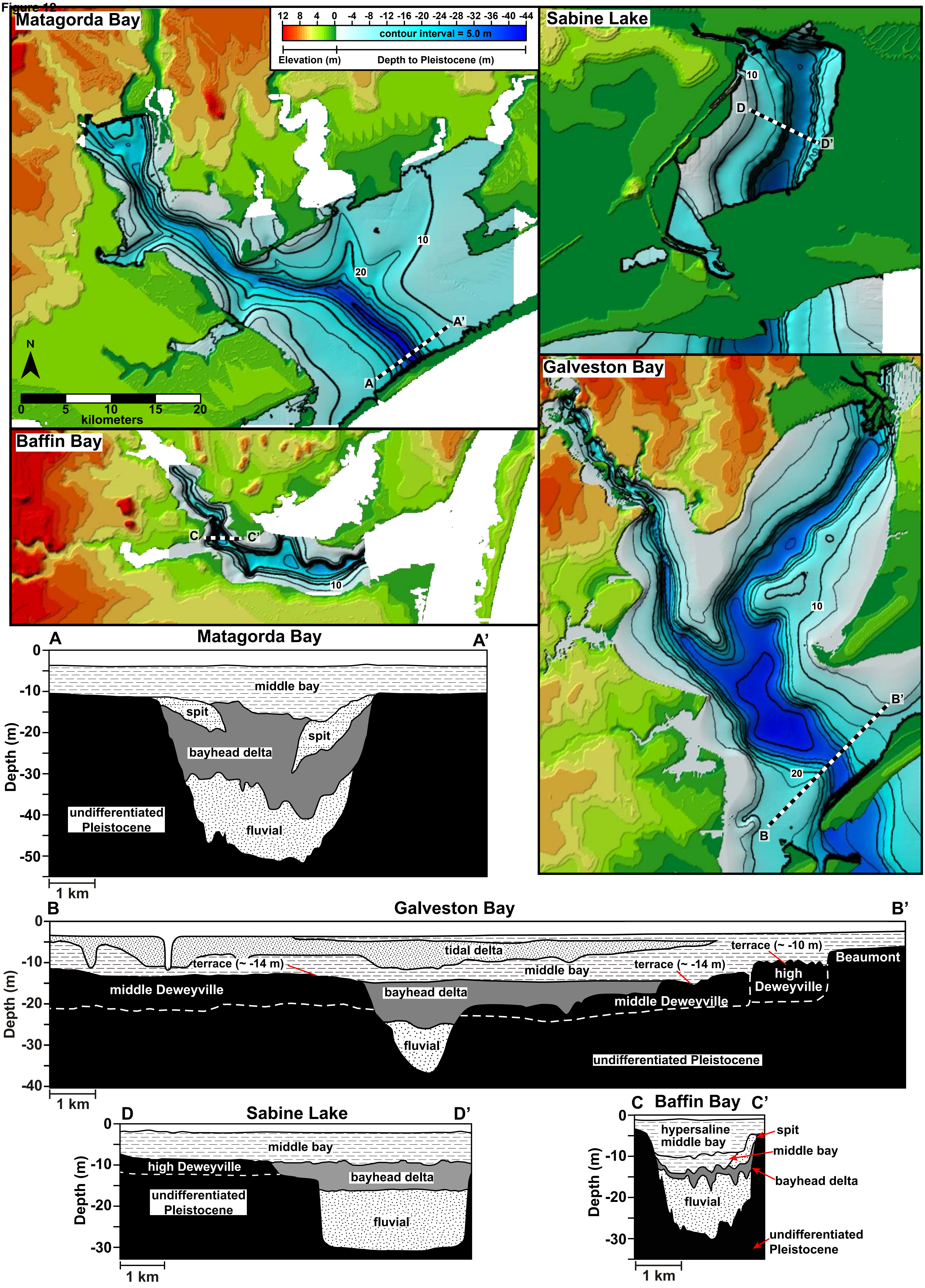

Matagorda Bay
12 8 4 0 -4 -8 -12 -16 -20 -24 -28 -32 -36 -40 -44
contour interval = 5.0 m
Elevation (m)
Depth to Pleistocene (m)
10
20
A
A'
N
0 5 10 15 20
kilometers
Sabine Lake
10
D
D'
Galveston Bay
10
20
B
B'
Baffin Bay
C
C'
10
A
Matagorda Bay
A'
middle bay
spit
spit
bayhead delta
undifferentiated Pleistocene
fluvial
Depth (m)
0 -10 -20 -30 -40 -50
1 km
B
Galveston Bay
B'
tidal delta
terrace (~ -10 m)
terrace (~ -14 m)
middle bay
terrace (~ -14 m)
Beaumont
high Deweyville
middle Deweyville
bayhead delta
middle Deweyville
fluvial
undifferentiated Pleistocene
Depth (m)
0 -10 -20 -30 -40
1 km
D
Sabine Lake
D'
middle bay
high Deweyville
bayhead delta
undifferentiated Pleistocene
fluvial
Depth (m)
0 -10 -20 -30
1 km
C
Baffin Bay
C'
hypersaline middle bay
spit
middle bay
bayhead delta
fluvial
undifferentiated Pleistocene
Depth (m)
0 -10 -20 -30
1 km

Figure 13

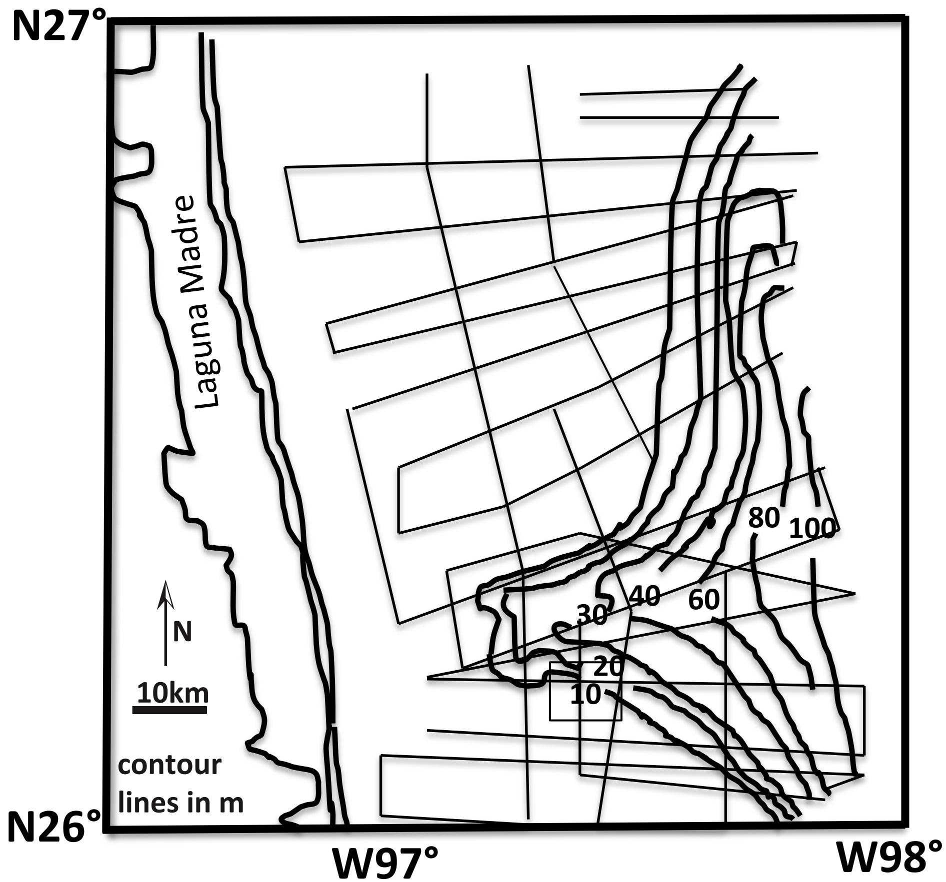
N27°
N26°
W97°
W98°
Laguna Madre
N
10km
contour lines in m
10
20
30
40
60
80
100

Figure 14

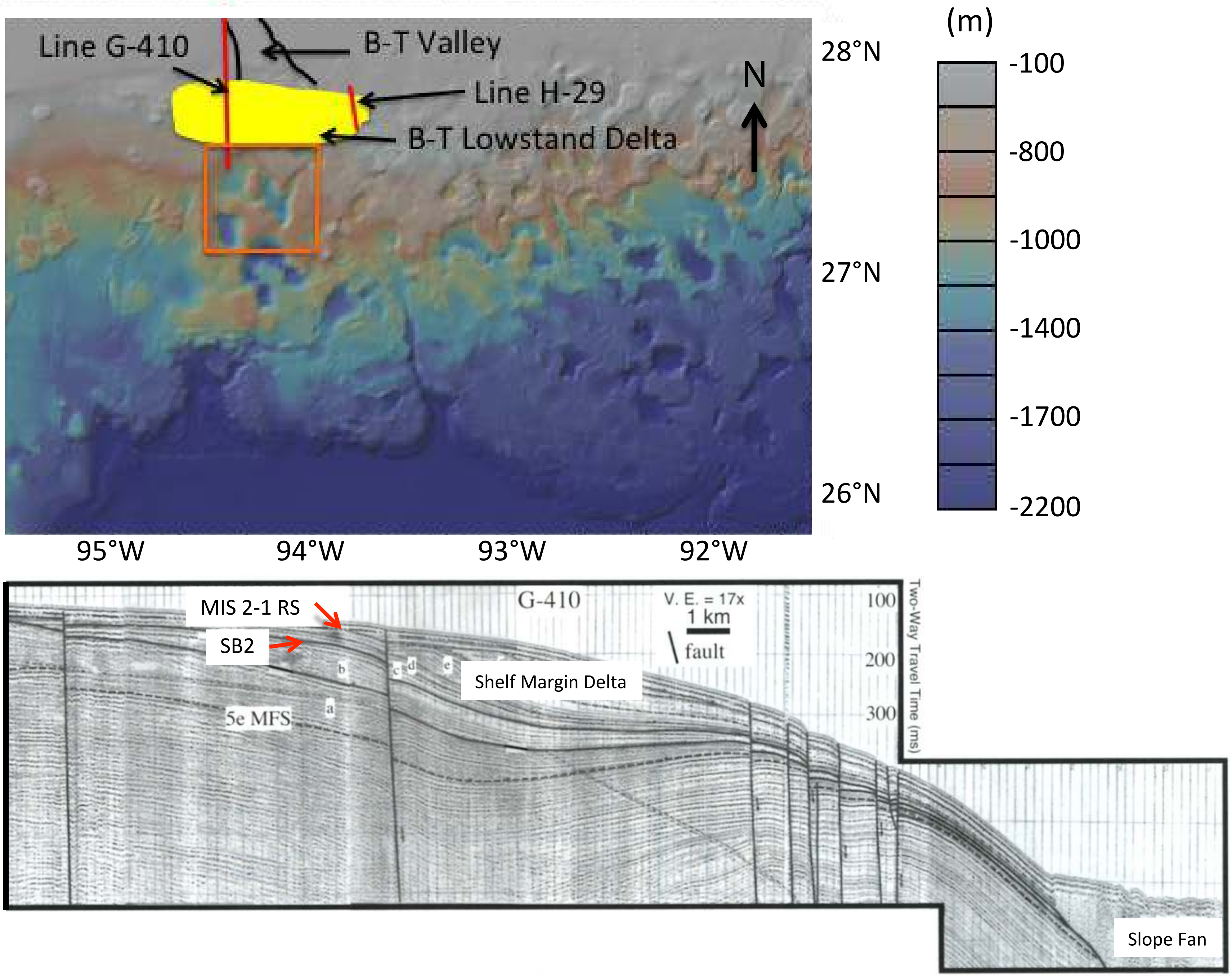
Line G-410
B-T Valley
Line H-29
B-T Lowstand Delta
N
28°N
27°N
26°N
95°W
94°W
93°W
92°W
(m)
-100
-800
-1000
-1400
-1700
-2200
MIS 2-1 RS
SB2
G-410
V. E. = 17x
1 km
fault
100
200
300
Two-Way Travel Time (ms)
Shelf Margin Delta
5e MFS
a
b
c
d
e
Slope Fan

Figure 15

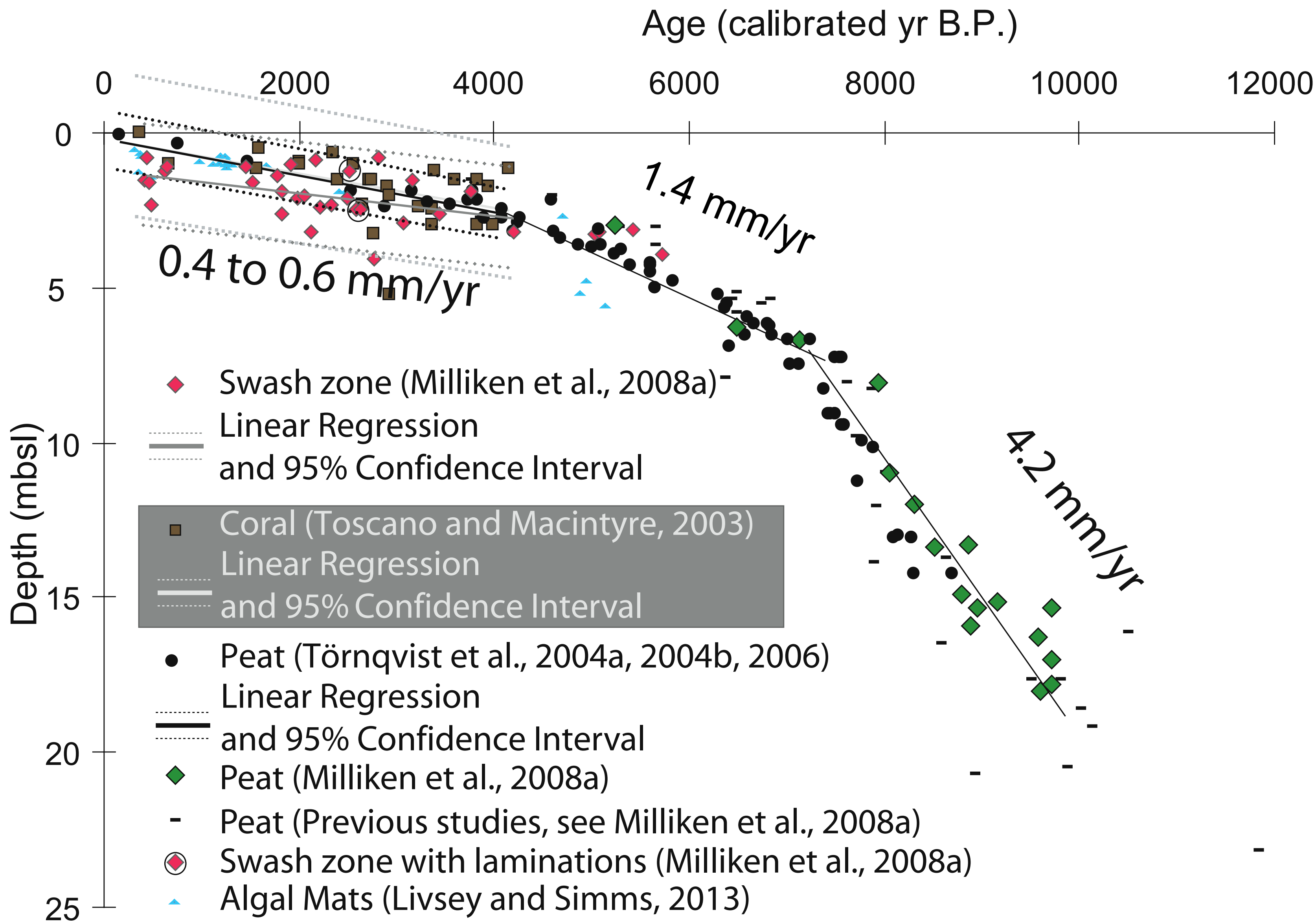

Age (calibrated yr B.P.)
0
2000
4000
6000
8000
10000
12000
Depth (mbsl)
0
5
10
15
20
25
1.4 mm/yr
0.4 to 0.6 mm/yr
4.2 mm/yr
Swash zone (Milliken et al., 2008a)
Linear Regression
and 95% Confidence Interval
Coral (Toscano and Macintyre, 2003)
Linear Regression
and 95% Confidence Interval
Peat (Törnqvist et al., 2004a, 2004b, 2006)
Linear Regression
and 95% Confidence Interval
Peat (Milliken et al., 2008a)
Peat (Previous studies, see Milliken et al., 2008a)
Swash zone with laminations (Milliken et al., 2008a)
Algal Mats (Livsey and Simms, 2013)

Figure 16

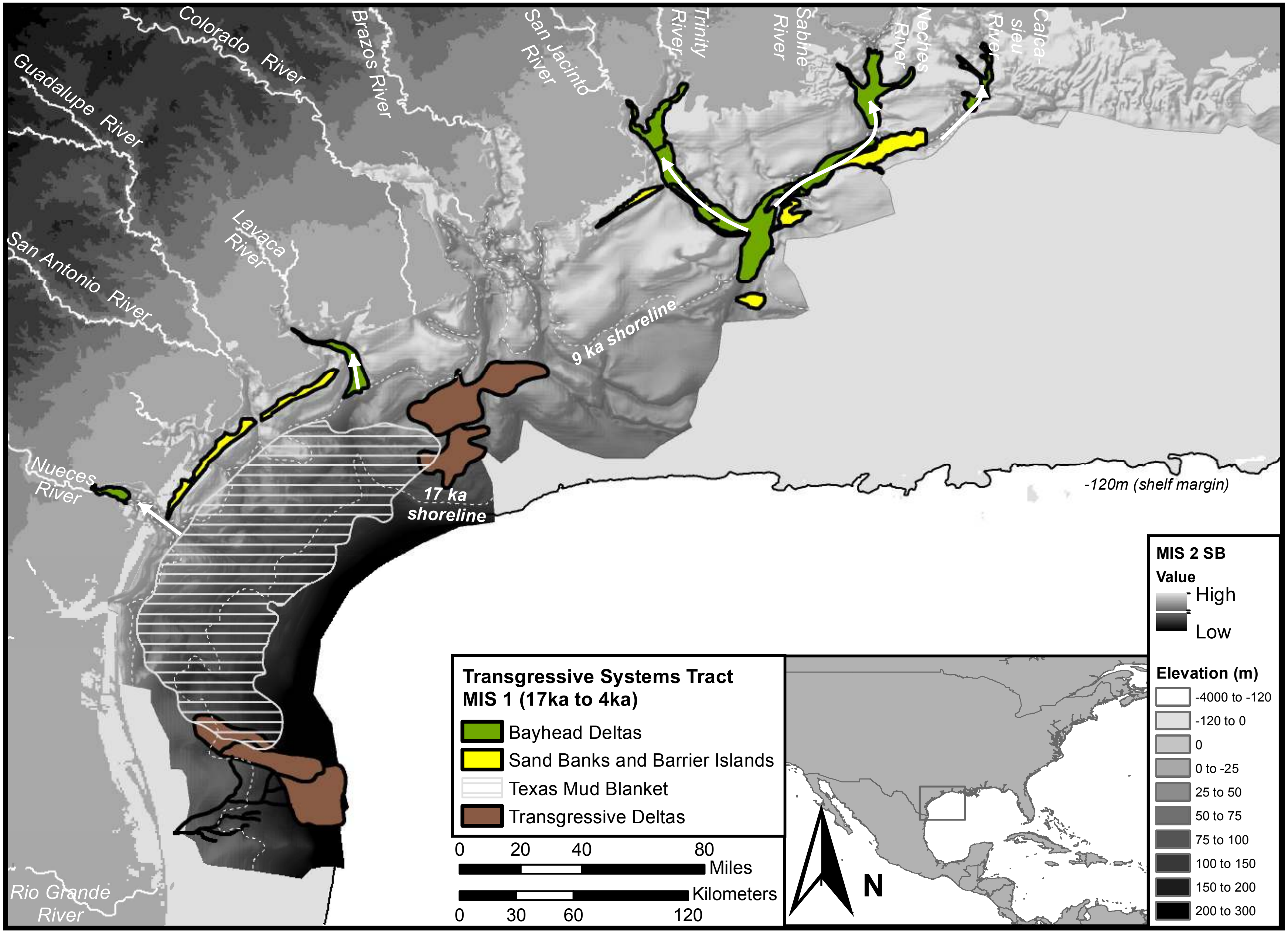

Colorado River
Brazos River
San Jacinto River
Trinity River
Sabine River
Neches River
Calcasieu River
Guadalupe River
Lavaca River
San Antonio River
Nueces River
Rio Grande River
9 ka shoreline
17 ka shoreline
-120m (shelf margin)
Transgressive Systems Tract
MIS 1 (17ka to 4ka)
Bayhead Deltas
Sand Banks and Barrier Islands
Texas Mud Blanket
Transgressive Deltas
0
20
40
80
Miles
Kilometers
0
30
60
120
N
MIS 2 SB
Value
High
Low
Elevation (m)
-4000 to -120
-120 to 0
0
0 to -25
25 to 50
50 to 75
75 to 100
100 to 150
150 to 200
200 to 300

Figure 17

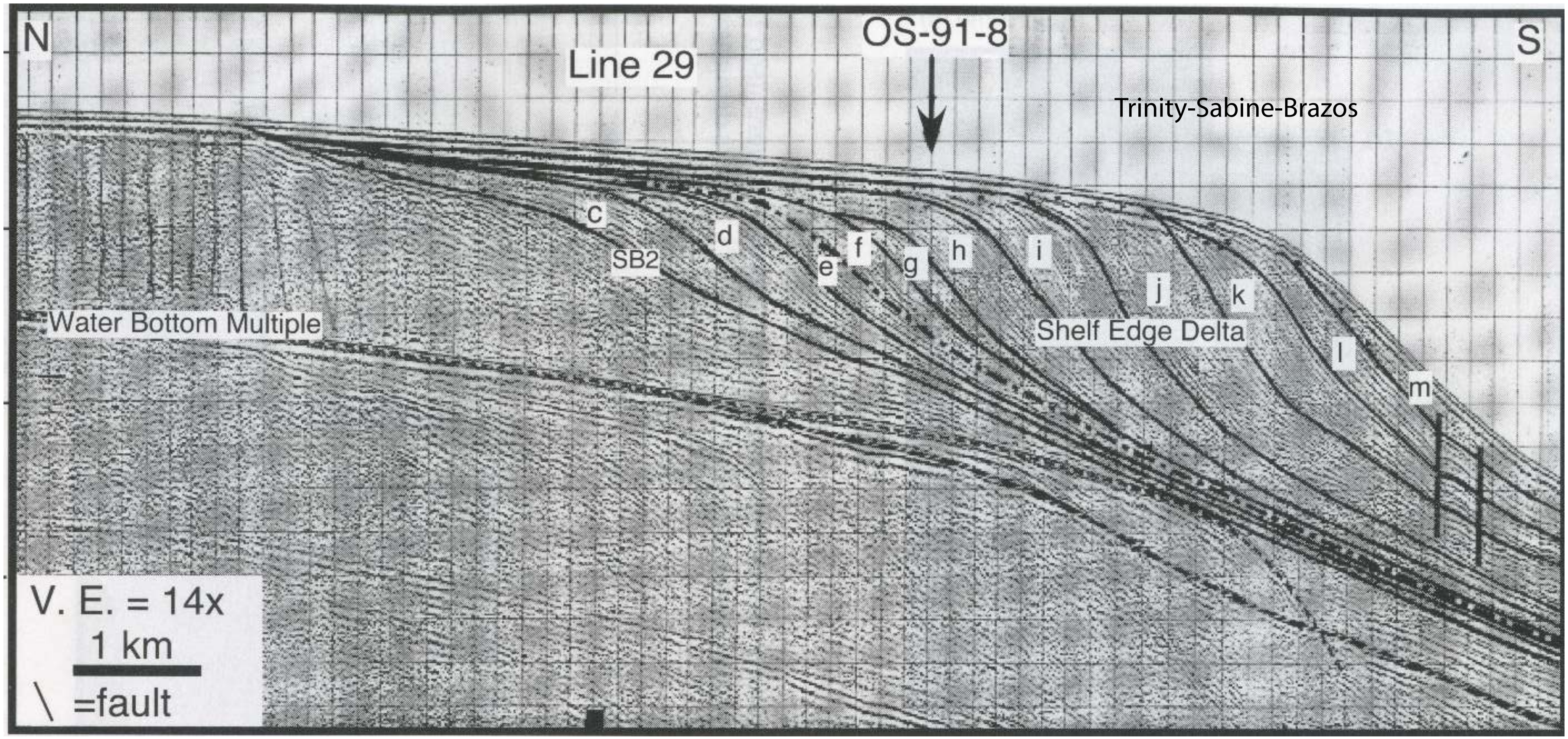
N
S
Line 29
OS-91-8
Trinity-Sabine-Brazos
c
SB2
d
e
f
g
h
i
j
k
l
m
Water Bottom Multiple
Shelf Edge Delta
V. E. = 14x
1 km
\ =fault

Figure 18

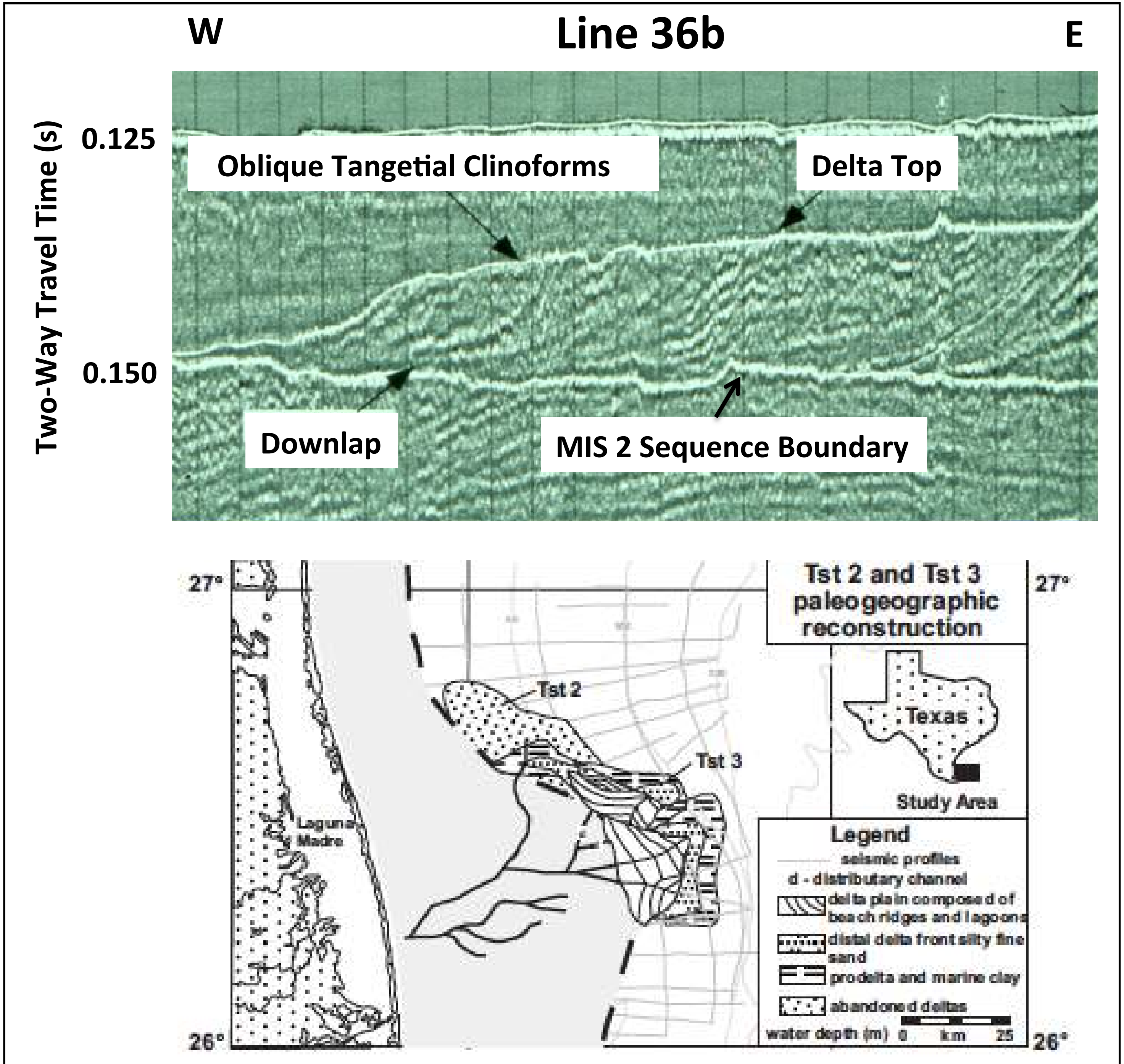

W
Line 36b
E
Two-Way Travel Time (s)
0.125
0.150
Oblique Tangetial Clinoforms
Delta Top
Downlap
MIS 2 Sequence Boundary
27°
26°
Tst 2 and Tst 3
paleogeographic
reconstruction
Tst 2
Tst 3
Laguna
Madre
Texas
Study Area
Legend
seismic profiles
d - distributary channel
delta plain composed of beach ridges and lagoons
distal delta front silty fine sand
prodelta and marine clay
abandoned deltas
water depth (m)
0
km
25

Figure 19

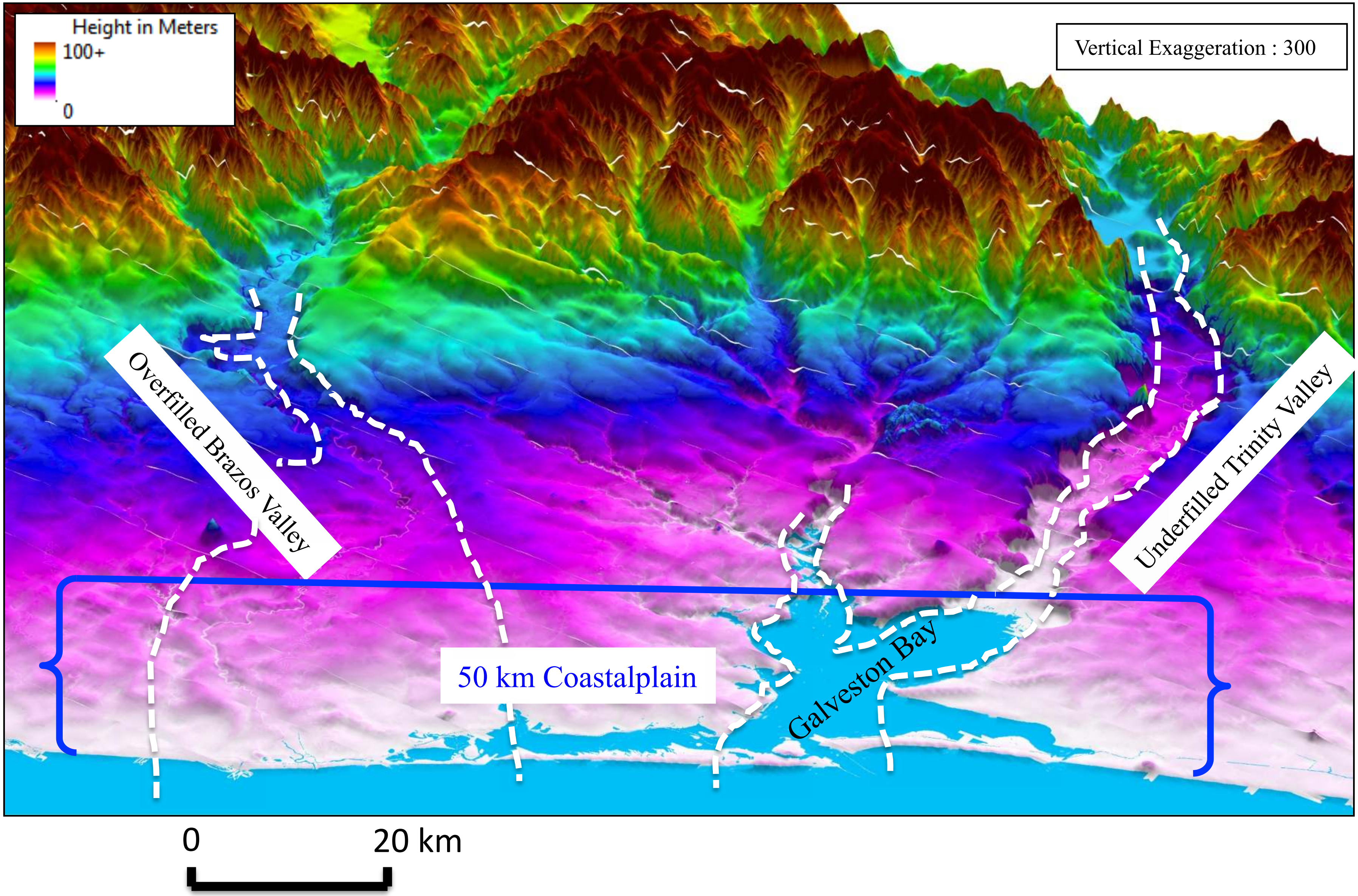

Height in Meters
100+
0
Vertical Exaggeration : 300
Overfilled Brazos Valley
Underfilled Trinity Valley
50 km Coastalplain
Galveston Bay
0
20 km

Figure 20

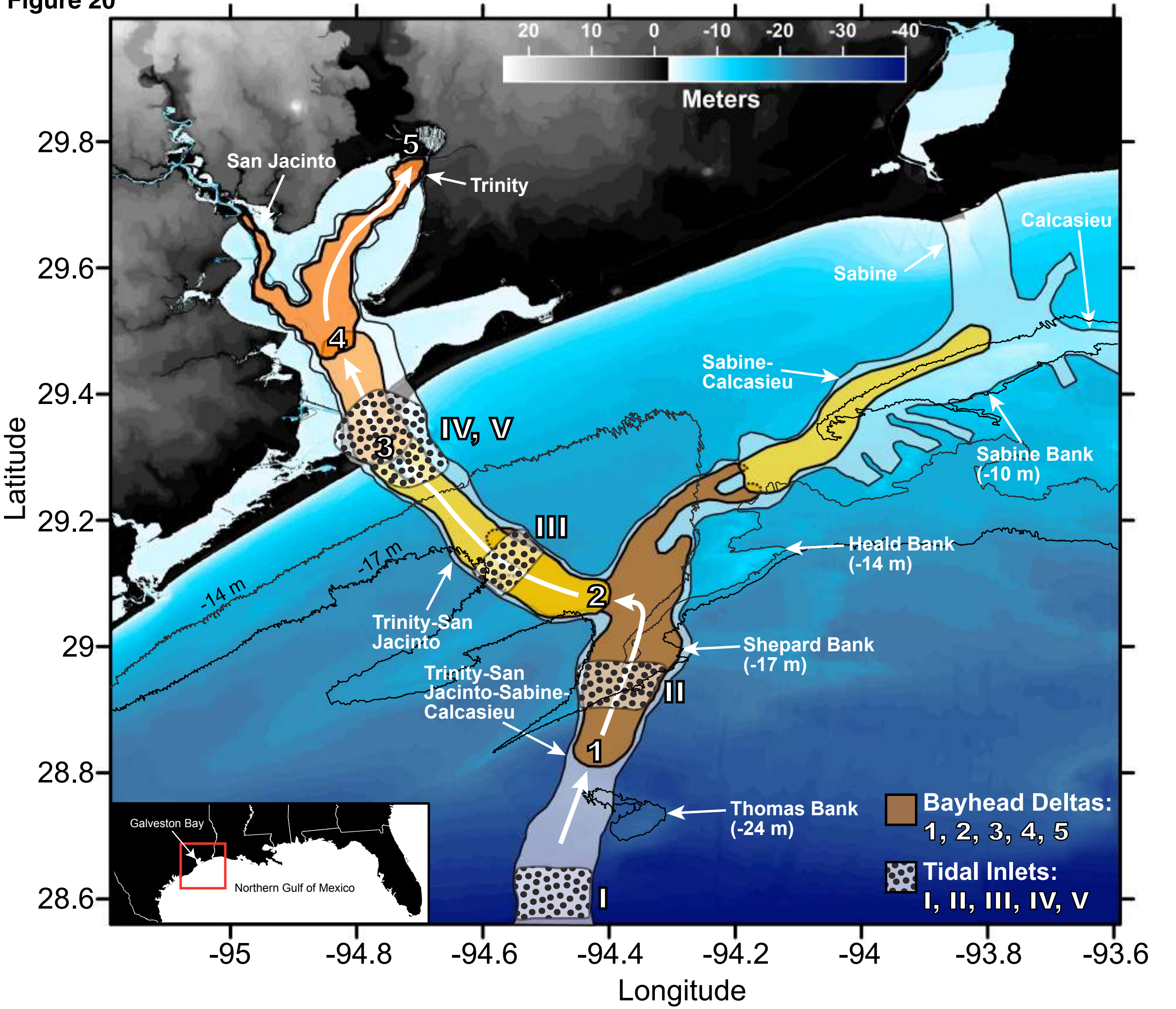

20
10
0
-10
-20
-30
-40
Meters
San Jacinto
5
Trinity
4
3
IV, V
III
2
1
II
I
Calcasieu
Sabine
Sabine-
Calcasieu
Sabine Bank
(-10 m)
Heald Bank
(-14 m)
Shepard Bank
(-17 m)
Thomas Bank
(-24 m)
-14 m
-17 m
Trinity-San
Jacinto
Trinity-San
Jacinto-Sabine-
Calcasieu
Bayhead Deltas:
1, 2, 3, 4, 5
Tidal Inlets:
I, II, III, IV, V
Galveston Bay
Northern Gulf of Mexico
29.8
29.6
29.4
29.2
29
28.8
28.6
Latitude
-95
-94.8
-94.6
-94.4
-94.2
-94
-93.8
-93.6
Longitude

Figure 21

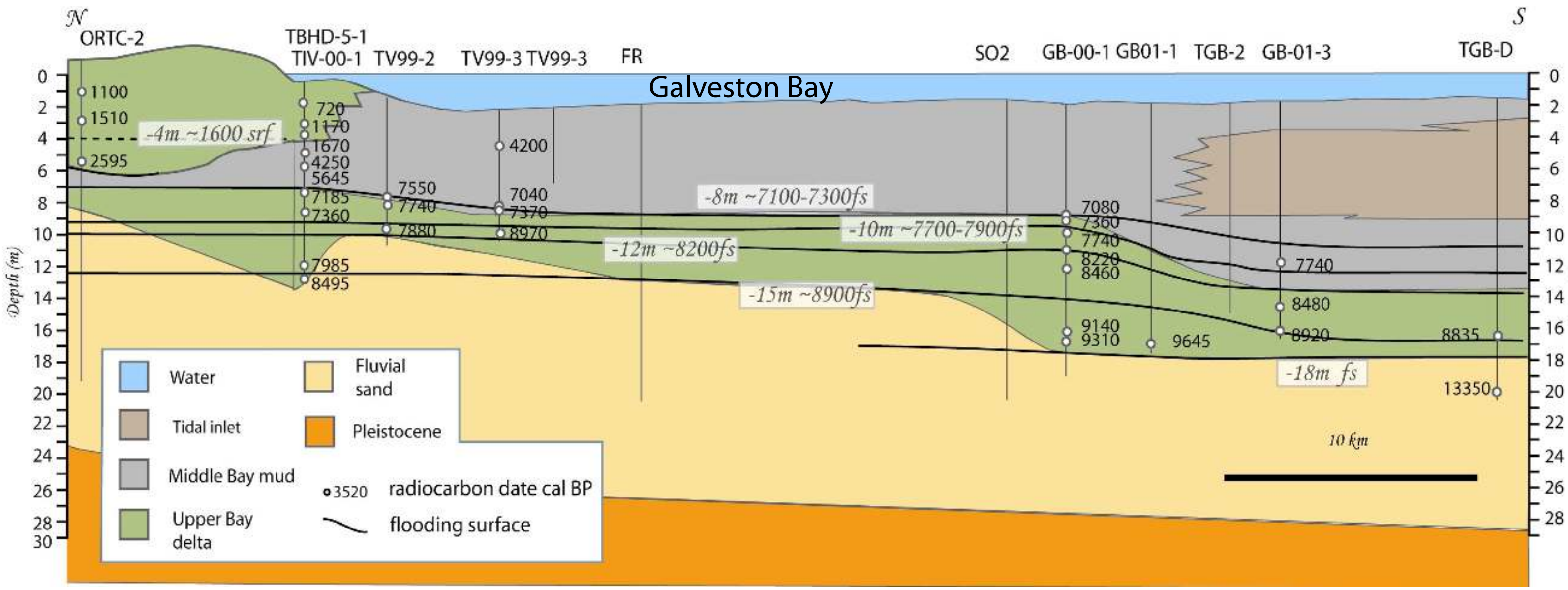

N
S
ORTC-2
TBHD-5-1
TIV-00-1
TV99-2
TV99-3 TV99-3
FR
SO2
GB-00-1 GB01-1
TGB-2
GB-01-3
TGB-D
Galveston Bay
-4m ~1600 srf
-8m ~7100-7300fs
-10m ~7700-7900fs
-12m ~8200fs
-15m ~8900fs
-18m fs
Depth (m)
10 km
Water
Fluvial sand
Tidal inlet
Pleistocene
Middle Bay mud
Upper Bay delta
3520 radiocarbon date cal BP
flooding surface

Figure 22

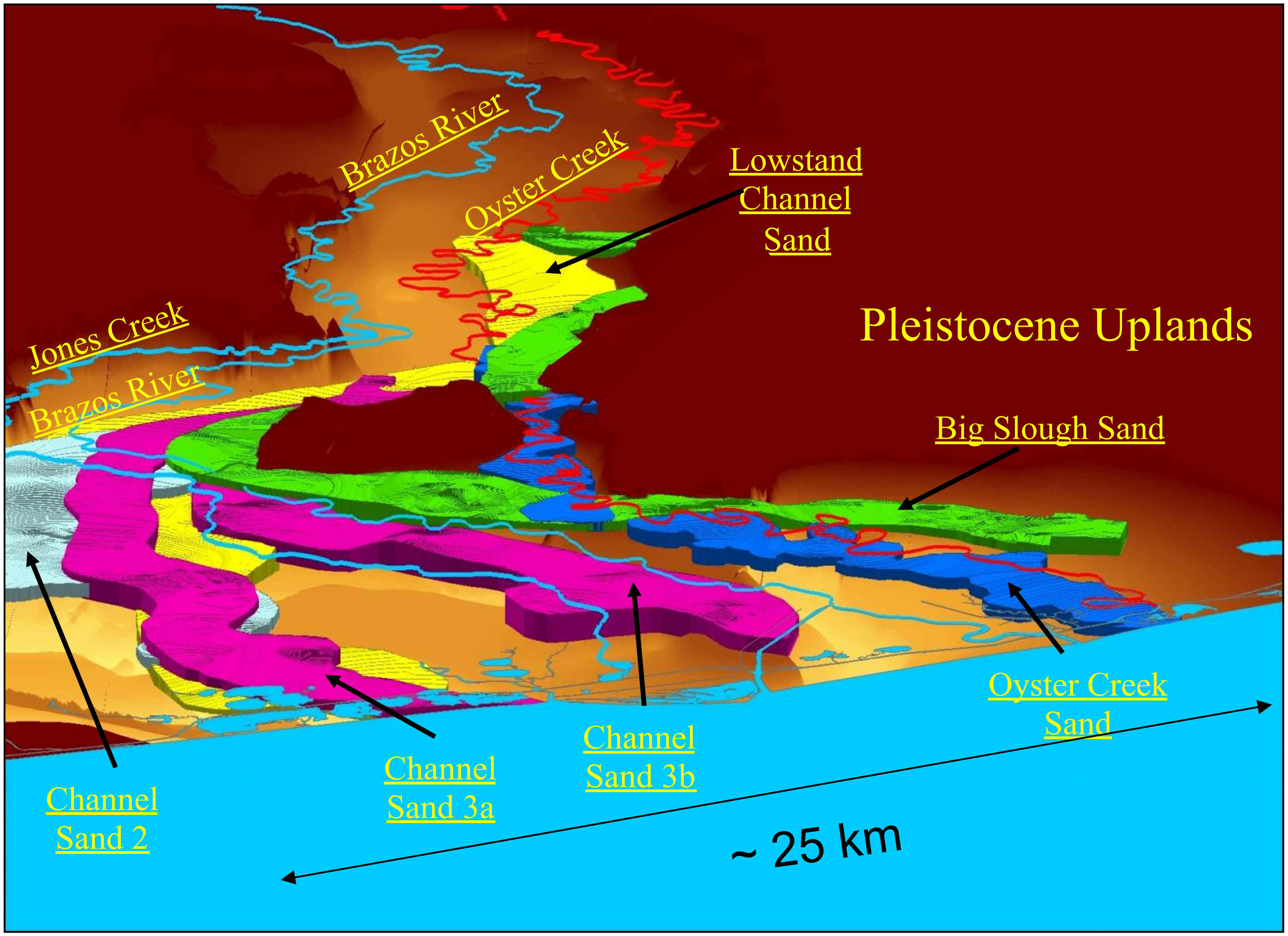

Brazos River
Oyster Creek
Lowstand Channel Sand
Jones Creek
Brazos River
Pleistocene Uplands
Big Slough Sand
Channel Sand 2
Channel Sand 3a
Channel Sand 3b
Oyster Creek Sand
~ 25 km

Figure 23

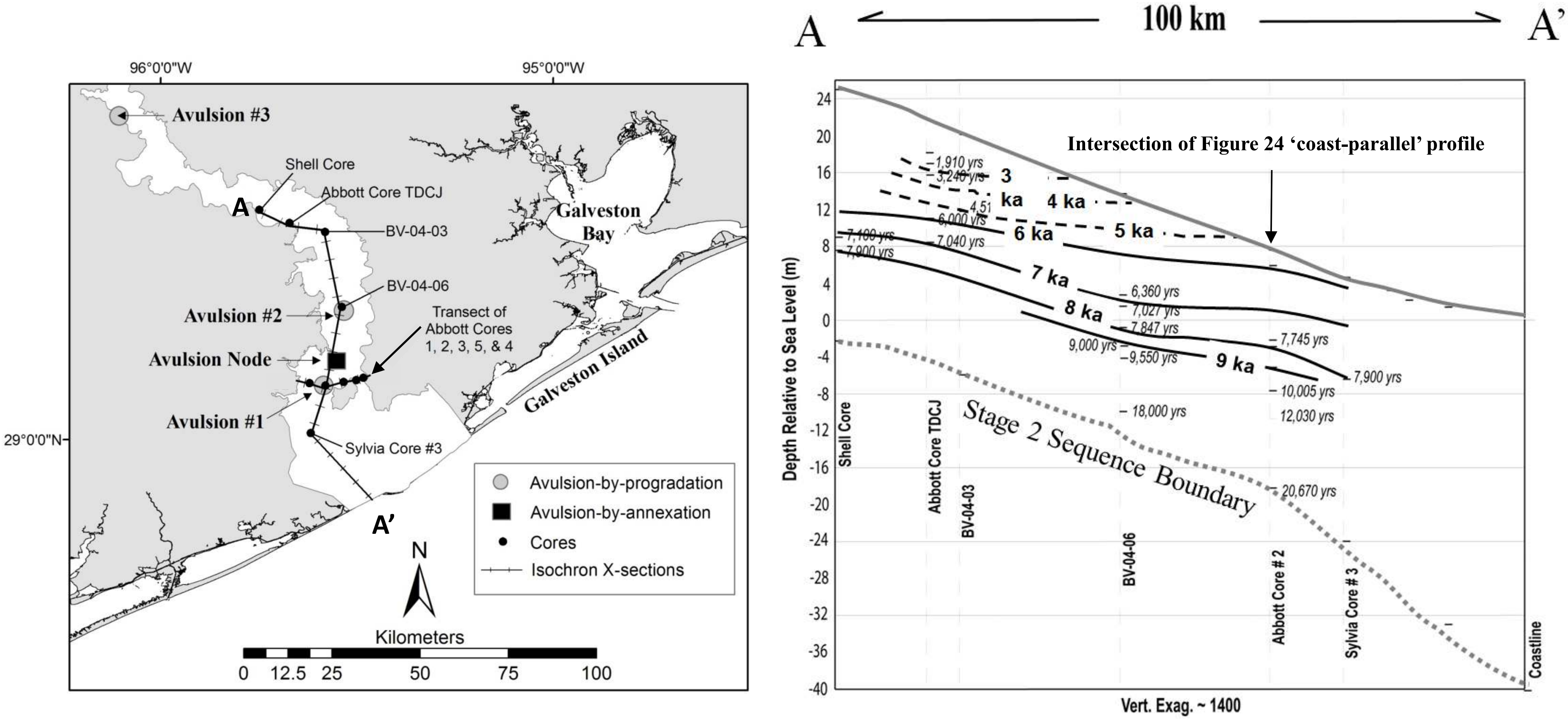
96°0'0"W
95°0'0"W
29°0'0"N
Avulsion #3
Shell Core
Abbott Core TDCJ
A
BV-04-03
Galveston Bay
BV-04-06
Avulsion #2
Transect of Abbott Cores 1, 2, 3, 5, & 4
Avulsion Node
Galveston Island
Avulsion #1
Sylvia Core #3
A'
Avulsion-by-progradation
Avulsion-by-annexation
Cores
Isochron X-sections
N
Kilometers
0 12.5 25 50 75 100
A
100 km
A'
Intersection of Figure 24 'coast-parallel' profile
Depth Relative to Sea Level (m)
24
20
16
12
8
4
0
-4
-8
-12
-16
-20
-24
-28
-32
-36
-40
1,910 yrs
3,240 yrs
3 ka
4 ka
5 ka
6 ka
7 ka
8 ka
9 ka
6,000 yrs
7,100 yrs
7,040 yrs
7,900 yrs
6,360 yrs
7,027 yrs
7,847 yrs
9,000 yrs
9,550 yrs
7,745 yrs
7,900 yrs
10,005 yrs
18,000 yrs
12,030 yrs
20,670 yrs
Stage 2 Sequence Boundary
Shell Core
Abbott Core TDCJ
BV-04-03
BV-04-06
Abbott Core # 2
Sylvia Core # 3
Coastline
Vert. Exag. ~ 1400

Figure 24

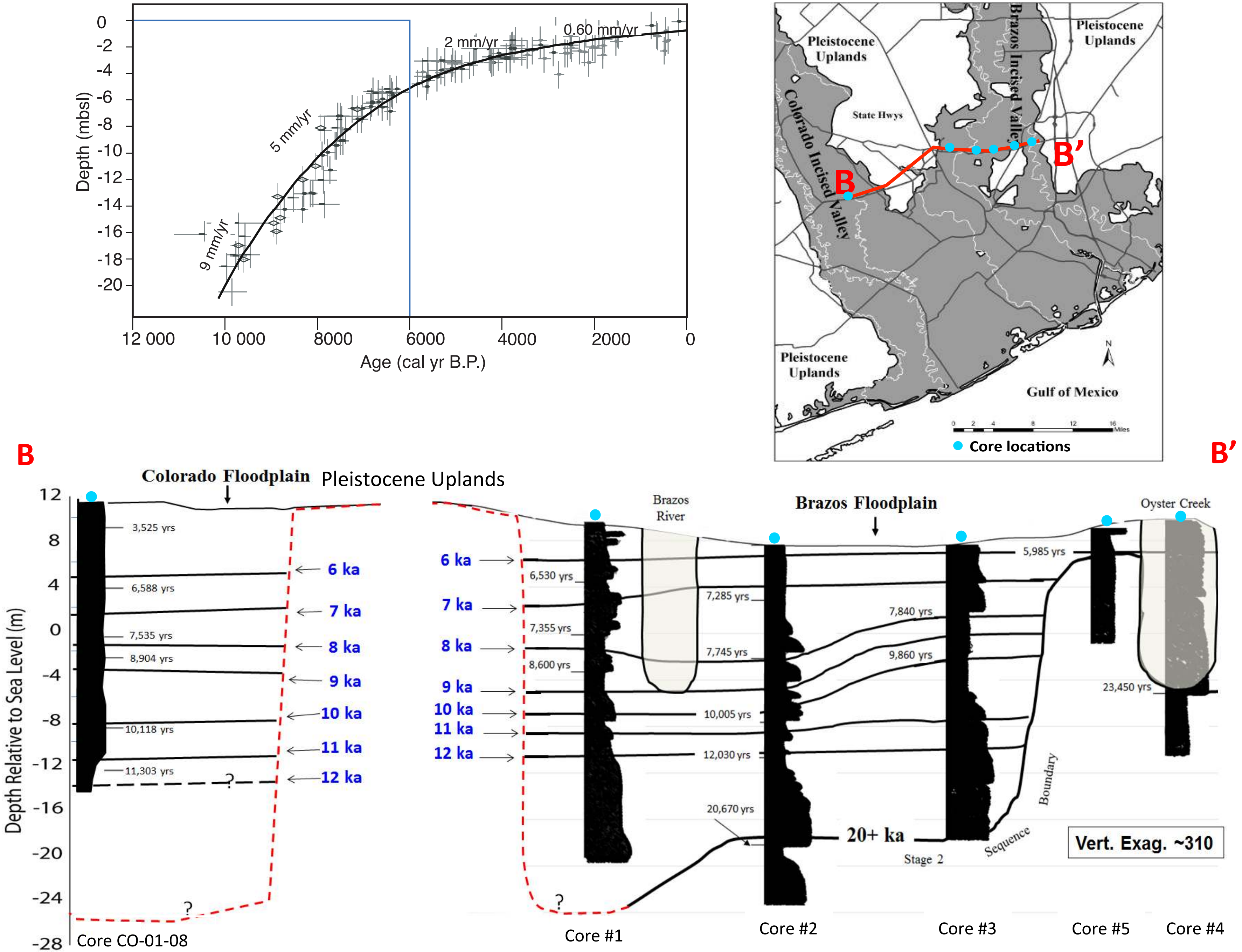

0
-2
-4
-6
-8
-10
-12
-14
-16
-18
-20
Depth (mbsl)
12 000
10 000
8000
6000
4000
2000
0
Age (cal yr B.P.)
9 mm/yr
5 mm/yr
2 mm/yr
0.60 mm/yr
Pleistocene Uplands
Pleistocene Uplands
Pleistocene Uplands
Brazos Incised Valley
Colorado Incised Valley
State Hwys
B
B’
Gulf of Mexico
Core locations
B
B’
Colorado Floodplain
Pleistocene Uplands
Brazos Floodplain
Brazos River
Oyster Creek
Depth Relative to Sea Level (m)
12
8
4
0
-4
-8
-12
-16
-20
-24
-28
3,525 yrs
6,588 yrs
7,535 yrs
8,904 yrs
10,118 yrs
11,303 yrs
6 ka
7 ka
8 ka
9 ka
10 ka
11 ka
12 ka
6,530 yrs
7,355 yrs
8,600 yrs
7,285 yrs
7,745 yrs
10,005 yrs
12,030 yrs
20,670 yrs
7,840 yrs
9,860 yrs
5,985 yrs
23,450 yrs
20+ ka
Stage 2
Sequence
Boundary
Vert. Exag. ~310
Core CO-01-08
Core #1
Core #2
Core #3
Core #5
Core #4

Figure 25

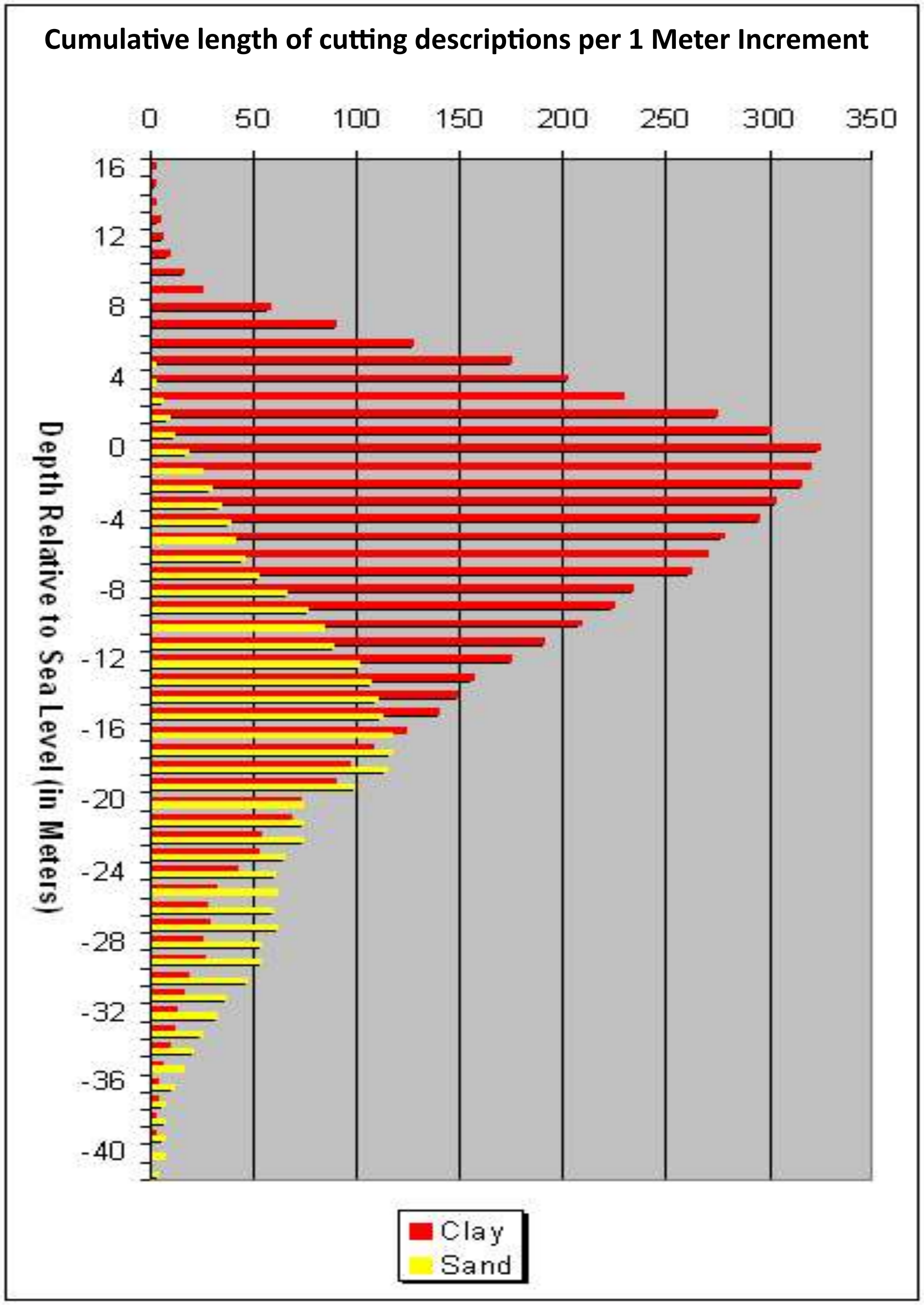

Cumulative length of cutting descriptions per 1 Meter Increment
0
50
100
150
200
250
300
350
16
12
8
4
0
-4
-8
-12
-16
-20
-24
-28
-32
-36
-40
Depth Relative to Sea Level (in Meters)
Clay
Sand

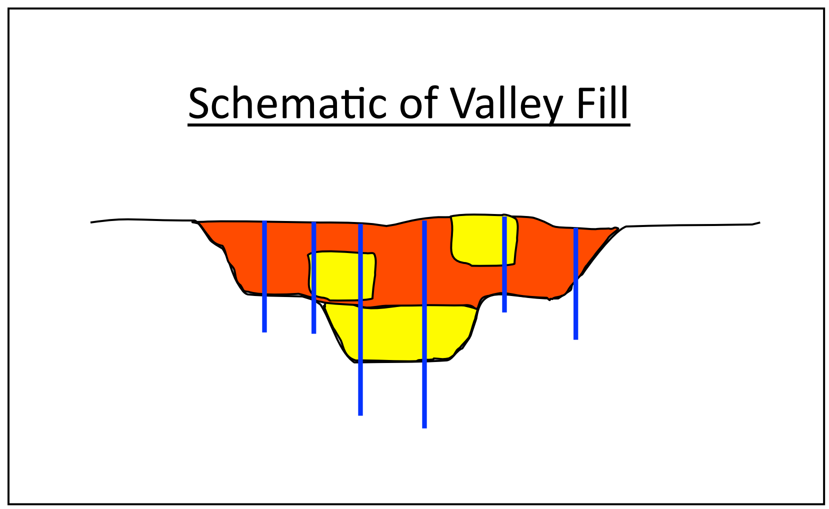

Schematic of Valley Fill

Figure 26

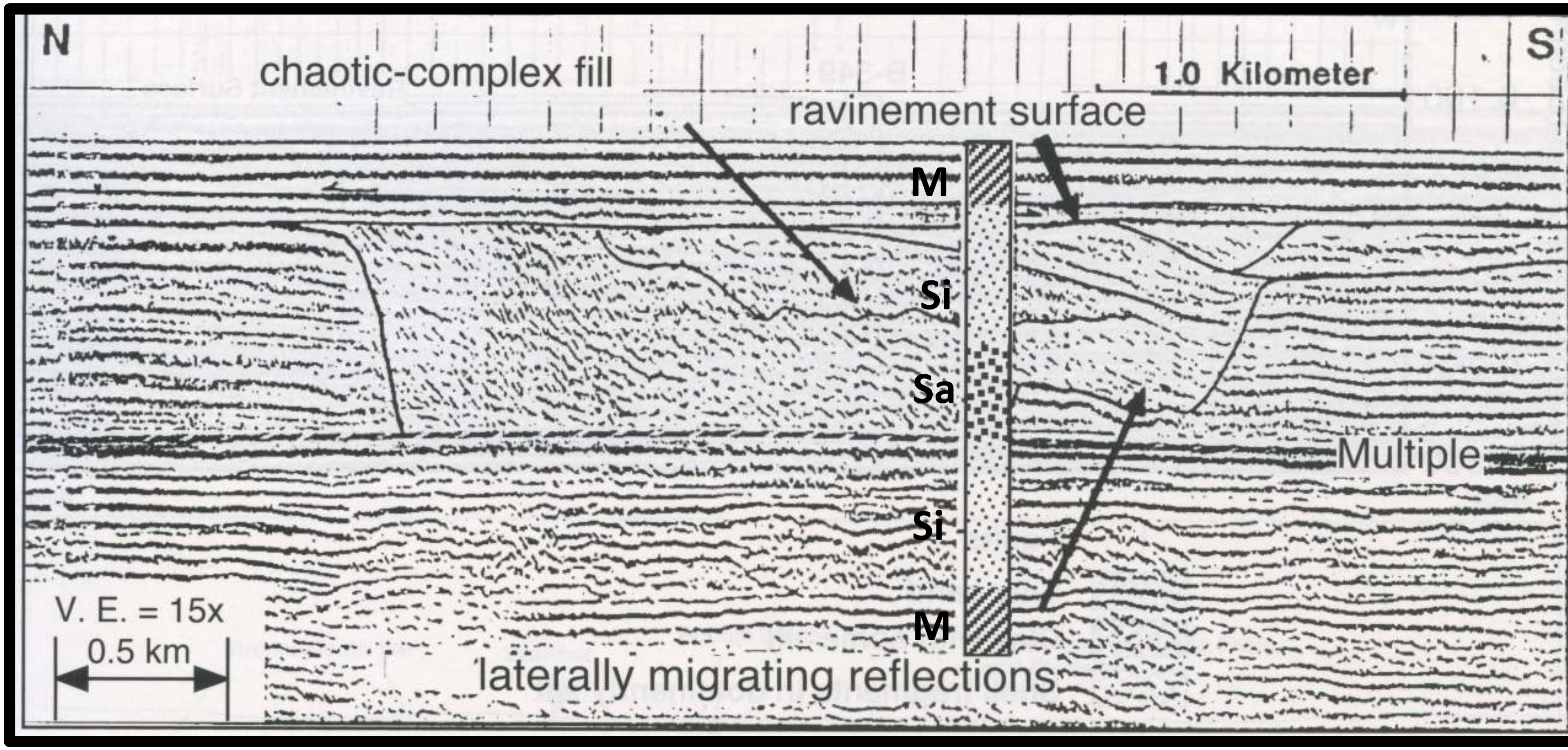
N
S
chaotic-complex fill
1.0 Kilometer
ravinement surface
M
Si
Sa
Si
M
Multiple
V. E. = 15x
0.5 km
laterally migrating reflections

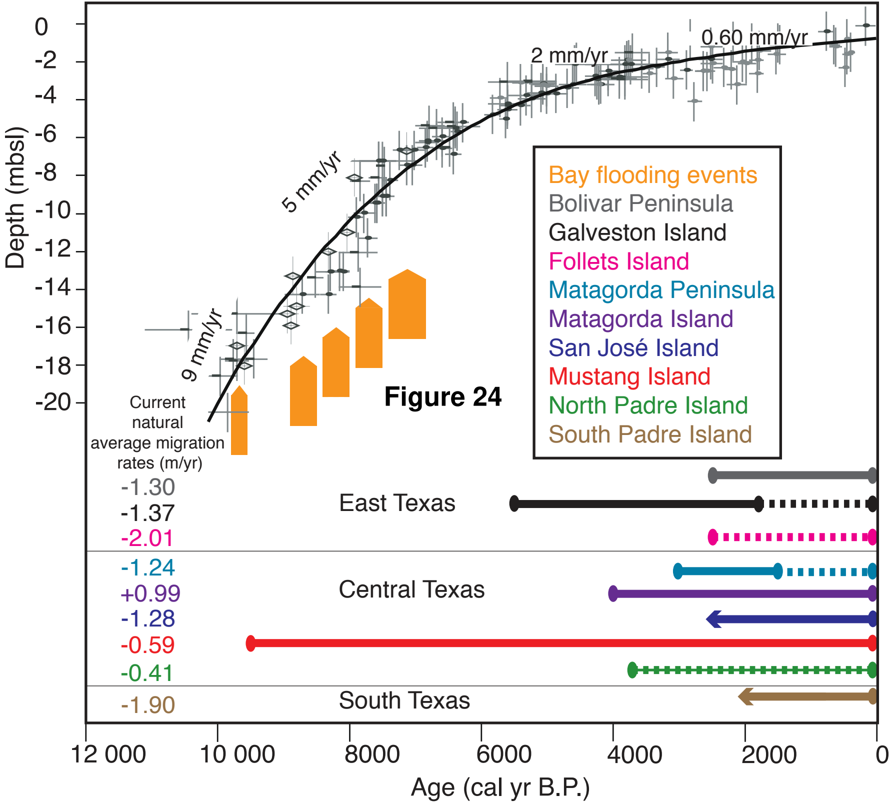

Figure 24
Depth (mbsl)
0
-2
-4
-6
-8
-10
-12
-14
-16
-18
-20
0.60 mm/yr
2 mm/yr
5 mm/yr
9 mm/yr
Bay flooding events
Bolivar Peninsula
Galveston Island
Follets Island
Matagorda Peninsula
Matagorda Island
San José Island
Mustang Island
North Padre Island
South Padre Island
Current natural average migration rates (m/yr)
-1.30
-1.37
-2.01
East Texas
-1.24
+0.99
-1.28
-0.59
-0.41
Central Texas
-1.90
South Texas
12 000
10 000
8000
6000
4000
2000
0
Age (cal yr B.P.)

Figure 28

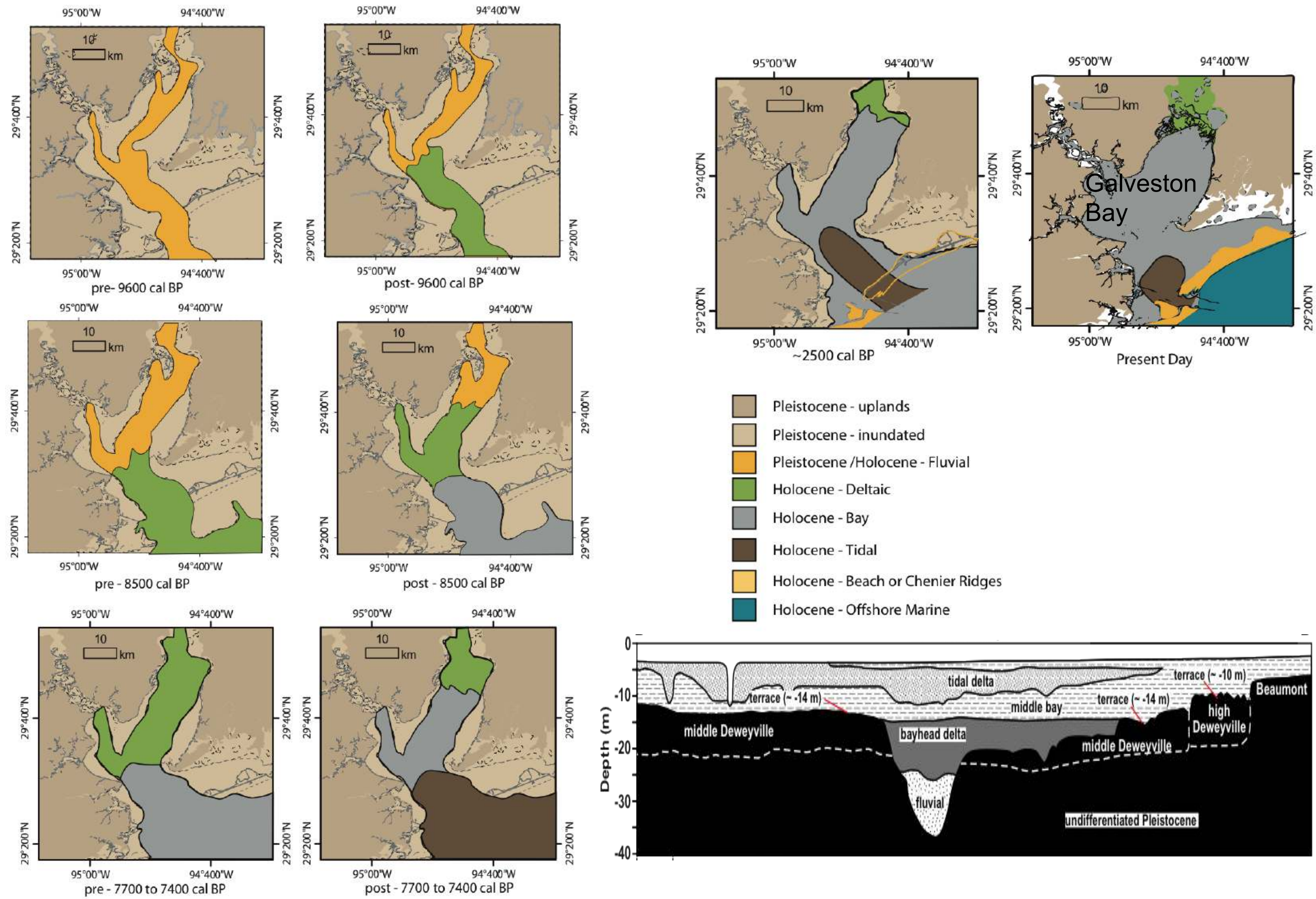

pre- 9600 cal BP
post- 9600 cal BP
pre - 8500 cal BP
post - 8500 cal BP
pre - 7700 to 7400 cal BP
post - 7700 to 7400 cal BP
~2500 cal BP
Present Day
Galveston Bay
95°00'W
94°400'W
29°400'N
29°200'N
10 km
Pleistocene - uplands
Pleistocene - inundated
Pleistocene /Holocene - Fluvial
Holocene - Deltaic
Holocene - Bay
Holocene - Tidal
Holocene - Beach or Chenier Ridges
Holocene - Offshore Marine
Depth (m)
0
-10
-20
-30
-40
tidal delta
terrace (~ -10 m)
Beaumont
terrace (~ -14 m)
middle bay
terrace (~ -14 m)
high Deweyville
middle Deweyville
bayhead delta
middle Deweyville
fluvial
undifferentiated Pleistocene

Figure 29

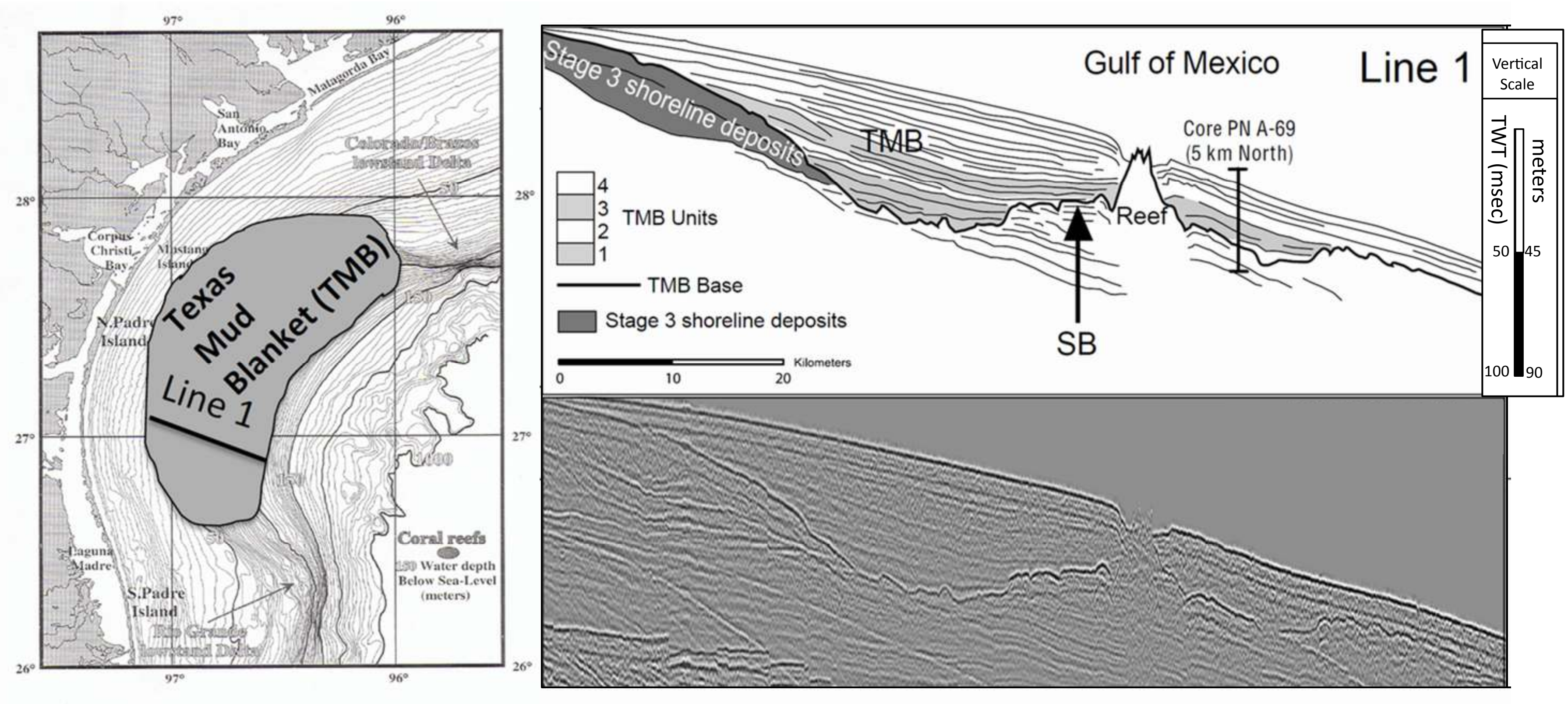
97°
96°
Matagorda Bay
San Antonio Bay
Colorado/Brazos lowstand Delta
28°
Corpus Christi Bay
Mustang Island
N.Padre Island
Texas Mud Blanket (TMB)
Line 1
27°
Laguna Madre
S.Padre Island
Rio Grande lowstand Delta
Coral reefs
150 Water depth Below Sea-Level (meters)
26°
Stage 3 shoreline deposits
Gulf of Mexico
Line 1
TMB
Core PN A-69 (5 km North)
4
3
2
1
TMB Units
TMB Base
Stage 3 shoreline deposits
Reef
SB
Kilometers
0
10
20
Vertical Scale
TWT (msec)
meters
50
45
100
90

Figure 30

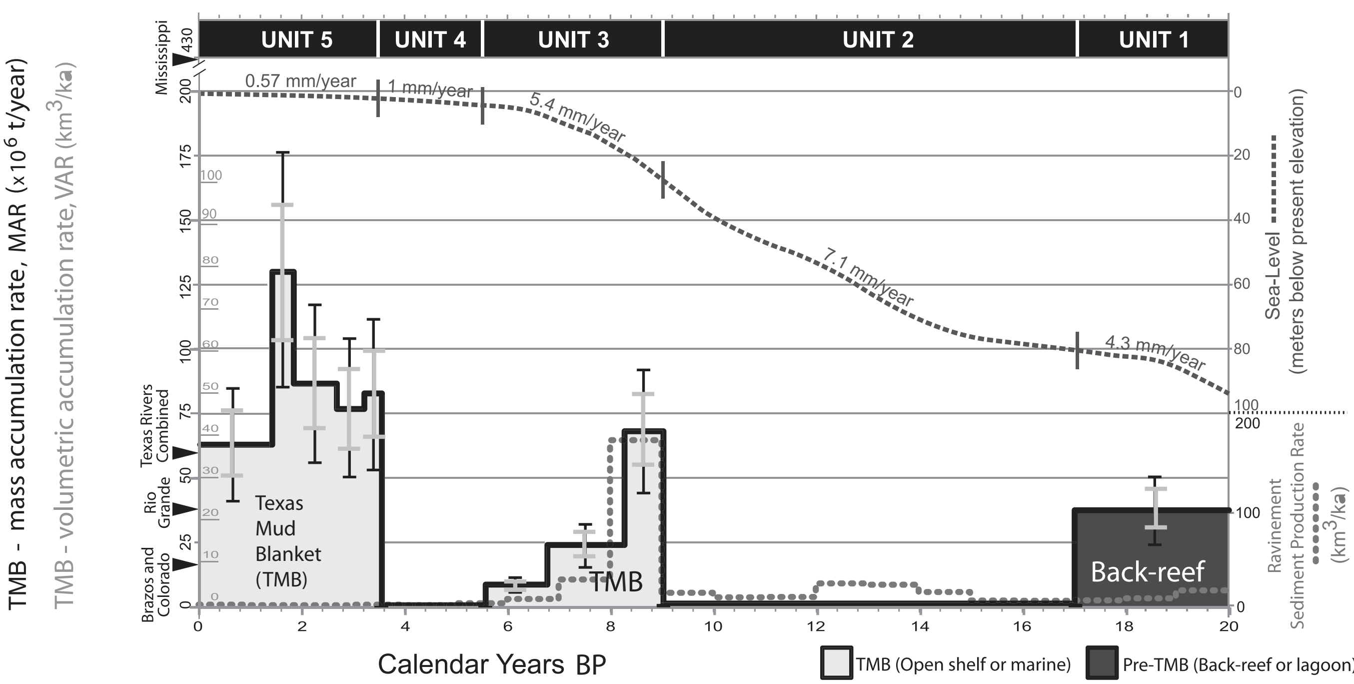

UNIT 5
UNIT 4
UNIT 3
UNIT 2
UNIT 1
0.57 mm/year
1 mm/year
5.4 mm/year
7.1 mm/year
4.3 mm/year
Mississippi
430
Texas Rivers Combined
Rio Grande
Brazos and Colorado
Texas Mud Blanket (TMB)
TMB
Back-reef
TMB - mass accumulation rate, MAR (x10^6 t/year)
TMB - volumetric accumulation rate, VAR (km^3/ka)
Sea-Level (meters below present elevation)
Ravinement Sediment Production Rate (km^3/ka)
Calendar Years BP
TMB (Open shelf or marine)
Pre-TMB (Back-reef or lagoon)

Figure 31

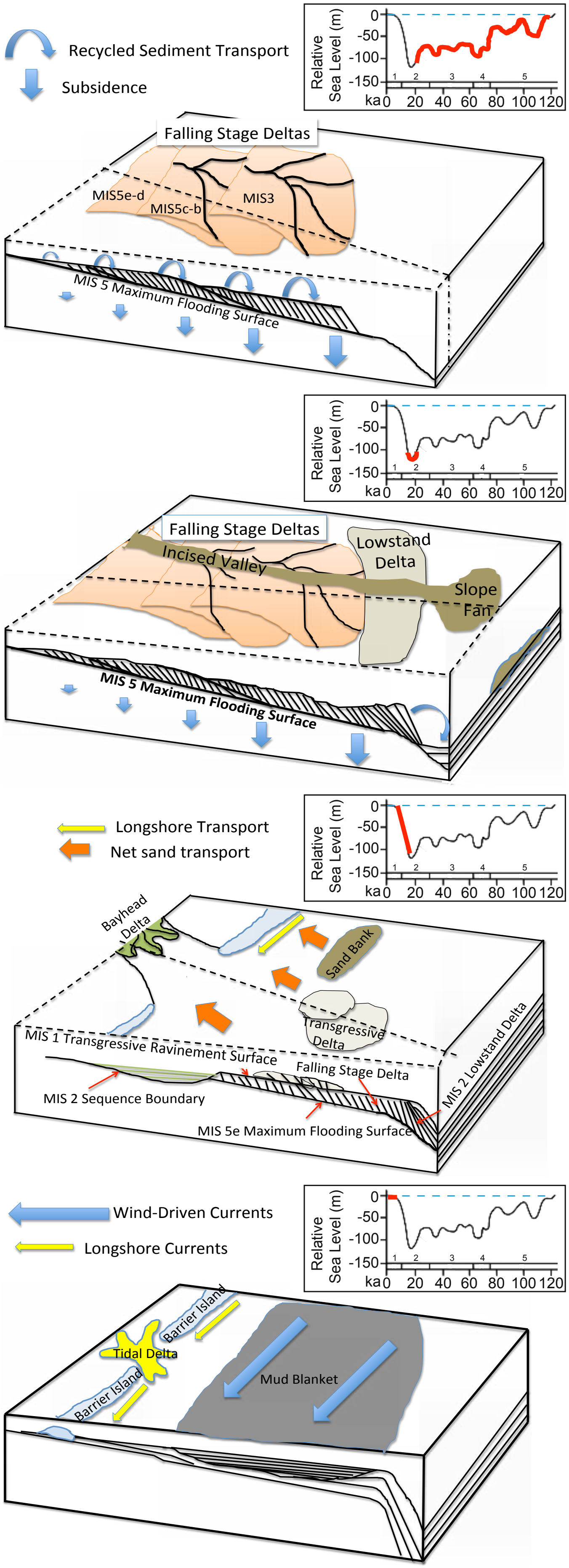

Falling Stage

1. Delta growth marked by episodic progradation and back-stepping due to sea-level oscillations
2. Recycling of sediments from the slowly subsiding inner shelf to the outer shelf results in increased sediment supply through time
3. Multiple episodes of channel incision and purging during fall and aggradation during rise contributes to variable sediment supply to deltas

Lowstand

1. Valley incision
2. Lowstand delta and slope fan formation
3. Continued erosion and recycling of sediments from inner to outer shelf

Transgression

1. Transgressive ravinement provides sand to evolving coast
2. Transgressive deltas formed during climatically-induced increase in sediment discharge of Brazos, Colorado, and Rio Grande rivers
3. Sand Banks formed by overstepping of barriers
4. Valley aggradation

Highstand

1. Most modern barriers formed
2. Sediment bypass in larger rivers
3. Mud blanket formed on central Texas shelf

Table 1

Depocenter	MIS Stage	Time Interval (ka)	Volume (km^3)	VAR km^3/kyr	MAR (10^6 t/y)*	*Modern River*	*Modern sediment discharge (10^6 t/y)*
Colorado Delta	Late MIS 3	40 - 23	21	1.24	1.96	*Rio Grande*	*(4)36.9*
Colorado Delta	MIS 2	22 - 11.5	77	7.33	11.66	*Nueces*	*(2)0.68*
Colorado Delta (volume from [5])	MIS 1	11.5 - 8.0	10.8	3.09	4.91	*Lavaca*	*(2)0.15*
Brazos Delta	MIS 5e-5b	120 - 90	33	1.10	1.75	*Brazos*	*(4)12.4*
Brazos Delta	MIS 5a-4	80 - 60	27	1.35	2.15	*Colorado*	*(4)2.8*
Brazos Delta	MIS 3	55 - 23	112	3.50	5.57	*San Jacinto/Trinity*	*(3)6.2*
Brazos Lower Incised Valley	MIS 1	20 - Present	28.6	1.43	2.27	*Sabine*	*(1)0.75*
Brazos Lower Incised Valley	MIS 1	8 - Present	24	3.00	4.77	*Mississippi*	*(4)427.9*
Trinity Valley Bay Deposits	MIS 1	10 - Present	9	0.90	1.43		
Purging of Brazos valley	MIS 1	20 - 12	24	3.00	4.77		
Texas Mud Blanket (from Weight et al., 2011)	MIS 1	9.0 - 8.0	41	41.00	68.50		
Texas Mud Blanket (from Weight et al., 2011)	MIS 1	3.5-Present	172	49.14	81.00		
Modern Coast	MIS 1	4 - Present	13	3.25	5.17		

*Assumptions unless otherwise noted:
100% Quartz, 40% porosity

(1) Milliman and Syvitski, 1992
(2) Shepard, 1953
(3) Seaber et al., 1987
(4) from Weight et al., 2011 using QBART (Syvitski and Milliman, 2007)
(5) Van Heijst et al., 2001